

**Polyaniline Incorporated MOF Modified Anode in Microbial Fuel Cell
for Enhanced Bioelectricity Generation**



By

Osama Naeem

(Registration No: 00000362446)

Department of Materials Engineering

School of Chemical and Materials Engineering

National University of Sciences & Technology (NUST)

Islamabad, Pakistan

(2024)

Polyaniline Incorporated MOF Modified Anode in Microbial Fuel Cell for Enhanced Bioelectricity Generation



By

Osama Naeem

(Registration No: 00000362446)

A thesis submitted to the National University of Sciences and Technology, Islamabad,

in partial fulfillment of the requirements for the degree of

Master of Science in
Surface and Materials Engineering

Supervisor: Dr. Usman Liaqat

School of Chemical and Materials Engineering

National University of Sciences & Technology (NUST)

Islamabad, Pakistan

(2024)

THESIS ACCEPTANCE CERTIFICATE



THESIS ACCEPTANCE CERTIFICATE

Certified that final copy of MS thesis written by Mr **Osama Naeem** (Registration No 00000362446), of School of Chemical & Materials Engineering (SCME) has been vetted by undersigned, found complete in all respects as per NUST Statues/Regulations, is free of plagiarism, errors, and mistakes and is accepted as partial fulfillment for award of MS degree. It is further certified that necessary amendments as pointed out by GEC members of the scholar have also been incorporated in the said thesis.

Signature: _____

Name of Supervisor: Dr Usman Liaqat

Date: 18-09-24

Signature (HOD): _____

Date: 19/09/24

Signature (Dean/Principal): _____

Date: 19/9/24

TH - 1

Form TH-1

National University of Sciences & Technology (NUST) MASTER'S THESIS WORK

Formulation of Guidance and Examination Committee (GEC)

Name: Osama Naeem NUST Reg No: 00000362446
Department: Department of Materials Engineering Specialization: Master of Science in Materials & Surface Engineering
Credit Hour Completed: 21.0 → 24 CGPA: 3.64 → 3.69

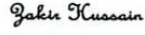
Course Work Completed

S/No:	Code:	Title:	Core/Elective:	CH:	Grade:
1.	MSE-811	Materials Thermodynamics	Compulsory	3.0	B+
2.	MSE-821	Mechanical Behaviour Of Materials	Compulsory	3.0	A
3.	RM-898	Research Methodology	Additional	2.0	Q
4.	NSE-842	Nano Materials For Energy Applications	Elective	3.0	B+
5.	MSE-812	Phase Transformation & Microstructures	Compulsory	3.0	B+
6.	MSE-851	Surface Engineering & Characterisation	Compulsory	3.0	B+
7.	MSE-954	Advanced Characterization Of Materials	Elective	3.0	B+
8.	MSE-963	Semiconductor And Optical Materials	Elective	3.0	A

Date 04 - Nov - 2022

Student's Signature

Thesis Committee

- Name: Usman Liaqat (Supervisor)
Department: Department of Materials Engineering
Signature: 
- Name: Waheed Miran (Cotutor)
Department: Department of Chemical Engineering
Signature: 
- Name: Sofia Javed (Internal)
Department: Department of Materials Engineering
Signature: 
- Name: Zakir Hussain (Internal)
Department: Department of Materials Engineering
Signature: 

Date: 04 - Nov - 2022

Signature of Head of Department:

APPROVAL

Date: 04 - Nov - 2022

Signature of Dean/Principal:

School of Chemical & Materials Engineering (SCME) (SCME) H-12 Campus,

- * 9. MSE-882 Corrosion & Control Engg Elective 3 A
10. MSE-952 Materials for Biomedical Application Add 3 A

TH - 4



National University of Sciences & Technology (NUST)

FORM TH-4

MASTER'S THESIS WORK

We hereby recommend that the dissertation prepared under our supervision by

Regn No & Name: 00000362446 Osama Naem

Title: Polyaniline Incorporated MOF Modified Anode in Microbial Fuel Cell for Enhanced Bioelectricity Generation.

Presented on: 08 Aug 2024 at: 1430 hrs in SCME Seminar Hall

Be accepted in partial fulfillment of the requirements for the award of Masters of Science degree in **Materials & Surface Engineering.**

Guidance & Examination Committee Members

Name: Dr Zakir Hussain

Signature: [Signature]

Name: Dr Sofia Javed

Signature: [Signature]

Name: Dr Waheed Miran (Co-Supervisor)

Signature: [Signature]

Supervisor's Name: Dr Usman Liaqat

Signature: [Signature]

Dated: 20-08-24

[Signature]

Head of Department

Date 21-8-2024

[Signature]

Dean/Principal

Date 21/8/24

School of Chemical & Materials Engineering (SCME)

AUTHOR'S DECLARATION

I Osama Naeem hereby state that my MS thesis titled “Polyaniline Incorporated MOF Modified Anode in Microbial Fuel Cell for Enhanced Bioelectricity Generation” is my own work and has not been submitted previously by me for taking any degree from National University of Sciences and Technology, Islamabad or anywhere else in the country/ world.

At any time if my statement is found to be incorrect even after I graduate, the university has the right to withdraw my MS degree.

Name of Student: Osama Naeem

Date: 11 June 2024

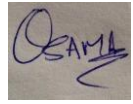
PLAGIARISM UNDERTAKING

I solemnly declare that research work presented in the thesis titled “Polyaniline Incorporated MOF Modified Anode in Microbial Fuel Cell for Enhanced Bioelectricity Generation” is solely my research work with no significant contribution from any other person. Small contribution/ help wherever taken has been duly acknowledged and that complete thesis has been written by me.

I understand the zero-tolerance policy of the HEC and National University of Sciences and Technology (NUST), Islamabad towards plagiarism. Therefore, I as an author of the above titled thesis declare that no portion of my thesis has been plagiarized and any material used as reference is properly referred/cited.

I undertake that if I am found guilty of any formal plagiarism in the above titled thesis even after award of MS degree, the University reserves the rights to withdraw/revoke my MS degree and that HEC and NUST, Islamabad has the right to publish my name on the HEC/University website on which names of students are placed who submitted plagiarized thesis.

Student Signature: _____



Name: Osama Naeem

DEDICATION

"To my very Supportive Parents and my supervisor."

ACKNOWLEDGEMENTS

I would like to begin by expressing my gratitude to Almighty **Allah** for bestowing his blessings and guiding me through this effort.

My sincere gratitude goes out to my supervisor, **Dr. Usman Liaqat**, and my co-supervisor, **Dr. Waheed Miran**, for their prompt counsel, helpfulness, and practical mindset throughout this project. It is crucial to remember that my project has only been completed because of his relentless effort. There were numerous obstacles and challenges during my investigation, but they stayed approachable and pursued me to do the task more effectively.

I would like to acknowledge the GEC members, **Dr. Zakir Hussain** and **Dr. Sofia Javed**, for their insightful insights and constructive criticism, which considerably improved the quality of this work.

A sincere thanks is extended to the **School of Chemical and Materials Engineering (SCME)** for cultivating a scholarly atmosphere that promotes outstanding performance. The department's invaluable resources, mentorship, and collaborative environment have significantly influenced the trajectory of this research undertaking.

I would like to convey my deepest appreciation to our department head, **Dr. Khurram Yaqoob**, and principal, **Dr. Amir Azam Khan**, for their unwavering commitment to the advancement of education and their exemplary leadership.

My sincere appreciation also extends to my family. Their steadfast motivation, assistance, and compassion served as fundamental components of my resilience. This accomplishment would not have been feasible without their unwavering dedication and kindness.

Osama Naeem

TABLE OF CONTENTS

ACKNOWLEDGEMENTS	IX
TABLE OF CONTENTS	X
LIST OF TABLES	XIII
LIST OF FIGURES	XIV
LIST OF SYMBOLS, ABBREVIATIONS AND ACRONYMS	XV
ABSTRACT	XVI
CHAPTER 1: INTRODUCTION	1
1.1 Background	1
1.2 MFCs Working Principle	2
1.3 MOFs	4
1.4 MFC Main Components	6
1.4.1 Anode	6
1.4.2 Cathode	7
1.4.3 Ion Exchange Membrane (IEM)	7
1.4.4 Anolyte and Catholyte	7
1.5 Types of MFCs	9
1.5.1 Single Chamber MFCs	9
1.5.2 Double Chamber MFCs	11
1.5.3 Stacked MFCs	12
1.5.4 Upflow MFCs	13
1.6 Microbial Electron Transfer Mechanism	13
1.6.1 Direct Electron Transfer (DET) Mechanism	13
1.6.2 Mediated Electron Transfer (MET) Mechanism	14
1.7 MFC Performance Evaluation	15
1.8 Factors Effecting MFC Performance	17
1.8.1 Effect of temperature	17
1.8.2 Effect of PH	18
1.8.3 Ionic Strength	18
1.8.4 Internal Resistance	19
1.8.5 External Resistance	19
1.8.6 Overpotential at the anode	19
1.8.7 Overpotential at the cathode	19
1.8.8 Anolyte Conversion Rate	20
1.8.9 Substrate Type	20
1.8.10 Inoculum	20
1.9 Applications of MFC	21
1.9.1 Electricity Generation	21
1.9.2 Biohydrogen Production	21

1.9.3	Wastewater Treatment	21
1.9.4	Remote and Off-grid Supply	22
1.9.5	Bioremediation	22
1.9.6	Desalination	22
1.9.7	Sensor and Environment Monitoring	22
1.10	Objectives	23
CHAPTER 2: LITERATURE REVIEW		24
2.1	MFCs	24
2.2	MFC Design	25
2.3	Pathway of organic matter conversion to electricity	26
2.4	Breakdown of fermentation products	26
2.4.1	Acetate	27
2.4.2	Propionate	29
2.4.3	Formate	29
2.4.4	Butyrate	30
2.5	Factors affecting MFC performance.	30
2.5.1	Anode Material	30
2.5.2	Cathode Material	33
2.5.3	Membrane	35
2.6	MFC Operational Parameters	36
2.6.1	PH	36
2.6.2	Temperature	37
2.6.3	External Resistance	38
2.6.4	Rint	39
2.6.5	Electrical Conductivity and Ionic Strength	39
2.6.6	Organic Loading	40
2.6.7	Electron Transfer Mechanism and Inoculum Type	41
CHAPTER 3: MATERIALS AND METHODS		43
3.1	Iron MOF Synthesis	43
3.2	PANI Synthesis	43
3.3	Fe-MOF/PANI Composite Synthesis	44
3.4	Preparation of anode	44
3.4.1	Hydrophilic treatment of anode	44
3.4.2	Coating of material on anode	44
3.5	Preparation of Cathode	45
3.6	Membrane pretreatment	45
3.7	Setting Up MFCs	45
3.7.1	MFC Construction	46
3.7.2	MFC Arrangement	46
3.7.3	Microbial Sludge	46
3.7.4	Anolyte	47
3.7.5	Catholyte	48
3.7.6	Operating MFC	48
3.7	Calculations and Analyses	48

CHAPTER 4: CHARACTERIZATION	50
4.1 Instruments	50
4.2 SEM	50
4.2.1 Working principle	50
4.2.2 Sample preparation	52
4.3 XRD	52
4.3.1 Working principle	52
4.4 FTIR Spectroscopy	54
4.5 CV	56
4.5.1 Working principle	57
4.6 Electrochemical Impedance Spectroscopy (EIS)	58
CHAPTER 5: RESULTS AND DISCUSSION	60
5.1 XRD	60
5.2 FTIR	61
5.3 Scanning Electron Microscope	62
5.4 Contact angle	64
5.5 Open and Close Circuit Voltage	65
5.6 Power Density	67
5.7 CV	68
5.8 EIS	71
CHAPTER 6: CONCLUSIONS AND FUTURE RECOMMENDATION	72
6.1 Conclusion	72
6.2 Future Recommendations	72
REFERENCES	74

LIST OF TABLES

Table 1.1: Basic Components of MFC [17, 18]	8
Table 1.2: Parameters for evaluating MFC performance [1, 31]	15
Table 2.1: Overview of biochemical reactions involved in the degradation of mixed end products in MFCs [66]	28
Table 2.2: Anode Materials Utilized in MFC [33, 74, 80, 83-87]	32
Table 2.3: Major Pros and Cons of Membrane and Membrane-Less MFCs [25, 53, 66, 79, 85, 89, 96-98]	35
Table 3.1: Mass Loading of Material onto GF.....	45
Table 3.2: Nutrient Medium Composition.	47

LIST OF FIGURES

Figure 1.1: Metal Organic Framework [12].....	6
Figure 1.2: Single Chamber MFC Configuration [18]	10
Figure 1.3: Double Chamber MFC Configuration [24].....	12
Figure 1.4: Stacked MFC Configuration [25].....	12
Figure 1.5: Upflow MFC Configuration [27].....	13
Figure 2.1: A) Single Chamber MFC, B) Dual Chamber MFC [60].....	25
Figure 2.2: Potential theoretical routes for electron movement within the anode section of MFCs originating from various fermentation byproducts. [66].....	27
Figure 4.1: SEM working principle [143]	51
Figure 4.2: Schematic representation of X-ray diffraction [146]	53
Figure 4.3: Schematic representation of Bragg's law [147]	54
Figure 4.4: Schematic representation FITR working [148].....	56
Figure 4.5: Cyclic voltammogram for an one-electron electrochemically reversible redox process [153].....	58
Figure 5.1: XRD Plots of Fe-MOF, PANI, PANI/Fe-MOF	60
Figure 5.2: FTIR Spectra of Fe-MOF, PANI, Fe-MOF/PANI	62
Figure 5.3: SEM images of (a) Fe-MOF (b) PANI (c) PANI/Fe-MOF (d) Bare GF (e) Fe-MOF Coated GF (f) PANI/Fe-MOF Coated GF (g) GF with attached Biofilm.....	63
Figure 5.4: Contact angle of a) Bare GF, b) Fe-MOF@GF, c) PANI/Fe-MOF@GF	64
Figure 5.5: a) OCV Bare GF MFC, Fe-MOF@GF MFC, PANI/Fe-MOF@ GF MFC, b) 1000 Ω Voltage cycle for all three MFCs.....	66
Figure 5.6: Power density and Current density Curves of all three MFCs.....	67
Figure 5.7: a) Cyclic Voltammogram of Bare GF, Fe-MOF@GF and PANI/Fe-MOF@GF, b) Cyclic Voltammogram of Bare GF MFC, Fe-MOF@GF MFC, PANI/Fe-MOF@GF MFC, c) First derivative of CV of Bare GF MFC, Fe-MOF@GF MFC, PANI/Fe-MOF@GF MFC	70
Figure 5.8: Nyquist plot of PANI/Fe-MOF@GF, Fe-MOF@GF, bare GF.....	71

LIST OF SYMBOLS, ABBREVIATIONS AND ACRONYMS

Microbial Fuel Cells	MFCs
Metal-Organic Frameworks	MOFs
Oxygen Reduction Reaction	ORR
Ion Transport Membrane	ITM
Cation Exchange Membrane	CEM
Direct Electron Transport	DET
Mediated Electron Transfer	MET
Internal Resistance	R_{int}
Open Circuit Voltage	OCV
Maximum Power	P_{max}
Coulombic efficiency	CE
Chemical Oxygen Demand	COD
Electrochemically Active Bacteria	EAB
Bio-electrochemical Systems	BES
Polytetrafluoroethylene	PTFE
Organic Loading Rate	OLR
Extracellular Electron Transfer	EET
Cyclic voltammetry	CV
Electrochemical Impedance Spectroscopy	EIS

ABSTRACT

Microbial fuel cells (MFC) are acknowledged as a highly promising device for generating environmentally friendly and sustainable electricity. The anode plays a crucial role in the electricity generation process in MFC. The microorganisms in the anodic chamber undergo oxidation of organic substrates, resulting in the release of electrons and protons. Subsequently, these electrons are transferred to the surface of the anode, resulting in the generation of an electric current. When protons originating from the anode traverse a proton exchange membrane (PEM) and electrons flowing through an external circuit react with oxygen to produce water at the cathode, the electrochemical circuit is finalized. Utilizing polyaniline/Fe-MIL-88B-NH₂ (PANI/Fe-MOF) as an anode material shows great potential in enhancing MFC performance. Fe-MOF is a material that possesses a substantial surface area and can have its chemical properties tuned. The objective is to optimize the catalytic properties of Fe-MOF to enhance the performance of MFCs. This will be achieved by depositing Fe-MOF onto the surface of the anode, thereby accelerating electron transfer. PANI can enhance the redox activity, stability, and conductivity of the electrode surface. The Fe-MOF is synthesized using a room temperature synthesis approach, and then the PANI is polymerized in-situ to form a composite of PANI/Fe-MOF. The MFC operated using the PANI/Fe-MOF@Graphite Felt (GF) anode, exhibited the highest power density of 277 mW/m² and a maximum output of 319 mV at an external resistance of 1000 Ω. This surpassed the power density and output voltage of both the Fe-MOF@GF (154 mW/m², 202 mV) and the unmodified GF (45 mW/m², 161 mV). The enhanced performance can be ascribed to the material's reduced charge transfer resistance (R_{ct}) in conjunction with its boosted affinity for bacteria, leading to an augmented efficiency in extracellular electron transfer (EET). This study demonstrates that the PANI/Fe-MOF composite exhibits promising potential as an anode for power generation in MFCs.

Keywords: Microbial Fuel Cell, Bioelectricity, Metal-organic framework, Fe-MIL-88B-NH₂, Polyaniline, MFC Power Density, Bio electrochemical System.

CHAPTER 1: INTRODUCTION

1.1 Background

Microbial Fuel Cells (MFCs) are an area of research in sustainable energy that shows great potential. They integrate the fields of microbiology, electrochemistry, and environmental engineering. Potter (1911) first proposed the concept of generation of electric current by harnessing the metabolic activity of microorganisms. Significant advancements have been made in understanding and improving MFCs for a range of applications, such as energy generation, wastewater treatment, and carbon emission reduction

The need for advancing clean and sustainable technology has been highlighted by the pressing global issues of escalating energy consumption, water scarcity, and climate change. MFCs use microorganisms' innate metabolic skills to transform organic molecules into electrical energy, offering a unique approach [1]. This strategy not only promotes the generation of renewable energy but also addresses the interconnected issues of wastewater treatment and carbon emissions.

MFC operates primarily on the ability of microbes, usually bacteria, to break down organic substances through their metabolic processes. During the oxidation process, electrons are released, and the MFC harness these electrons to generate an electric current [2]. MFCs are a dynamic technology capable of producing power by combining microbial metabolism with electrochemical processes. At first, MFC designs utilized simple organic substrates like acetate and glucose. Nevertheless, recent advancements have expanded the potential by enabling the utilization of more complex waste materials as substrates [3].

MFCs not only produce electric current but also offer an innovative approach to wastewater treatment. MFCs utilize microorganisms to decompose organic pollutants in water, resulting in the generation of electricity and the elimination of contaminants, thereby purifying the water. The dual functionality of MFCs aligns with the principles of green engineering, which seek to integrate the treatment of environmental pollutants with the generation of valuable resources [4].

Moreover, MFC aids in mitigating carbon emissions by providing an environmentally friendly alternative to conventional methods of energy production. Converting organic waste into electricity aids in mitigating the release of methane, a potent greenhouse gas, which is generated

during traditional wastewater treatment methods [5]. This facet of MFC technology centers on the global imperative to reduce carbon footprints and transition to sustainable energy methods.

Scientists have concentrated their efforts on enhancing the MFC's performance, specifically regarding the materials utilized for the electrodes, due to the wide variety of applications. Recent researches have investigated the use of Metal-Organic Frameworks (MOFs) as anodes in MFCs to enhance the production of bioelectricity [6]. This is achieved by improving the efficiency at which electrons are transferred and increasing the attachment of microorganisms on anode surface.

1.2 MFCs Working Principle

MFCs harness the unique metabolic abilities of microorganisms to generate electricity through the integration of microbiology and electrochemistry. MFCs operate by utilizing the microbial oxidation of organic substances, resulting in electron transmission from microbial cells to an external circuit, ultimately producing electrical energy. The MFC consists of two separate compartments, namely a cathode chamber and an anode chamber, which are separated by an ion-selective membrane [1]. One part of the reaction takes place in anodic chamber which usually involves the microbial oxidation, and the other half of the reaction takes place in cathodic chamber which usually involves the reduction reaction. The microorganisms employed in MFCs, typically electrogenic bacteria, primarily serve the purpose of producing and subsequently transferring electrons because of their extracellular electron transfer (EET) capability.

The process of microbial oxidation begins when bacteria metabolize organic substrates in the anode chamber. Electrons are produced as secondary products of the microbial respiratory chain during this metabolic process. In the conventional cellular respiration process, the electrons are directly utilized by an electron acceptor that is typically located within the same compartment. However, in an MFC, there is an intentional lack of an external electron acceptor in the microbial environment. This causes the release of electrons into the extracellular space.

In a MFC, bacteria utilize the surface of the anode as a substrate for growth and attachment, resulting in the formation of a dense bacterial community known as a biofilm. The electroactive biofilm acts as a channel that links the microbial cells to the anode, allowing electrons to pass more

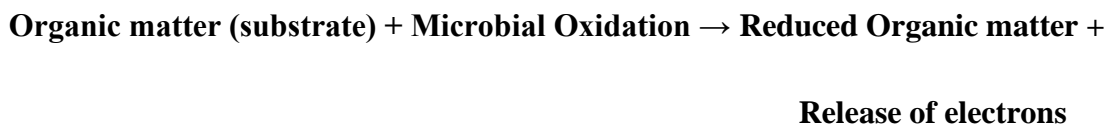
efficiently from the bacteria's outer membrane to the anode's surface. Electrons that have been released from the outer cell membrane of electrogenic bacteria travel through the conductive structure of the anode, typically made of materials like carbon fiber or graphite, leading to the development of an electrically conductive biofilm on the anode's surface [2]. When the electrons reach the anodic interface, they flow via the external circuit, generating an electric current. This electric current can subsequently be utilized for various purposes.

Simultaneously, in the cathode chamber, a corresponding reduction reaction occurs. The typical cathodic electron acceptor used is oxygen or another oxidizing agent. Water or other reduced compounds are created at the cathode when protons and electrons from the external circuit combine with the cathodic electron acceptor, completing the electrochemical circuit.

The proton exchange membrane (PEM), positioned between the cathodic and anodic chambers, acts as a barrier that only allows the movement of protons generated during microbial oxidation while blocking the flow of electrons. The selective transport of protons is essential for maintaining electrical equilibrium in both compartments and ensuring the continuous flow of electrochemical reactions

General Chemical reaction of chambers is as follow:

At the Anode:



At the Cathode:



The fundamental concept of MFCs involves harnessing the innate metabolic processes of microorganisms to produce electricity in a sustainable manner. As research progresses in investigating methods to improve the overall output of MFCs, specifically by modifying the anode

materials to enhance their conductivity through the exploration of materials such as MOFs, the potential of MFCs as a feasible and environmentally friendly energy source becomes more evident.

1.3 MOFs

A new family of porous materials known as metal-organic frameworks (MOFs) or porous coordination polymers (PCPs) is made up of organic linkers and metal-containing nodes (as shown in Fig 1.1), sometimes known as secondary building units, or SBUs [7]. Ditopic or polytopic organic carboxylates (and other comparable negatively charged compounds) are the organic units utilized. These units combine to create structurally robust crystalline MOF structures when they are joined with units that contain metal. These structures usually have a porosity that exceeds 50% of the volume of the MOF crystal [8]. The ability to be designed and the capability to have finely adjustable and their uniform pore structures make them extremely promising materials for a variety of applications. Typically, MOFs can be readily created and produced by combining different organic ligands with metal ions or components due to the combined behavior of the functional units [9].

Nevertheless, the majority of MOFs possess inherent insulation properties as a result of the presence of low-energy barriers to charge transfer and the lack of free charge carriers. These characteristics significantly limit their potential for electrochemical applications. The electrical conductivity of MOFs can enhance their catalysis efficiency and electrochemical process and. Furthermore, these materials can be effectively utilized in various applications such as secondary batteries, sensors, and electrochemical devices. Many conductive MOFs have been produced recently using techniques such composite formatting, post-synthesis modification, and guest molecule introduction [10].

Furthermore, through the utilization of the cooperative advantages of functional units, the deliberate integration of MOFs with other functional materials such as graphene, semiconductors, or conductive polymers holds the promise of generating advanced composites that exhibit superior performance compared to the performance of each individual component. Polyaniline (PANI) and Polypyrrole are two examples of conductive polymers, which are functional materials. This scenario may occur when the MOFs are integrated with other functional materials.

These compounds can be classified as a subclass of coordination polymers and can be further organized into one-dimensional, two-dimensional, and three-dimensional structures. MOFs are categorized into mesoporous, nanoporous and macroporous materials based on the size of their pores. Typically, the last two mentioned are amorphous. MOFs show remarkable properties that can be linked to the existence of coordination bonds, including considerable porosity, a substantial specific surface area, and exceptional thermal stability. The pores of the material can accommodate various types of molecules, including neutral molecules like anions, solvent molecules and cations. Depending on the MOF's total charge, certain molecules, such as gas molecules and biomolecules, may be integrated.

The coordination bonds that develop between metal ions and organic ligands are referred to as molecular interactions. Conversely, weak interactions such as hydrogen bonds and π - π interactions are included in the category of intermolecular interactions [10].

Reaction duration, temperature, solvent selection, organic ligand and metal ion properties, nodal size and structural characteristics, the presence of counterions, and crystallization kinetics which control nucleation and crystal growth all have an impact on the synthesis of MOFs. Usually, liquid phase solutions of the ligand and metal salt are combined to synthesize MOFs. Each reaction's activation energy and thermodynamics are significantly influenced by the solvent. Typically, MOFs are created through solvo (hydro)thermal synthesis, which involves subjecting them to high temperature and pressure conditions. This is the conventional approach for synthesizing MOFs. In recent years, various alternative synthetic methods, including sonochemical methods mechanochemical, microwave, and, electrochemical have also been developed [11].

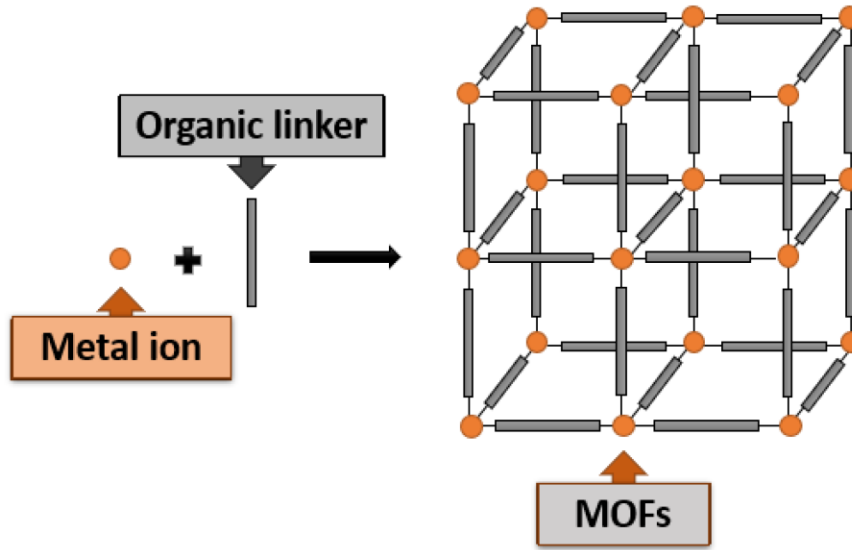


Figure 1.1: Metal Organic Framework [12]

1.4 MFC Main Components

The primary constituents of MFC that had an impact on their performance are concisely outlined below and presented in Table 1.1. The performance of MFCs is greatly influenced by their structural characteristics. The availability of the substrate, temperature, the microbial species or community employed, the anolyte's composition, and the materials utilized for the MFC's anode, cathode, and separator are other variables that impact how well the device's function.

1.4.1 Anode

An important constituent is the anode, where the process of oxidation and electron generation occurs. Stable biofilm is formed by the attachment of bacteria onto the anode surface and it depends upon properties of anodic materials. Efficient electron transfer requires the establishment of a stable biofilm. Additionally, it must possess biocompatibility with the electroactive microbes and exhibit improved electron conductivity. Furthermore, the anode material must possess characteristics such as robust mechanical strength, resistance to corrosion, and chemical stability. Typically, the roughness of the anode materials is intentionally increased to promote the attachment of bacteria, thereby enabling higher power density. Furthermore, the increased surface roughness strengthens the electrode's resistance to swelling and breakdown brought on by the redox condition [13].

1.4.2 Cathode

At the cathode, a reduction reaction takes place. The MFCs power density and electrochemical performance are greatly impacted by the cathode material selection. The oxygen reduction reaction (ORR) normally occurs at the cathode, where it functions as the reaction that sets a limit on the cathode's total rate. Selecting the right cathode is essential since it affects the ORR directly.

Air cathodes and aqueous air cathodes, which may or may not include catalysts, are the two main types of cathodes. These days, the most common catalysts are titanium and platinum [14].

1.4.3 Ion Exchange Membrane (IEM)

Membranes serve as the physical barriers that separate the anodic and cathodic chambers. Membranes are essential to the development of MFCs. Membranes allow protons to travel more easily but prevent oxygen from diffusing. Additionally, the membranes help with ionic and chemical conjugation. Nevertheless, the obstacles related to membranes include their high cost, fouling, and rise in internal resistance.

The selection of a membrane for the separation of the cathode and anode entails a choice between two competing interests: (i) Enhanced proton selectivity improves the efficiency of the MFC cell and diminishes membrane resistance. (ii) Membranes must exhibit exceptional stability to cope with the challenges of a colloidal and nutrient-rich environment.

IEMs can be categorized into three groups based on the kind of ion transport they facilitate: Cation Exchange Membrane (CEM), Bipolar Membrane (BPM) and Anion Exchange Membrane (AEM) [15].

1.4.4 Anolyte and Catholyte

The main emphasis of the MFC biological phenomena is on the anodic chamber. Anolytes of various kinds are employed in MFC, comprising unique exo-electrogens derived from either pure or mixed cultures. Studies on MFC also show the use of biofilm electrodes and other substances that work together to improve performance, particularly in terms of current density or power density

The substrates frequently used in MFCs encompass starch, glucose, sodium formate, acetate, lactate, urban wastewater, and artificial wastewater, among other options. When these substrates encounter suitable bacteria (inoculums), they decompose the substrate to produce.

Positively charged particles and negatively charged particles. Oxygen has been widely used as a catholyte in most studies on MFCs due to its unlimited ability to accept electrons. The redox potential is distinguished by its accessibility and elevated standard. Ferricyanide, potassium permanganate, and manganese dioxide are frequently employed as cathodic electron acceptors in two-chambered MFC [16].

Table 1.1: Basic Components of MFC [17, 18]

Items	Materials	Remarks
Anode	carbon paper, Graphite, reticulated vitreous carbon (RVC) carbon-cloth (CC), graphite felt (GF), Pt, Pt black	Necessary-Must be noncorrosive, chemically stable, conductive, biocompatible, and non-toxic
Cathode	RVC, GF, Pt black, carbon paper, Pt, Graphite, CC	Necessary
PEM	Nafion, polyethylene, Ultrex, porcelain septum, Salt bridge, Poly(styrene-co-divinylbenzene), or solely electrolyte	Permeable to O ₂ , ferricyanide, organic matters (drawbacks), ions, Optional,
Electrode Catalyst	Pt, Fe ³ , PANI, MnO ₂ , Pt black	To overcome high overpotential for O ₂ reduction, Optional
Anodic Chamber	Plexiglass, Glass, polycarbonate	Necessary

Cathodic Chamber	Polycarbonate, plexiglass, Glass,	Not Necessary
-------------------------	-----------------------------------	---------------

1.5 Types of MFCs

MFCs have experienced significant diversification in their design and configuration to improve their performance for various applications. MFCs can be categorized based on their structural characteristics, operational parameters, and usage.

Understanding treatment orate distinctions of each category is essential for tailoring MFCs to meet precise needs, such as maximizing energy generation, enhancing wastewater treatment, or exploring novel biotechnological applications biotechnological uses. substrate [17].

1.5.1 Single Chamber MFCs

In comparison to the double-chamber configuration, the MFC single-chamber configuration is somewhat simpler. The system consists of an air-cathode that is exposed to air and an anode that is housed in an anodic chamber (as shown in Fig 1.2) [19]. In this arrangement, the electron is transported from the anode through the external circuit to the cathode following anaerobic digestion.

At the cathode, oxygen from the surrounding air then absorbs the electron. The IEM is placed near the inner surface of the cathode. Protons are better able to pass to the cathode when a membrane and a porous cathode are present, as this stops oxygen from diffusing into the anodic chamber [20].

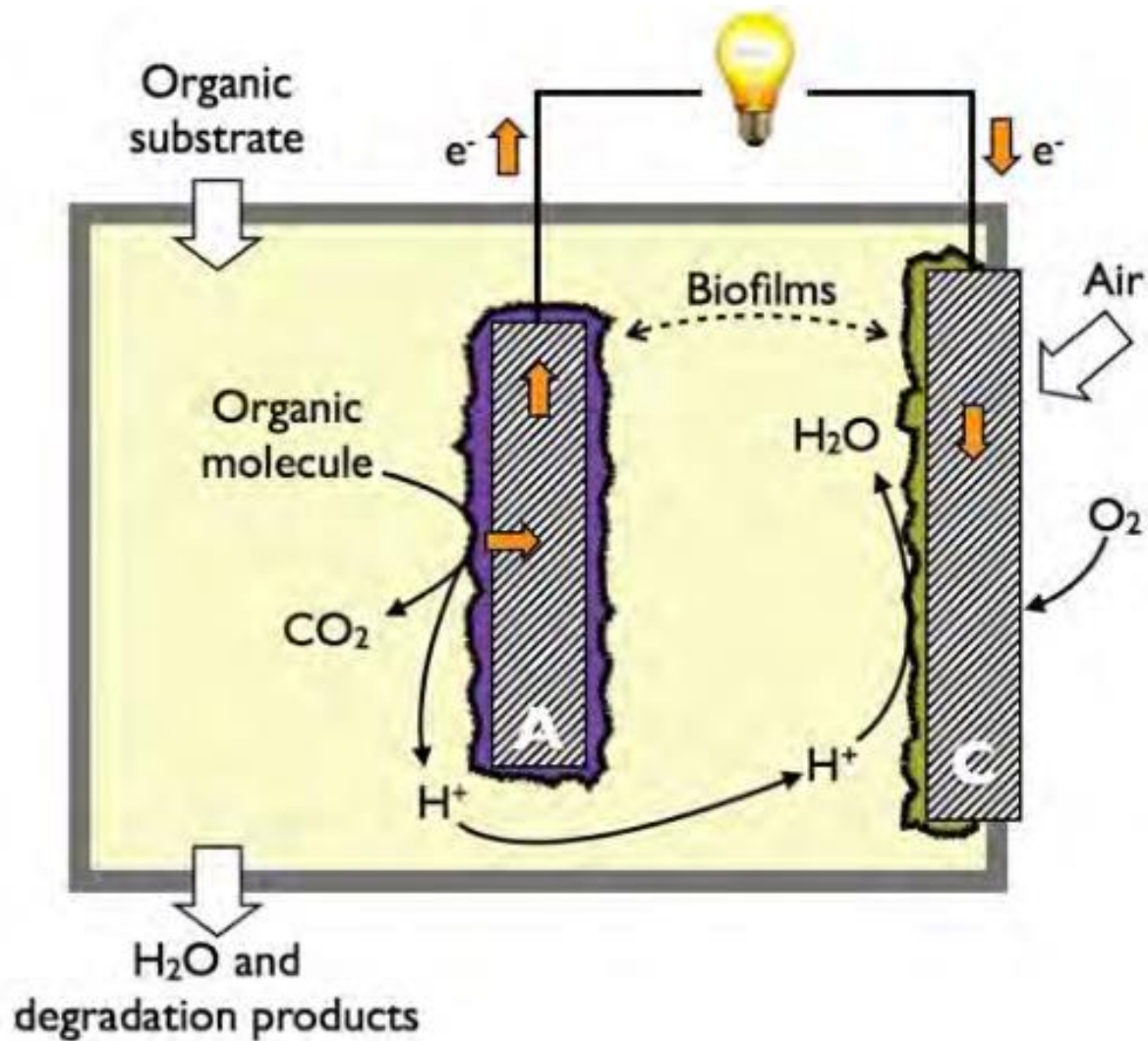


Figure 1.2: Single Chamber MFC Configuration [18]

The lack of a cathodic chamber makes this construction more cost-effective. Furthermore, it does not require the introduction of oxygen into the catholyte. The single-chamber structure has lower internal resistance, greater oxygen reduction at the cathode, and enhanced power production.

Nevertheless, there exist certain constraints to this configuration when it comes to commercial applications. It is not possible to increase the volume of the chamber while maintaining a small electrode spacing, which results in a decrease in power density when the set-up is expanded [21].

1.5.2 *Double Chamber MFCs*

Dual-chamber MFCs consist of two chambers, one anodic and one cathodic, which are separated by membranes (as shown in Fig 1.3) [22]. The microorganisms in the biofilm on the anode within the anodic chamber perform anaerobic digestion of the substrate, generating electrons.

The external wire transports electrons to the cathode, whereas the membrane transports protons. The ORR occurs at the cathode. The cathodic compartment requires continuous oxygen supply.

The double-chamber MFCs have been adapted and investigated in various configurations, such as cylinder type, flat plate type, H-type, tubular type, and so on. These modifications have been implemented to optimize the operational efficiency of large-scale operations [23].

The H-type MFCs exhibit diminished proton transfer because of their reduced surface area. Consequently, they exhibit reduced power density. Conversely, flat plate-type MFCs offer a greater membrane surface area, which enhances the transfer of protons. Furthermore, it decreases the distance between the electrodes, resulting in a decrease in internal resistance [19].

Tubular MFCs have also become a viable choice for large-scale operations. Double-chamber MFCs offer a significant benefit in their ability to be utilized for the large-scale treatment of wastewater to generate energy.

The necessary operational parameters for scaling up include maintaining an appropriate pH level, ensuring sufficient oxygen availability, reducing internal resistance, and adding electron mediators [20].

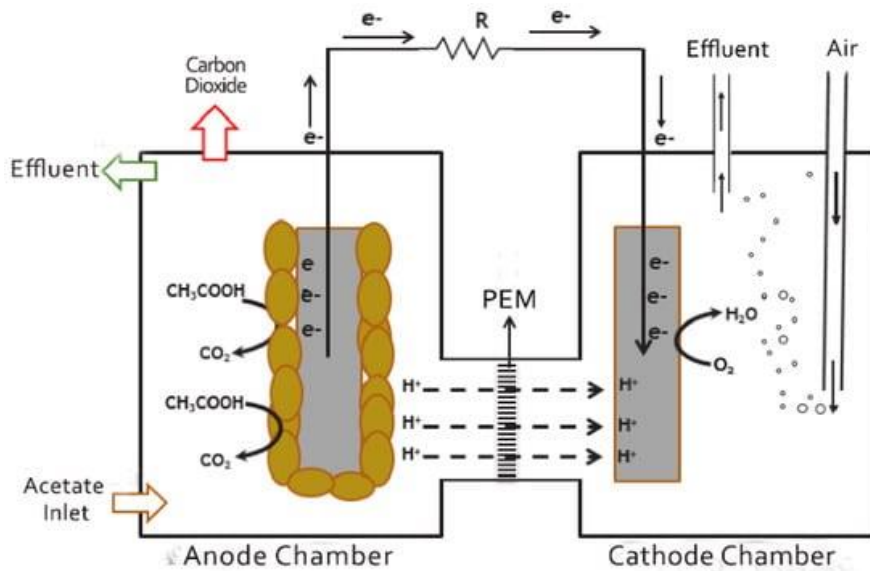


Figure 1.3: Double Chamber MFC Configuration [24]

1.5.3 Stacked MFCs

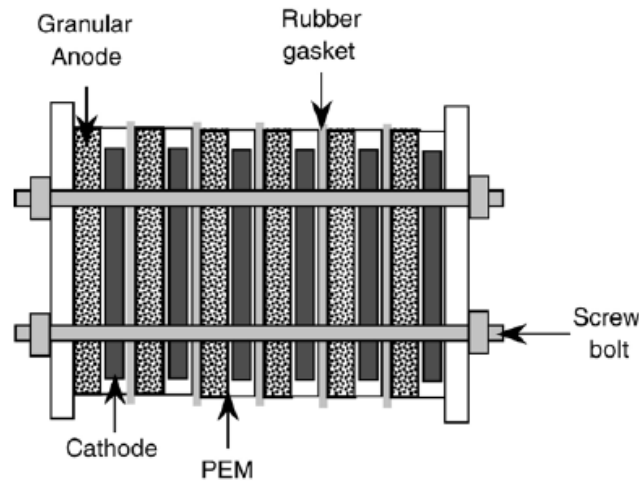


Figure 1.4: Stacked MFC Configuration [25]

Another form being studied is stacked MFC. In this design, the MFCs can be connected in series or parallel (as shown in Fig 1.4). This study intends to maximize power generation and improve pollutant removal efficiency in wastewater treatment [22]. The series connection enables a higher voltage and a shorter treatment duration. Conversely, a parallel connection enhances both the magnitude of electric current and the amount of power per unit volume. The MFCs can be connected either horizontally or vertically [20]. The primary constraints of this arrangement are

voltage reversal and a significant initial investment. Once these problems are addressed, this method has the potential to serve as a viable option for efficiently treating wastewater and generating power on a large scale [19].

1.5.4 Upflow MFCs

Upflow MFCs are a new class of microbial electrochemical devices designed especially to generate electricity and improve wastewater treatment. This configuration makes use of the benefits of upflow operation, in which incoming wastewater is directed upward via the anode chamber (as shown in Fig 1.5), promoting efficient microbial activity and substrate utilization [26].

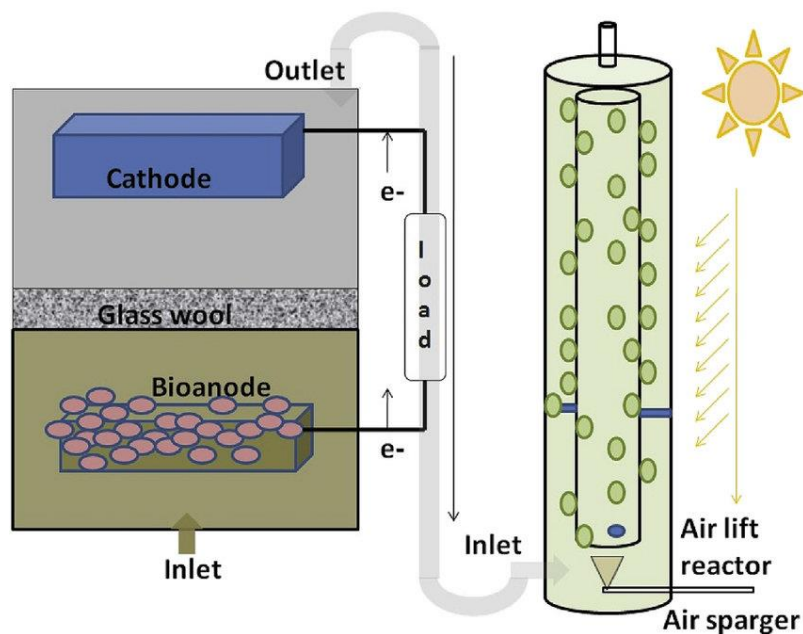


Figure 1.5: Upflow MFC Configuration [27]

1.6 Microbial Electron Transfer Mechanism

There are various ways in which electron transfer occurs between microorganisms and conductive solid surfaces.

1.6.1 Direct Electron Transfer (DET) Mechanism

In this method, electrons are directly passed from material bacterial membrane to electrode material. There should be enough physical contact between electrode material and the microbial

cell membrane. Research has shown that *Rhodospirillum rubrum* sp., *Shewanella* sp., and *Geobacter* sp. have excellent DET efficiency [28]. In general, redox elements that are dissolved do not participate in electron transfer when direct electron transfer occurs. The processes of self-assembled attachments, conductive pili known as nanowires, and outer/external membrane cytochromes all contribute to somewhat direct electron transfer. Transferring electrons to an external terminal electron acceptor such as the anode of a MFC is facilitated by redox proteins. Microbial cells have C-type cytochromes, also referred to as redox proteins, on their outer membrane. DET was found to be possible with the use of multiheme proteins and c-type cytochromes. The main drawback of this process is that electron transfer cannot take place until bacteria attach themselves to the anode's surface and form a biofilm. Most gram-positive bacteria are believed to engage in DET by forming a biofilm using teichoic acid. This compound enables the bacteria to adhere to the surface of the anode through direct contact [28, 29].

1.6.2 Mediated Electron Transfer (MET) Mechanism

Many microorganisms are unable to undergo direct electron transfer when they are not in contact with the anode surface. In such cases, they can utilize an alternative method known as mediated electron transfer, where the transfer of electrons is facilitated by a mediator. This process transfers electrons to the terminal electron acceptor by means of a redox carrier that serves as a transporter. In this process, redox mediators collect electrons from the microbial cell and transfer them to the anode material in a reduced state. The MFCs then undergo oxidation of the anode material. The following process of electron transfers could be started by the oxidized stages of electrons. Certain properties are crucial for effective mediators: the ability to be reversibly oxidized and reduced, they should be able to penetrate microbial surfaces, be non-toxic to microorganisms, dissolve in the anolyte solution, be readily available, inexpensive, and generate sufficient redox potential to facilitate electron transfer [28]. Exogenous or endogenous redox mediators can be found, depending on the factor under consideration. Redox mediators, also referred to as endogenous mediators, are created by the microbes themselves. Exogenous mediators are compounds that can be added externally, such as redox mediators [29].

1.7 MFC Performance Evaluation

When assessing MFCs, it is crucial to consider their ability to generate voltage and treat organic wastes. Both aspects play a significant role in their overall evaluation. A brief discussion of the parameters that are frequently used to evaluate MFC performance is provided in Table 1.2. From these parameters maximum power (P_{max}), open circuit voltage (OCV), internal resistance (R_{int}) can be determined using the polarization curve. By utilizing a potentiostat or multiple resistors to measure the current at different voltages, a polarization curve may be used to show the relationship between voltage and current. The relationship between the cell potential and the current is shown by a polarization curve.

$$E_{cell} (V) = OCV (V) - I (A) \cdot R_{int} (\Omega)$$

R_{int} is the slope of the polarization curve. Power (P) is calculated as

$$P (W) = I (A) \cdot E_{cell} (V)$$

As a result, the polarization curve can be used to determine the power curve. Numerous elements, including the substrate type, mediator type, exoelectrogen type, reactor configuration, anode and cathode materials, and environmental parameters like pH level and temperature, affect the power density in MFC [1, 30].

Table 1.2: Parameters for evaluating MFC performance [1, 31]

Parameter	Unit	Description
OCV	V	OCV refers to the highest voltage generated in MFC when there is no current flowing between the anodes and cathodes.
Coulombic efficiency (CE)	Ω	The quantification of the overall internal losses in an MFC process can be achieved by calculating the gradient of the polarization curve.

CE	%	CE is determined by quantifying the quantity of charge (measured in coulombs) that is transferred during an electrochemical reaction and comparing it to the theoretical charge that could be generated based on the substrate used. (estimated from the total chemical oxygen demand (COD) value).
Power density (per volume)	W m^{-3}	Power density per unit volume in an MFC refers to the amount of electrical power produced by the MFC relative to the volume of the reactor.
Power density (per area)	W m^{-2}	The power output is standardized by normalizing it to either the area of the anode or the area of the cathode. The Pmax value is commonly employed. When the structure of an electrode is complex (such as being made of felt or cloth), a projection area is used instead of a physical surface area.
Current density	A m^{-2}	Current density in a MFC refers to the amount of electrical current produced per unit area of the electrode surface.
Loading rate	$\text{Kg m}^{-3} \text{d}^{-1}$	An efficiency evaluation index for MFC as a waste treatment method. The quantity of organic matter, quantified as (COD; kg), that is added to the MFC is modified to consider the total volume of the anode (m^3) and the time period (d).
Effluent quality	kg m^{-3}	The effluent released from the anode chamber contains a measure of the concentration of organic compounds, specifically measured as COD.

Treatment efficiency	%	COD-removal efficiency, also referred to as chemical oxygen demand removal efficiency, is determined by dividing the concentration of COD in the effluent by the concentration of COD in the influent.
Energy efficiency (EE)	%	The energy-recovery process of the MFC is assessed by determining the ratio of power produced by the MFC to the heat energy acquired from the combustion of the added substrates. The ratio plays a pivotal role in assessing the effectiveness of the MFC process.
Rint		The determination of the Rint of the MFC system involved analyzing the gradients of polarization curves. This entailed calculating the ratio of the change in voltage to the change in current intensity for the corresponding polarization curve, which mainly indicates ohmic losses.

1.8 Factors Effecting MFC Performance

The generation of electricity in a MFC is influenced by both electrochemical and biological processes. The following are the crucial parameters for optimizing electroactive biofilms, along with a concise discussion on their significance.

1.8.1 Effect of temperature

The temperature is an important factor in the process of generating electricity. The temperature of the anolyte regulates the metabolism of electrochemically active bacteria EAB by modulating the enzymatic reactions [32]. Every enzyme has a range of temperatures where it functions at its best and produces the most. The high temperatures would denaturize the enzymes necessary for life support and metabolism. The operation temperature had a significant impact on the change in the microbial community and metabolic processes. It was noticed that an increase in temperature from 30 to 40 °C led to an 80% increase in current generation [33, 34].

1.8.2 Effect of PH

Microorganisms require a specific pH range for their survival, so any difference in acidity or alkalinity between the cathode and anode negatively impacts their growth and activity [35]. A pH outside of the appropriate range considerably inhibits the activity of microorganisms. For example, pH variations can cause changes in the charge that biological macromolecules like proteins and nucleic acids carry, which can affect how they function biologically. Similarly, the electrical charge of cell membranes can cause disruptions in the ability of microbial cells to absorb nutrients [36]. Determining the ideal pH values for both electrogenic and degrading bacteria depends on how well the microbes in a bioelectrochemical system (BES) adapt to different pH situations.

Hence, the pH level of the anolyte plays a crucial role in BESs as it directly regulates the production of electrons and protons, thereby impacting the metabolic activity of the microbes that are specific to the substrate. An optimal condition for achieving higher electricity generation and organic matter removal is to have a neutral pH at the cathodic side and a slightly alkaline pH (around 7.5) at the anodic side [37].

1.8.3 Ionic Strength

Higher solution ionic strength/conductivity can decrease R_{int} and improve power generation. The power output of a single-chambered air-cathode MFC increased from 720 to 1330 mW/m^2 when the solution's ionic strength was raised from 100 to 400 mM by adding NaCl [38]. Alongside this rise in power production, the solution conductivity increased from 10 to 40 mS/cm. By raising the phosphate buffer solution's concentration from 50 mM (7.5 mS/cm) to 200 mM (20 mS/cm), power output was improved. Nevertheless, exceeding a solution conductivity of 40 mS/cm had an adverse impact on the performance of the MFC. The decline in power generation at the significantly elevated solution conductivity was caused by an augmented overpotential of the anode, leading to a reduced circuit voltage. This suggests that the high salinity suppressed bacterial activity [39, 40].

1.8.4 Internal Resistance

The internal resistance is determined by the combined resistance of the electrolyte between the electrodes and the resistance of the membrane. To achieve maximum efficiency, it is necessary to position the anode and cathode in close proximity to each other. Furthermore, the migration of protons has a substantial impact on losses related to resistance. However, these losses can be minimized by ensuring proper mixing [41].

1.8.5 External Resistance

It is an essential electrical component in power generation that controls the correlation between the electric current and the operating voltage. The attainment of maximum power output is contingent upon the alignment of the external resistance with the internal resistance of MFC. The presence of external resistance can affect the microbial composition of the anodic biofilm. Using an external resistance that is equal to or lower than the internal resistance can promote the development of biofilm and maximize the power generation of MFCs. [42, 43].

1.8.6 Overpotential at the anode

The performance of anodes in a MFC is influenced by several factors, such as the electrode's surface characteristics, its electrochemical properties, electrode potential, as well as the kinetics and mechanism of electron transfer and current flow. [44].

1.8.7 Overpotential at the cathode

The losses in the cathode compartment are caused by overpotentials, like those in the anodes. Even minimal electric currents passing through the surface of the electrode require careful consideration due to the associated losses. To reduce the activation overpotentials, it is necessary to introduce catalysts to the electrode or employ a suitable mediator to facilitate the transfer of electrons from the cathode to oxygen. In order to achieve sustainability, it is preferable for MFC cathodes to be open-air cathodes [45].

1.8.8 Anolyte Conversion Rate

The result depends on various factors, including the quantity of bacterial cells, the mechanisms of mixing and mass transfer in the reactor, the kinetics of the bacteria, the rate at which organic material is loaded onto the biomass [22], the efficiency of the proton exchange membrane in moving protons, and the electrical potential across the microbial fuel cell [44].

1.8.9 Substrate Type

The power generated by MFCs is primarily influenced by the characteristics of the substrate [46]. Basic forms of substrate, such as sucrose, acetate, and glucose, are more readily broken down and generate higher power output compared to complex organic substrates, such as real wastewater. Acetate is frequently utilized as a substrate because it is inert towards other biological conversion mechanisms, such as fermentations. Additionally, it serves as the final result of multiple metabolic pathways that break down intricate organic substances [39, 47].

1.8.10 Inoculum

The function of the BES can be achieved by employing either a homogeneous strain or a combination of bacteria. Bacterial strains that are free from impurities can be separated and concentrated from the anode of a BES or selected based on their known ability to produce electricity. Utilizing a genetically homogeneous bacteria strain in a MFC is highly advantageous for investigating the mechanism of electron transfer [48, 49]. Studies have shown that the electron transfer efficiency of MFC systems composed of a single species of bacteria is higher compared to MFCs that contain a combination of different bacteria. Moreover, the introduction of domesticated electrogenic bacteria into a BES can augment the electrical output of the system in challenging circumstances. In practical application, we can employ indigenous microorganisms to directly oxidize the substrate and transfer the electrons to the anode, leading to a simple and economical process. Furthermore, employing a combination of different inoculants can effectively reduce the accumulation of metabolites on the anode. This could be due to the microorganisms utilizing diverse carbon sources and deriving advantages from a synergistic interaction [37].

1.9 Applications of MFC

Despite being in its early stages, MFC technology holds promise due to its numerous distinctive attributes. Although MFCs have been studied as a prospective alternative energy source, their current applications are limited to specific markets. The subsequent sections address the main areas of primary importance concisely:

1.9.1 Electricity Generation

MFCs are primarily utilized to produce electricity through the process of oxidizing organic substrates. Various organic waste streams have been researched as fuel sources for MFCs, demonstrating their capacity for decentralized and sustainable electricity production [1].

1.9.2 Biohydrogen Production

Modifying MFCs allows for the simultaneous production of electricity and hydrogen. During typical operation, protons generated by the anodic reaction migrate towards the cathode, where they combine with oxygen to create water. The thermodynamics of hydrogen production in a MFC is unfavourable. Nevertheless, in an MFC circuit, if an external potential is applied to raise the cathode potential and surpass the thermodynamic obstacle, the protons and electrons generated by the anodic reaction merge at the cathode to produce hydrogen.

1.9.3 Wastewater Treatment

MFCs offer a twofold benefit in the treatment of wastewater: they effectively eliminate organic pollutants while simultaneously generating electricity. Microbial oxidation at the anode facilitates the breakdown of organic materials in wastewater, providing a sustainable approach to water filtration [50].

MFCs have the potential to reduce the electricity consumption in wastewater treatment by half compared to conventional methods that require a significant amount of power for aerating activated sludge. MFCs produce a significantly reduced amount of solid waste, ranging from 50 to 90% less, that needs to be disposed of [51, 52].

1.9.4 Remote and Off-grid Supply

MFCs are suitable for remote and off-grid power supply applications due to their adaptability in various operating conditions. MFCs have the potential to serve as a reliable and environmentally friendly energy solution in areas lacking reliable access to traditional power sources. This is achieved by utilizing locally available organic waste as a fuel source [53].

1.9.5 Bioremediation

The MFC technology has been researched for the purpose of in-situ bioremediation of polluted soils, sediments, groundwater, and surface water resources. This is a biodegradation process carried out by a naturally occurring microbial community in streams, which has the ability to break down pollutants into less harmful substances [54]. The use of bioelectroremediation, a form of bioremediation performed in microbial fuel cells (MFCs), offers economic benefits compared to conventional technologies like mycoremediation, phytoremediation, and bacterial bioremediation. This is because bioelectroremediation allows for energy production and can enhance bioremediation rates by utilizing certain pollutants in the system [55].

1.9.6 Desalinisation

The MFCs possess the capability to simultaneously carry out desalination, wastewater treatment, and energy production. To achieve this, a supplementary chamber is incorporated into a standard DC MFC configuration, positioned between the anodic and cathodic chambers. The chambers are divided by an AEM and CEM [55, 56].

1.9.7 Sensor and Environment Monitoring

Research has been conducted on the utilization of MFCs for supplying energy to sensor networks and environmental monitoring equipment. MFCs have the ability to function autonomously and for long durations as a result of continuous microbial processes. This characteristic makes them suitable for situations where regular maintenance is challenging difficult [57].

In summary, MFCs have demonstrated their efficacy in various applications, such as wastewater treatment, remote power supply, environmental monitoring, and electricity generation.

The ongoing research in this field continues to seek innovative methods to enhance the performance of MFCs and expand their scope of practical applications.

1.10 Objectives

The objective of this research work is as follows:

- Synthesis of a **conductive MOF and its composite** as an anode material
- Enhancing the active surface area of the anode to promote greater bacterial attachment.
- Increasing microbe-anode interaction by forming dense and robust biofilm.
- Enhancing the interaction between electroactive microorganisms and the modified anode to boost the process of electron transfer thereby amplifying power output

CHAPTER 2: LITERATURE REVIEW

2.1 MFCs

MFCs are incredibly efficient bio electrochemical systems that belong to a special category of alternative energy-harnessing devices. They have the potential to significantly reduce pollutants through microbial metabolic activities [58]. What sets them apart is their ability to generate environmentally friendly energy while simultaneously addressing waste management. Thus, MFCs serve a dual purpose.

Utilizing MFC-assisted food waste treatment has the capacity to convert our present energy requirements into future energy production. The benefits of MFCs as an environmentally friendly waste treatment method are as follows: (a) turning substrate energy into electricity with high efficiency, (b) producing less sludge than aerobic processes, (c) operating efficiently in a variety of settings, and (d) eliminating the need to treat off gasses. (e) lower energy demand for aeration, and (f) broader applicability, particularly in distant areas with poor electrical infrastructure. However, MFCs still face various challenges, such as problems with generating voltage, expensive electrode materials, slow reaction rates, limitations in efficiency, and losses caused by polarization. [59].

The MFC is a bio electrochemical device that consists of an anaerobic chamber where substrate oxidation takes place, and an aerobic chamber that is physically separated from the anaerobic chamber by a separator or membrane.

In the anode compartment, the electroactive microbes break down organic matter and release protons and electrons. An illustration of acetate oxidation in the anode compartment is provided by the following equation:



An electron acceptor utilizes electrons within the cathode chamber. Oxygen is commonly utilized as an electron acceptor in MFCs due to its significant oxidation potential. The generated protons pass through the proton exchange membrane/separator, while the electrons travel to the cathode via the external circuit. At the cathode, electrons interact with protons and oxygen to form

water, producing bioelectricity [1]. The potential difference between the anodic and cathodic chambers' oxidative and reductive processes, which generate current flow, is what generates the electromotive force. The equation below represents the half-cell reaction of acetate in the cathode chamber.



2.2 MFC Design

Various laboratory settings have utilized different types of MFCs in the past, including single chamber, double chamber, H-shape dual chamber, cylindrical, and tubular designs. Food waste-fed MFCs are commonly used in two primary configurations: single chamber and dual chamber, as depicted in Fig 2.1

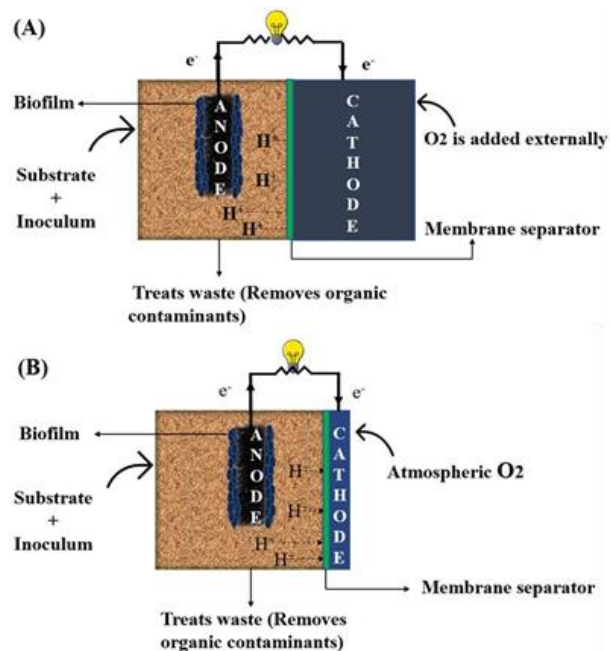


Figure 2.1: A) Single Chamber MFC, B) Dual Chamber MFC [60]

A dual chamber MFC is made up of two chambers: an anaerobic anode chamber and an aerobic cathode chamber, which are separated by a cation exchange membrane. The anaerobic chamber stores the anolyte/fuel, and the cathode chamber stores the catholyte or oxygen. The cation exchange membrane allows protons to pass through while blocking the diffusion of oxygen from the aerobic cathode to the anaerobic anode chamber.

A single-chamber MFC, also referred to as an air cathode MFC, consists of only one chamber where the cathode is directly exposed to air. The arrangement of the reactor has a substantial influence on the efficiency of the microbial fuel cell's output. [61]. Dual chambers are generally more efficient at maintaining an anaerobic environment by reducing the oxygen diffusion in the reactor, in contrast to single chamber setups. A single-chamber MFC enhances the transfer of oxygen from the cathode to the anode chamber, leading to a reduction in the CE of the reactor. However, the complexity of the application and the large amount of space required for installation limit the use of a dual-chamber MFC. [62].

2.3 Pathway of organic matter conversion to electricity

The process of converting complex organic matter into simpler substrates is facilitated by hydrolytic and fermentative bacteria, such as *Clostridium* and *Bifidobacterium* [63]. The less complex compounds are subsequently transformed into volatile fatty acids (VFAs), H₂, and CO₂ by acidogenic bacteria like *Lactobacillus*. Electrogenic bacteria, such as *Geobacter sulfurreducens*, convert VFAs into electricity through the process of electrogenesis. Electrogenesis is a process that involves two pathways for transferring electrons from bacterial cells to the anode: direct and indirect electron transport [64].

The direct electron transport pathway entails the creation of a single layer of microorganisms on the anode's surface. This enables the direct transportation of electrons through the cytochrome C protein. Additional microorganisms are discovered further away from the surface and use electrically conductive extensions known as pili or nanowires to transmit electrons from bacterial cells to the anode. Electrons are carried indirectly utilizing electron shuttles or mediators, which can be both endogenously produced by bacteria and exogenously injected to promote the flow of electrons from the cell to the anode [61, 65].

2.4 Breakdown of fermentation products

In general, fermentative bacteria convert complex molecules into simpler molecules. The by-products can undergo additional oxidation in MFCs to generate electricity, as illustrated in Fig 2.2.

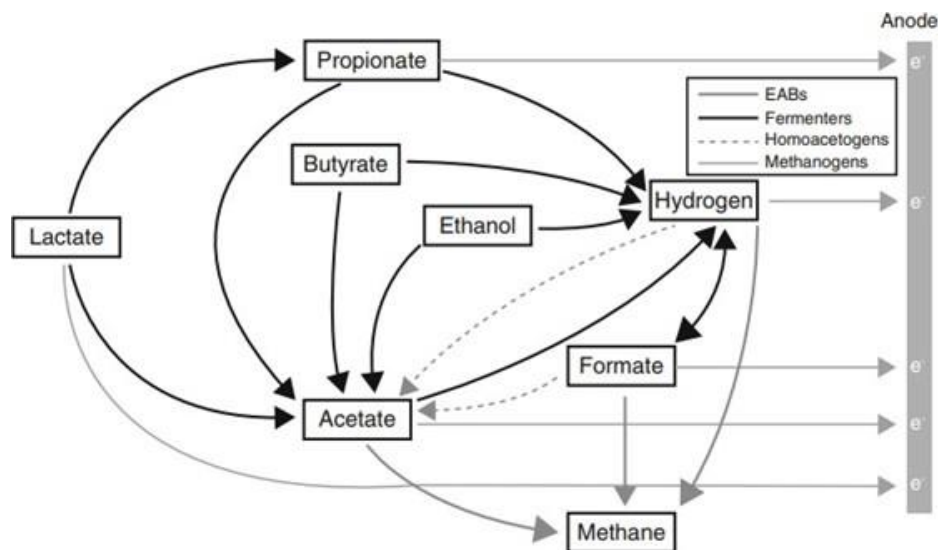


Figure 2.2: Potential theoretical routes for electron movement within the anode section of MFCs originating from various fermentation byproducts. [66]

2.4.1 Acetate

Acetate is a common product of the process of acetic acid fermentation. Acetate can be converted into electricity through two different pathways: either by electroactive biofilms or by producing hydrogen. Acetate oxidation is thermodynamically favorable under standard conditions. Electroactive biofilms, such as those formed by *Geobacter sulfurreducens*, adhere to the direct pathway. *Geobacter sulfurreducens* utilizes acetate as a source of electrons and electrodes as a recipient of electrons [1].

Another route for the conversion of acetate involves the generation of hydrogen. Hydrogen scavengers are crucial for facilitating the transfer of electrons from acetate to anode. This is because acetate is less readily available compared to the soluble chemical electron acceptors in the solution, which are more easily accessible to the microbes. Thus, the process of acetate oxidation is thermodynamically favorable in proximity to the anode [65]. As the biofilm becomes thicker, it becomes harder to access the electrode, causing hydrogen to build up and leading to an increase in partial pressure. *Geobacter sulfurreducens* is unable to undergo acetate fermentation under these conditions due to the reaction becoming endergonic. The reaction can only occur if the hydrogen partial pressure is sufficiently low, which can be achieved in the presence of hydrogen scavengers. Hydrogen scavengers consist of three distinct metabolic groups: homo-acetogenic bacteria,

electrogenic biofilms that consume hydrogen, and hydrogenotrophic methanogens. The symbiotic relationships among these three metabolic groups rely on the exchange of hydrogen between different species [67].

In BES featuring a mixed microbial community, the process of methanogenesis poses a significant challenge to the production of electrical current. Methanogens could break down acetate and hydrogen to produce methane. This creates competition with electroactive biofilms for the use of these substrates, which ultimately reduces the efficiency of the process. With a decrease in external resistance, the rate of electrogenesis increases because of greater substrate consumption, reduced methane production, and a higher coulombic efficiency of 67%. At high external resistance, a low rate of electrogenesis increases the likelihood of methanogenesis, resulting in a 25% decrease in CE [67]. The table provides a concise overview of the biochemical reactions that occur during the degradation of mixed end products in MFCs.

Table 2.1: Overview of biochemical reactions involved in the degradation of mixed end products in MFCs [66]

Substrates	Products	ΔG° (kJ mol ⁻¹)
Acetate + 4 H ₂ O	2 HCO ₃ ⁻ + 9H ⁺ + 8e ⁻	-35.5
Acetate + H ⁺ + H ₂ O	2 CO ₂ + 4H ₂	104.6
Propionate + 5H ₂ O	2CO ₂ + HCO ₃ ⁻ + 14 H ⁺ + 14 e ⁻	-72.95
Propionate + 3 H ₂ O	Acetate + H ⁺ + HCO ₃ ⁻ + 3 H ₂	76.1
Formate + H ₂ O	HCO ₃ ⁻ + 2H ⁺ + 2e ⁻	-49.6
Formate + H ₂ O	HCO ₃ ⁻ + H ₂	1.3
Butyrate + 2 H ₂ O	2 Acetate + H ⁺ + 2H ₂	48.1

H₂	$2\text{H}^+ + 2\text{e}^-$	-34.9
----------------------	-----------------------------	-------

2.4.2 *Propionate*

Propionate is a prevalent byproduct of anaerobic processes, specifically in methanogenic systems. Microbial community analysis reveals three distinct pathways for the conversion of propionate into electricity. The initial route involves the direct exergonic oxidation through electroactive biofilms and can be performed by *Geothrix fermentans*, either with or without electronic shuttles [68].

Furthermore, *Geothrix fermentans* possesses a c-type cytochrome that enables the direct transfer of electrons to the anode. The second route involves the process of fermentation, which leads to the production of acetate and subsequently hydrogen. Nevertheless, under standard conditions, this reaction is endergonic and requires a symbiotic relationship between fermenters and hydrogen scavengers. The third pathway involves the conversion of a substance into acetate and subsequently into formate. This process is classified as endergonic. The process of propionate oxidation is characterized by intricate and poorly understood interactions. Gaining a more comprehensive understanding of propionate fermenters and their interactions could provide valuable insights into the intricate mechanisms of electron flow within their pathways [69].

2.4.3 *Formate*

Formic acid is a product of glucose fermentation and is classified as a short-chain organic acid. The analysis of microorganisms in the MFC fueled by formic acid indicates three distinct pathways for the conversion of formic acid to electricity. These pathways include direct conversion through electroactive biofilms, indirect conversion through homoacetogenesis, or indirect conversion through hydrogen. The oxidation of formate is a thermodynamically favorable reaction under standard conditions. The second method of converting formate into current involves the initial conversion of formic acid to acetic acid through the activity of homoacetogens. This reaction is exergonic under standard conditions, as indicated in Table 2.1. *Geobacter sulfurreducens* can efficiently convert acetate into electrical current, making up approximately 50% of the microbial communities on the anode. The third pathway involves the conversion of formate into hydrogen,

which is an energy-requiring reaction. This process relies on a mutually beneficial relationship between microbes to maintain a low hydrogen partial pressure [70].

2.4.4 Butyrate

Under conditions of low oxygen, the process of fermenting organic materials produces a significant amount of butyrate as a byproduct [71]. Under normal conditions, the process of butyrate oxidation is energetically unfavourable. This means that it requires a cooperative relationship between hydrogen scavengers and butyrate oxidizing bacteria to overcome thermodynamic limitations. The microbial community profiles suggest that there is only one pathway for the conversion of butyrate into electrical current. The process entails the initial oxidation of butyrate to acetate, followed by the subsequent conversion of acetate to hydrogen, facilitated by the enzymatic activity of *Pelomonas saccharophila*. *Geobacter sulfurreducens* can carry out the exergonic process of converting acetate and hydrogen into electricity. This is the second step of the process that occurs under normal conditions. Multiple studies suggest that the process of converting butyrate into electricity exhibits a low level of efficiency, specifically achieving a conversion efficiency of only 10% [72].

2.5 Factors affecting MFC performance.

Like fuel cells, the essential elements of MFC include an anode, a cathode, an external circuit, and a separator, all of which have an impact on the performance of MFC.

2.5.1 Anode Material

The selection of an appropriate anode material is crucial in MFCs as it enables the formation of electroactive biofilms by electroactive bacteria, regulates the mechanism of electron transfer, and influences the kinetics of substrate oxidation in an MFC [73].

The attainable power output is contingent upon the choice of anode material. This determines the upper threshold for power density and can have a substantial impact on the performance of the MFC [74]. Hence, anode materials must possess qualities such as excellent biocompatibility, superior conductivity, chemical stability, low internal resistance, mechanical strength, corrosion resistance, and toughness. Furthermore, it is essential for the anode to have a

substantial surface area to enhance bacterial adhesion and thereby optimize the performance of the MFC. In previous experiments, different anode materials have been examined in a laboratory setting to enhance the performance and economic feasibility of MFCs for large-scale deployment.

Carbonaceous materials, such as graphite fiber brush and rods, carbon cloth, carbon felt, and reticulated vitreous carbon, are mainly utilized as anode materials [75]. Table 2.2 illustrates various anode materials employed in previous research on MFCs. Initially, 2D carbon materials were widely used as anodes in MFC research because they were easy to construct and allowed for accurate measurement of biofilm growth. Nevertheless, the brittle structure of these materials diminished their suitability as the preferred choice for anode material in MFC. Graphite sheets and plates, along with other 2D materials, exhibit low power density because of reduced bacterial adhesion and limited biofilm attachment to smooth surfaces.

The utilization of three-dimensional (3D) anode materials has become increasingly popular due to recent advancements in MFC and breakthroughs in materials and nanotechnology. In their study, Logan et al. (2007) created a 3D graphite fiber brush anode for use in a single chamber MFC. This anode demonstrated a remarkable maximum power density of 2400 mW/m². 3D anode materials offer large surface areas that facilitate bacterial adhesion and efficient colonization of biofilm. This enhances the accessibility of the substrate to anode-respiring bacteria and, as a result, reduces mass transfer limitation [75].

Furthermore, electrode pre-treatments involving acid, ammonia, and heat have shown promise in enhancing the efficiency and power output of MFC. As an illustration, Wang et al. (2009) employed CC that was treated with concentrated ammonia and then subjected to heat treatment in a muffle furnace. They observed an enhanced power density as a result of greater bacterial attachment to the surface of the anode [76]. In addition, Cai et al. (2013) obtained a significant CE of 71% by modifying the carbon mesh through electrochemical oxidation of the anode in nitric acid. The presence of oxygen-containing functional groups on the anode surface can be attributed to the enhanced overall efficiency of the system [77]. Zhu et al. (2019) and Li et al. (2020) utilized anode modification techniques and observed a substantial enhancement in extracellular electron transport. Zhu et al. (2019) employed a carbon-felt anode modified with bio-

reduced graphene oxide, leading to enhanced adhesion of *Shewanella putrefaciens* onto the anode's surface [78].

The alteration improved the movement of electrons between the anode and cathode, resulting in a maximum power density of 240 mW/m², which is four times higher than the control. Li et al. (2020) improved the electron transport mechanism by altering CC with polydopamine and reduced graphene oxide, leading to a highest power density of 2,047 mW/m². The outstanding performance demonstrated by the modified anode can be attributed to the numerous electrochemical sites generated on the anode surface through modification, as well as the hydrophilic characteristics of polydopamine, which improve the attachment of the biofilm to the anode. [79].

The utilization of non-traditional carbonaceous materials, such as graphene-based anodes and stainless steel with surface modifications, has increased recently. According to Chen et al., composite graphene materials show promise for surpassing traditional carbon felt anode in power density, with 427 mW/m³ [80]. Comparably, both single-walled and multi-walled carbon nanotubes and carbon nanofibers have demonstrated improved performance in terms of power generation and bacterial adhesion. Compared to bare graphene, Shen et al. reported a 54% increase in power density when using graphene modified with carbon nanofiber [81, 82].

Overall, because of their excellent output performance and financial viability, carbonaceous anode materials—among the many materials used in the past—remain widely used as MFC anodes. A viable path for increasing overall efficiency is the further improvement of anode efficiency through surface modification and elemental dosing.

Table 2.2: Anode Materials Utilized in MFC [33, 74, 80, 83-87]

Anode material	Substrate	Inoculum	Anode surface area	Max Power Density	Max current density
3D carbon material	Acetate	Domestic wastewater	5.11	NR	25.3

3D carbon fiber	Artificial wastewater	Wastewater	NR	NR	30
Graphite rod	Artificial wastewater	Domestic wastewater	11.5	NR	5.17
Polycrystalline carbon rod	Artificial wastewater	Domestic wastewater	15	NR	9.21
Graphite foil	Artificial wastewater	Domestic wastewater	15	NR	0.07
Carbon mesh	Acetate	Domestic wastewater	7	1330	NR
Multi-brush Anode	Acetate	Effluent from MFC	8	1200	4.2
3D carbon scaffold anodes from polyacrylonitrile	PO ₄ -buffered basal medium	<i>Escherichia coli</i>	2	30.7	2.91
Graphene Sponges	Glucose	Wastewater	NR	1570	1.32

2.5.2 Cathode Material

The air-cathode and aqueous phase cathodes are the typical configurations for cathodes. An air-cathode MFC allows for direct exposure of the reaction area to the air, thereby eliminating the need for aeration and enhancing the power density in the MFC. An air-cathode MFC typically consists of a hydrophobic diffusion layer that is exposed to air, a catalyst layer/binder that is exposed to water, and a conductive supporting material that may also serve as a diffusion layer [88]. On the other hand, an aqueous phase cathode consists of a catholyte contained in a distinct reaction chamber and is composed of a conductive supporting layer with a catalyst/binder layer.

Nevertheless, the effectiveness of aqueous air-cathodes is hindered by the low oxygen solubility in water, which is 4.6×10^{-6} (25°C), in contrast to the 0.21 solubility in air. As a result, air-cathodes are considered a more favorable and feasible design for MFC and have garnered greater interest compared to other cathodes [41].

The selection and design of the cathode material pose significant difficulties in the development of an MFC, as the efficiency of an MFC is typically hindered by slow cathode reactions [89]. Carbon-based materials are commonly used as cathodes due to their abundance, low cost, and versatility. These materials mentioned above, such as anode materials, serve as a base for cathodes [90]. The cathode is commonly designed with a carbon base (paper or cloth) that is impregnated with platinum (Pt) catalyst on one side, either with or without the use of a binder solution [66, 91]. A group of researchers has devised a more pragmatic and cost-effective method for creating air-cathodes by utilizing stainless steel as a supportive material, as opposed to carbon paper and carbon cloth. You et al. utilized a more cost-effective stainless-steel mesh and attained a power density comparable to that achieved with carbon cloth.

Although anode materials can serve as cathodes, the only difference lies in the requirement of incorporating a catalyst layer to enhance the ORR. For example, Pt or ferricyanide are frequently employed as catalysts for dissolved oxygen or gas diffusion cathodes [75, 92]. Nevertheless, non-precious metals, such as iron-based compounds and activated carbon, were also subjected to testing as a catalyst in laboratory settings [93, 94]. To apply a catalyst on the cathode, a binder or polymer is necessary. The two most frequently utilized binders in MFC are perfluorosulfonic acid (Nafion) and polytetrafluoroethylene (PTFE). In addition, they conducted a comparison between PTFE and Nafion to assess their capability to achieve a high-power density in a single chamber MFC. The results indicated that the Nafion binder was able to achieve a power density that was more than 20% higher than that of PTFE. The PTFE binder exhibited a relatively low power density due to the formation of a loose and thin biofilm using that material. Nevertheless, the significant power density attained with Nafion cannot be economically justified for large-scale commercial use due to its exorbitant cost, which is 500 times higher than that of PTFE on a per unit mass basis [90].

2.5.3 Membrane

Membrane separators provide several benefits, including the prevention of oxygen diffusion and the inhibition of substrate crossover between the anode and cathode. Nevertheless, the inclusion of a membrane significantly increases the expenses associated with the design of MFCs and restricts their potential for widespread commercial use [95]. Hence, the choice of membrane is a crucial aspect in the design of MFCs, given that membranes account for 60% of the overall cost of MFCs [66]. Moreover, membranes contribute to the elevation of internal resistance and occasionally facilitate the diffusion of oxygen, resulting in a decline in the efficiency of the MFC. Membrane biofouling is a significant issue that hampers the practicality of using membrane MFCs in real-world scenarios. Table 2.3 displays the primary benefits and constraints associated with the utilization of membrane/separators and membrane-less MFCs.

Table 2.3: Major Pros and Cons of Membrane and Membrane-Less MFCs [25, 53, 66, 79, 85, 89, 96-98]

Membranes	Advantages	Disadvantages
None	High power density, high proton transfer rate, simple configuration, lesser cost	Due to large electrode spacing high Rint, Serious oxygen penetration, cathode biofouling, and deactivation, high substrate loss
IEMs	Low oxygen diffusion, low substrate loss, better isolation of anode and cathode	Restrained proton transfer, high costs, membrane fouling, pH splitting
Microporous filtration membranes	Low pH accumulation, moderate costs, high proton transfer	High Rint, high oxygen permeation

Course-pore filters	Low pH accumulation, high proton transfer, low costs	Inferior durability, biofilm formation on the filter causes substrate loss
Salt bridge	Low costs and simple configuration	High Rint and low power density

Membranes or separators that possess a high internal resistance have the effect of reducing the ion exchange capacity and impeding the movement of protons from the anode to the cathode. As a result, there is a reduction in power density and current densities. [99]. On the other hand, membranes that are porous and have low resistance, like microfiltration membranes, decrease the CE and power density because they enable substrate crossover and oxygen permeation through the membrane. [84]. The oxygen diffusion from the cathode to the anode poses a notable challenge as it leads to reduced efficiency of the MFC and a decrease in voltage due to an elevation in redox potential caused by aerobic microbes utilizing the substrate instead of anaerobic electrogens.

Furthermore, oxygen, being a more favorable electron acceptor, vies with the anode for electron reception, thereby reducing the cathode efficiency and overall efficiency of the MFC. However, the presence of oxygen diffusion does not have a lasting effect on the performance of MFC. This is because anaerobic bacteria can still function efficiently once oxygen is eliminated from the anodic chamber and MFC power is restored. [100].

2.6 MFC Operational Parameters

2.6.1 PH

The pH of the electrolyte is a critical factor that significantly affects the growth and substrate metabolism of electrogenic bacteria. At first, it was recommended to maintain a pH level of 6 in order to achieve optimal efficiency in MFC performance [101]. Subsequently, it was noted that the impact of pH on the performance of MFCs is significantly contingent upon the composition of the microbial community (whether it is pure or mixed) and the specific substrate employed [102]. Therefore, the pH microenvironment of the MFC system fluctuates depending on the composition of the microbial community in the anodic chamber. An optimal pH range of 6.5-

7.5, which is either neutral or close to neutral, is ideal for the growth and functioning of various bacteria, particularly electroactive biofilms [34]. Bacterial metabolism typically releases weak acids to regulate the intracellular pH, which has a tendency to decrease the pH of the anolyte [103]. Thus, it is advisable to maintain a slightly elevated pH when using MFCs to achieve equilibrium between the biological and electrochemical reactions. The favorable pH range for the anode was determined to be between 7 and 9. This is because higher pH levels result in a more negative anode potential, which in turn enhances the power density [104].

Microbes' electrogenic activity is significantly impacted by pH levels that are either highly basic (>9) or highly acidic (<5) due to the likelihood of severe damage to the active sites of enzymes involved in biochemical reactions [66]. Borole et al. showed that acidophiles at a pH below 5 can be utilized for electricity generation in MFC. This study indicates that operating MFCs at a low pH mitigates diffusional limitations more effectively than MFCs operated under neutral pH conditions. Under acidic conditions, the increased driving force is anticipated to enhance the rate of proton transfer and alleviate any limitations in proton availability at the cathode. However, this condition is only relevant for exceptionally effective systems that possess extraordinary electron transfer rates (equivalent to a power density of 1 W/m² or greater) [105]. This experiment proves the feasibility of generating electricity at a low pH. However, the main disadvantage of having an acidic anodic pH in MFCs is the higher probability of electrons being redirected to other electron acceptors. Conversely, numerous benefits of utilizing an alkaline pH level greater than 9 in MFC have been documented. Such benefits include decreased competition for substrates by methanogens and lower electrical potentials at the anode [106]. However, the expense of maintaining such elevated pH levels in MFCs is an added cost that undermines the primary objective of MFCs and would not be viable on a commercial level.

2.6.2 *Temperature*

Temperature is a crucial factor that impacts the performance of MFCs by influencing various factors, including the conductivity of the substrate, activation energy, charge transfer rates, biochemical processes of microbial communities, and diffusion coefficient. The cumulative impact of these factors can significantly affect the efficiency of MFC and power density [107, 108]. These systems are most effective at temperatures that are typical for the environment, specifically

temperatures between 20 and 45°C, which are known as mesophilic temperatures [109]. A small variation in temperature affects the kinetic and thermodynamic characteristics as well as the composition of microbial communities [110].

The biochemical reactions and the enzymes involved typically exhibit optimal performance at their ideal pH. Conversely, the rate of electrochemical reactions has a direct relationship with temperature. Furthermore, it is important to mention that electroactive biofilms exhibit lower sensitivity to fluctuations in external temperature compared to other bacteria. They are capable of adapting to both cold temperatures below 20°C (psychrophilic) and high temperatures above 50°C (thermophilic) [111]. MFCs have been evaluated for their capacity to produce electricity at cold temperatures, while also utilizing low-temperature wastewater directly. An important drawback of this system is the gradual decrease in power production over time caused by the deactivation of enzymes at extremely low temperatures. In contrast, thermophilic MFCs offer advantages such as enhanced solubility of substrates, greater electrogenic activity, minimal contamination risk, and reduced mass transfer limitations [106]. Nevertheless, the costly expenses associated with sustaining elevated temperatures restrict its usage on a commercial level.

2.6.3 *External Resistance*

The performance of MFCs is influenced by various factors, including microbial metabolism, microbial diversity, anode potential, biofilm morphology, power output, and stability, all of which are affected by external resistance [86]. Furthermore, it has an impact on the CE and the rate at which organic matter is removed. The substrate degradation proceeds slowly at high external resistance due to the sluggish microbial metabolism [112]. The maximum power is achieved when the external resistance is equal to the internal resistance. While anodic microbes can overcome the resistance in the system, the power losses can be reduced by carefully choosing the appropriate external resistance. Aelterman et al. observed that setting the external resistance close to the internal resistance in a mixed consortium-inoculated MFC resulted in reduced methane production and increased, consistent power density. Power generation diminishes when the external resistance exceeds or falls short of the internal resistance [42]. Katuri et al. employed various external resistances ranging from 0 to 4 kilohms (Ω) and observed significant variations in microbial communities at different resistance levels [113].

Research revealed that the biofilm undergoes maturation, resulting in the generation of high voltage under conditions of elevated external resistance. This phenomenon contributes to the production of sustainable power and enhances the removal of substrate. A separate study has shown that increasing the external resistance during the start-up phase of the system leads to a shorter start-up time. This is because the growth of microbes is accelerated under high external resistance conditions [96]. In contrast, a decrease in external resistance results in reduced microbial development and growth, which in turn leads to the formation of a thin biofilm. It is recommended to initially operate MFCs at a high external resistance during the start-up phase and then gradually decrease the resistance in order to generate a high current [114].

2.6.4 Rint

Internal resistance in an MFC is the total of all R_{int} losses and is comprised of two components: ohmic resistance and non-ohmic resistance [97, 115, 116]. The ohmic resistance is caused by the cation exchange membrane/separator (if present) and electrolytes, which impede the transfer of electrons and the conduction of ions, resulting in a loss of power in the MFC. To decrease the ohmic resistance, one can enlarge the geometric area between the anode and cathode, typically by increasing the surface area of the CEM [115]. The non-ohmic resistance consists of diffusion resistance and charge-transfer resistance. It can be decreased by increasing the surface area of the anode and cathode and by using electrodes with enhanced catalytic activities [116].

2.6.5 Electrical Conductivity and Ionic Strength

Electrical conductivity refers to its ability to carry electric current and is quantified in Siemens per meter (S/m). The conduction of electric current primarily occurs as a result of the existence of ionic compounds in the aqueous phase of the substrate [66]. The electrical conductivity is directly correlated with the levels of dissolved solids and salinity. To decrease internal resistance in MFC, one can enhance electrical conductivity and increase the ionic strength of the anolyte, thereby improving the mechanism of proton transfer [58]. Jang et al. demonstrated a 75% enhancement in current production by elevating the salt concentration in the catholyte from 100 mM to 1 M [44]. Liu et al. showed that the power output can be increased by 85% by adding NaCl (300 mM), highlighting the significance of anolyte conductivity [85].

Aaron et al. showed that raising the ionic strength of the solution from 0.037 M to 0.37 M led to a reduction in internal resistance from 22.5 Ω to 13.0 Ω , resulting in a 71% increase in power density [117]. Nevertheless, the conductivities of anolytes can only be increased within the acceptable limits of anodic bacteria. A salt concentration of 5 g L⁻¹ strongly hinders the process of methanogenesis. However, an excessive rise in salinity in a MFC is also unfavorable for electrogenic bacteria [66].

Lefebvre et al. conducted a study to examine the impact of elevated salt concentration on the performance of MFCs. They found that the introduction of NaCl in amounts exceeding 20 g L⁻¹ had a harmful effect on the anode respiring bacteria [118]. In environments with high salinity, the internal resistance of a MFC increases because the electroactive bacteria and other microorganisms in the anode chamber become dehydrated. This dehydration leads to a decrease in the rate at which electrons are transferred within the system.

2.6.6 *Organic Loading*

The organic loading rate (OLR) is an essential factor in the determination of the substrate conversion rate in MFCs. Multiple studies have investigated the impact of OLR on MFC performance and have determined that OLR is directly correlated with the degradation of organic matter and the production of power, while being inversely correlated with CE [119]. Rikame et al. did an experiment in which they handled food waste leachate in MFCs with varying levels of COD. They discovered that a lower initial COD concentration of 5,000 mg/L resulted in a 90% decrease in organic concentrations while maintaining a steady open-circuit voltage [120]. However, when the concentration of COD was raised to 20,000 mg/L, only 62.7% of the COD was effectively eliminated. The decline in microbial activity resulted from the suppression of anodic microorganisms as a consequence of the increased COD in the anode chamber. The decline in performance at elevated substrate concentrations can be ascribed to the buildup of volatile fatty acids (VFA), leading to a further decrease in pH, modifications in the composition of the microbial community, and an augmentation in charge transfer resistance due to heightened internal resistance. [121].

Mohanakrishna et al. conducted a comparison of different OLRs in a fermented vegetable waste-fed MFC. The OLRs tested were 3.13, 1.91, and 0.93 kg COD/m³-day, all with the same

hydraulic retention time. The findings indicated that the lowest OLR resulted in a high-power density of 111.76 mW/m². Furthermore, when the OLR was as low as 0.93 kg COD/m³-day, it resulted in the highest removal rates of 80% for COD, 79% for VFA, and 78% for carbohydrates [122]. Velvizhi and Mohan found that as the OLR increases, the power output decreases because the substrate gradually degrades. Conversely, at lower OLR, energy loss occurs due to the high Rint caused by limited substrate availability. Hence, it is crucial to maintain a balance between efficient electron recovery and COD removal when scaling up MFC. Therefore, it is crucial to maintain an optimal OLR in order to ensure efficient operation of the MFC and maximize power generation [119].

2.6.7 Electron Transfer Mechanism and Inoculum Type

The generation of electricity is heavily influenced by the type of inoculum used and the mode of EET. The anaerobically developed anodic biofilm plays a crucial role in the processes of biodegradation and electrogenesis [123]. Hence, it is crucial to comprehend the EET mode and the specific type of inoculum employed for the oxidation of the substrate in the anodic chamber. The performance of MFC was investigated using various pure cultures, including *Geobacter* sp., *Shewanella* sp., and *Rhodospirillum rubrum* sp., which possess a distinct capability to perform EET through both direct and indirect pathways [124, 125]. The current output of the system is influenced by various microbial inoculum, which in turn contribute to the internal resistance of the system.

Pure culture-fed MFCs have demonstrated greater power densities compared to mixed cultures for two main reasons. Firstly, most studies on pure culture-fed MFCs have utilized electroactive bacteria that have the ability to form biofilms and transfer electrons to the anode. Secondly, the start-up time and acclimatization period to the external environment are significantly shorter for pure cultures [126]. In contrast, the utilization of mixed consortia leads to an elevation in internal resistance due to the limited ability of certain microbes to donate electrons outside their cells. Furthermore, the process of acclimatization and biofilm formation is prolonged in mixed microbial consortia [127]. However, MFCs that are solely fed with pure cultures present various challenges, including a significant susceptibility to microbial contamination and restricted types of substrates that can be utilized by pure strains. In the case of large-scale applications, mixed cultures

are typically favored over pure cultures because they are more readily available in large quantities and generally exhibit greater tolerance to environmental disturbances.

DET and MET are two crucial mechanisms that facilitate electron transport [128]. The DET mechanism entails the direct transfer of electrons from the electroactive biofilm to the electrode material. Hence, it is clear that in DET, there must be sufficient physical contact between the electrode material and the electroactive biofilm to enhance electrogenesis [129]. Research has demonstrated that *Shewanella* sp., *Rhodospirillum rubrum* sp., and *Geobacter* sp. exhibit high efficiency in the DET mechanism. DET occurs via either membrane cytochromes or conductive pili, also referred to as nanowires [130-132]. The majority of gram-positive bacteria are believed to utilize the DET pathway for biofilm formation by means of teichoic acid, a substance that facilitates the attachment of biofilms to the anode [132]. In contrast, certain microorganisms are unable to undergo DET and instead utilize electron shuttles to carry out MET. The electron shuttle facilitates the predominant pathway of electron transfer utilized by various microbes, including *Shewanella oneidensis*, *Pseudomonas aeruginosa* [89], and *Escherichia coli* [133]. Typically, these redox mediators gather electrons from the microbes and transport them to the anode electrode. Endogenous mediators refer to mediators that are produced within the organism itself, while exogenous mediators are mediators that are added from outside the organism. Nevertheless, the use of externally introduced mediators in MFCs is hindered by several disadvantages, such as toxicity, operational instability, and notably, high expenses [127].

CHAPTER 3: MATERIALS AND METHODS

3.1 Iron MOF Synthesis

Fe-MIL-88B-NH₂ (Fe-MOF) was synthesized at room temperature. Fe-MOF particles were synthesized by combining two solutions at room temperature for a duration of 20 hrs. The initial solution consisted of 2.16 grams of Iron chloride hexahydrate (FeCl₃·6H₂O, Sigma Aldrich, ≥98%) dissolved in a mixture of 7.6 ml of deionized water (DI water) and 12.4 ml of N,N-dimethylformamide (DMF, Sigma–Aldrich, > 99%). 20 mL of DMF was supplemented with 0.720 g of 2-Aminoterephthalic acid (NH₂-TPA, Sigma Aldrich, 99%) in the second solution.

The mixed solution (with a molar composition of FeCl₃·6H₂O:NH₂-BDC: DMF: H₂O in a ratio of 1:1:52:52) was subjected to magnetic stirring. After the completion of the reaction, it was washed with DI water and then with ethanol several times using centrifugation. The ultimate powder was dehydrated at a temperature of 60 °C for the entire night in a vacuum oven and then gathered and grinded. [134, 135].

3.2 PANI Synthesis

Solution A was prepared by dissolving 100 µl of aniline (C₆H₅NH₂, Sigma Aldrich) in 50 ml of 1 mol·L⁻¹ Sulfuric acid (H₂SO₄ Sigma Aldrich, 99%) and mixing it thoroughly at room temperature in a beaker. Simultaneously, 0.25 grams of ammonium persulfate (NH₄)₂S₂O₈, Sigma Aldrich) is fully dissolved in a 50 ml solution of 1 mol·L⁻¹ of H₂SO₄ in a separate container, referred to as solution B.

The aniline monomer and (NH₄)₂S₂O₈ were mixed in a 1:1 molar ratio, and then poured into a round bottom flask. The system was continuously stirred for 3 hrs at room temperature to ensure complete polymerization. The presence of a dark green color signifies the formation of PANI emeraldine salt. The filter collection products undergo a process of washing with DI water and ethanol, followed by drying at room temperature in a vacuum oven before being collected [136, 137].

3.3 Fe-MOF/PANI Composite Synthesis

The preparation procedure for PANI/Fe-MOF composite is identical to that of Fe-MIL-88B-NH₂. The same procedure for synthesis was followed as previously described for Fe-MOF. Upon addition of solution B to solution A, 300 mg of prepared PANI was added, and the resulting solution was agitated at room temperature for 20 hrs. The filter collection products are subjected to a process of washing with deionized water and ethanol, the samples were then dried at room temperature in a vacuum oven overnight before collection [134, 138].

3.4 Preparation of anode

The anode electrode is prepared through a two-step process.

3.4.1 *Hydrophilic treatment of anode*

The GF was cut into pieces measuring (3.3 cm length × 3.3 cm width × 0.5 cm thickness). These pieces were then soaked in an acetone (C₃H₆O) solution for a duration of 24 hrs to eliminate any oil contaminants on the surface. Subsequently, the GF was subjected to a 30-minute ultrasound cleaning process using ethanol.

Afterwards, it underwent treatment with a solution containing 10% hydrogen peroxide (H₂O₂) and 10% hydrochloric acid (HCl) in a water bath at a temperature of 90 °C for a duration of 3 hrs. After a comprehensive process of washing with DI water GF was vacuum dried at 60 C overnight, a hydrophilic GF material was obtained [139].

3.4.2 *Coating of material on anode*

The initial step involved the formation of a slurry, which was subsequently applied onto the GF using the dip and dry method. To prepare the slurry, 55 mg of material was measured using a measuring balance. Then, 0.22 ml of Nafion 117 solution was added as a binder, followed by 3.3 ml of ethanol. Finally, 0.55 ml of DI water was added to form the final solution.

The solution was subjected to ultrasonication for a duration of 3 hrs until uniform suspension was formed. Subsequently, a slurry was applied onto the GF using the dip and dry technique, ensuring that the coating was uniformly distributed [140, 141].

The GF that had been coated was subsequently dried at a temperature of 70°C for the duration of one night in a vacuum oven. The weight of the GF was measured both before and after the coating process to determine the mass loading. Mass Loading is mentioned below in table 3.1

Table 3.1: Mass Loading of Material onto GF

Graphite Felt	Mass Loading
Fe-MOF Coated GF	91.32%
PANI/Fe-MOF Composite Coated GF	96.54 %

3.5 Preparation of Cathode

CC was utilized as a cathode. One side of the CC was covered with PTFE because PTFE improves the kinetics of ORR.

3.6 Membrane pretreatment

The Nafion 117 membrane underwent pre-treatment in three distinct stages. The membrane was initially subjected to heating at a temperature of 80 C in DI water for a duration of 1 hr. Subsequently, it was immersed in a 3% H₂O₂ solution at the same temperature for a period of 2 hrs.

Finally, it was treated with a 0.5 M H₂SO₄ solution at 80°C for 2 hrs. Subsequently, the PEM was immersed in DI water for storage prior to utilization [142].

3.7 Setting Up MFCs

The dual chamber MFC setup was used for these experiments as shown in Fig. 1.3. Each chamber within the reactor possesses a volume of 100 ml.

3.7.1 MFC Construction

The entire MFC setup was manually constructed. A sheet of plexiglass was purchased from the market and subsequently cut into various sizes by means of a laser cutting machine. Afterwards, the pieces were joined together using adhesive to construct two distinct chambers that are impervious to leaks. Subsequently, a rubber gasket was affixed to each side of both chambers. Drilling was performed on the top plate to create necessary holes for sample collection, nitrogen purging in the anodic chamber, and air purging in the cathodic chamber. Once the membrane is positioned between the chambers, the chambers are securely fastened together using nuts and screws.

3.7.2 MFC Arrangement

After assembling the MFC reactor, a membrane was initially positioned between the chambers and subsequently tightened together using screws and nuts. The anode was then inserted into the anodic chamber, which was filled with anolyte. To prevent any air from entering, the anodic chamber was completely sealed using silicon sealant. Similarly, the cathode was placed inside the cathodic chamber and filled with catholyte. A pipe for air purging was installed within the cathode. The entire MFC setup was positioned on a magnetic stirring plate to ensure continuous stirring for the uniform dispersion of the anolyte. Automatic heating rod set at an optimal temperature of 34°C was placed nearby to ensure the desired temperature for bacteria.

3.7.3 Microbial Sludge

The initially inoculum (anaerobic reactor sludge) was collected from a membrane bioreactor wastewater treatment plant at NUST University in Islamabad, Pakistan. The foreign particles were eliminated through the process of sieving the sludge and continuously stirring it at a speed of 180 rpm. This resulted in the creation of a uniform liquid phase for the final microbial inoculum. Following pretreatment, the sludge was introduced to fresh growth media and supplemented. The flask was outfitted with ports to facilitate the introduction of new media and the removal of used media.

3.7.4 Analyte

The anodic media comprises the compounds specified in table 3.2, along with their corresponding quantities. Sodium acetate was employed as an organic substrate in conjunction with nutrient media [142]. The medium was purged with 100% nitrogen gas to establish an oxygen-free environment. Additionally, the medium is prepared fresh each time to prevent any pre-existing bacterial growth or consumption. Following each decrease in voltage values, the depleted medium (70%) was subsequently separated by decantation and substituted with a new nutrient medium. This practice is reiterated after each cycle.

Table 3.2: Nutrient Medium Composition.

Sr.No.	Salt Name	Amount (g/L)
1	Manganese Sulphate ($\text{MnSO}_4 \cdot \text{H}_2\text{O}$)	0.50
2	Sodium Chloride (NaCl)	1.00
3	Iron sulphate ($\text{FeSO}_4 \cdot 7\text{H}_2\text{O}$)	0.10
4	Calcium Chloride ($\text{CaCl}_2 \cdot 2\text{H}_2\text{O}$)	0.10
5	Zinc Sulphate ($\text{ZnSO}_4 \cdot 7\text{H}_2\text{O}$)	0.18
6	Copper Sulphate ($\text{CuSO}_4 \cdot 5\text{H}_2\text{O}$)	0.01
7	Boric Acid (H_3BO_3)	0.01
8	Ammonium Chloride (NH_4Cl)	1.00
9	Sodium Citrate ($\text{Na}_3\text{C}_6\text{H}_5\text{O}_7$)	0.3
10	L-ascorbic Acid	0.1
11	Cobalt Chloride (CoCl_2)	0.1

12	Nickel Nitrate ($\text{Ni}(\text{NO}_3)_2 \cdot 6\text{H}_2\text{O}$)	0.03
13	Magnesium Chloride (MgCl_2)	0.06

3.7.5 Catholyte

The catholyte consisted of a 0.5 M solution of phosphate buffer (PBS) with a pH of 7 [142]. An air pump was used to continuously supply oxygen (air) to the cathode compartment for efficient reduction. The PBS solution is completely restored in the cathodic side whenever it dries out because of evaporation.

3.7.6 Operating MFC

A total of three MFCs were constructed and operated simultaneously for the purpose of conducting a comparative study. The MFC installed with bare GF is designated as the control MFC, while the second MFC employs an Fe-MOF anode. The third one being investigated utilizes the PAN/Fe-MOF composite anode. Data was continuously captured using a Picolog (Model PP547) data logger after arranging and operating the MFCs as outlined above. Picolog was attached to a personal laptop, and data was consistently recorded at 2-minute intervals. Several cycles were taken at a COD level of 1000, as well as multiple cycles at a COD level of 500. Additionally, multiple cycles were recorded at a COD level of 500 while applying a load of a 500 Ω resistor

3.7 Calculations and Analyses

The voltage differential between the two electrodes was measured under two conditions: open circuit and with a fixed load of 1000 Ω . The current (I) was determined using the following equation.

$$I = \frac{V}{R}$$

And Power density (mW/m^2) is given by:

$$P = \frac{VI}{A}$$

The variables employed in this particular context are denoted as I for current, V for voltage, and approximate cross-sectional area of the anode is represented by A. A polarization curve was plotted by varying the external resistance from 10 to 10000 Ω and recording the corresponding voltage values. The maximum power density of MFC can be determined by identifying the peak of the graph that plots current density on the x-axis and power density on the y-axis.

Cyclic voltammetry (CV) measurements were performed with a Gamry potentiostat Interface. The MFC anode served as the working electrode, the MFC cathode as the counter, and the reference electrode was Ag/AgCl (Ag/AgCl, sat. KCl). The area enclosed by the CV curve can be employed to signify the number of electrons moved at the electrode, hence indicating the electrode's capacitance. The capacitance can be calculated using the following formula.

$$C_p = \frac{\int_{v_1}^{v_2} i(V)dv}{2Av(V_2 - V_1)}$$

In CV scanning, V1 and V2 denote the boundaries of the chosen potential window, $i(V)$ signifies the instantaneous current, A represents the anode surface area (1x1 cm²), and v indicates the scanning rate.

CHAPTER 4: CHARACTERIZATION

4.1 Instruments

The samples were analyzed for their morphology through Scanning Electron Microscope (SEM) using JEOLJSM-6490A (Tokyo, Japan). The structural information was examined using X-ray diffraction (XRD) on a Seimens D5005 STOE & Cie GmbH (Darmstadt, Germany). The analysis was performed at an angle (2θ) ranging from 10° to 40° . The Fourier Transform Infrared Spectroscopy (FTIR) measurement was carried out using a PerkinElmer SpectrumTM100 spectrophotometer with potassium bromide (KBr) pellets and dried powder samples. The electrochemical behavior of the prepared samples was measured using a Gamry electrochemical workstation (Interface 1010E potentiostat, USA) with a standard three-electrode setup. The working electrode was a GF/ Modified GF, the counter electrode was a platinum wire, and the reference electrode was Ag/AgCl.

4.2 SEM

SEM is the technique most often employed for characterizing materials. The process entails utilizing a high-energy electron beam to scan the surface of a sample in a raster scan pattern, resulting in the creation of a high-resolution image. The image produced by the interaction of electron beam with the surface of the sample being studied provides insights into the sample's surface topography and chemical composition.

4.2.1 Working principle

To produce SEM images, electrons are generated within the electron gun. Typically, a V-shaped thin tungsten filament is utilized as the electron source, known as a thermionic cathode, as shown in Fig 4.1. This cathode is heated by an electric current, causing the emission of electrons. The electrons produced are directed towards an anode. A voltage differential is established between the anode and the thermionic cathode by connecting the cathode to the negative terminal and the anode to the positive terminal of a high voltage source. The voltage difference referred to as the accelerating voltage ranges from 0.2 to 40 keV, determining the wavelength and energy of electrons in the beam.

The intense electric field between the anode and the cathode propels the incident primary electrons towards the sample, causing the release of different emissions from its surface. These emissions include backscattered electrons, which have kinetic energies like that of the incident beam (around 50eV), secondary electrons with energies below 50eV, auger electrons generated through the de-excitation of atoms, and characteristic x-rays produced by the release of excess energy during atom de-excitation.

Analyzing the X-ray energy emitted by a sample can determine its chemical composition, as this energy is specific to the element it came from.

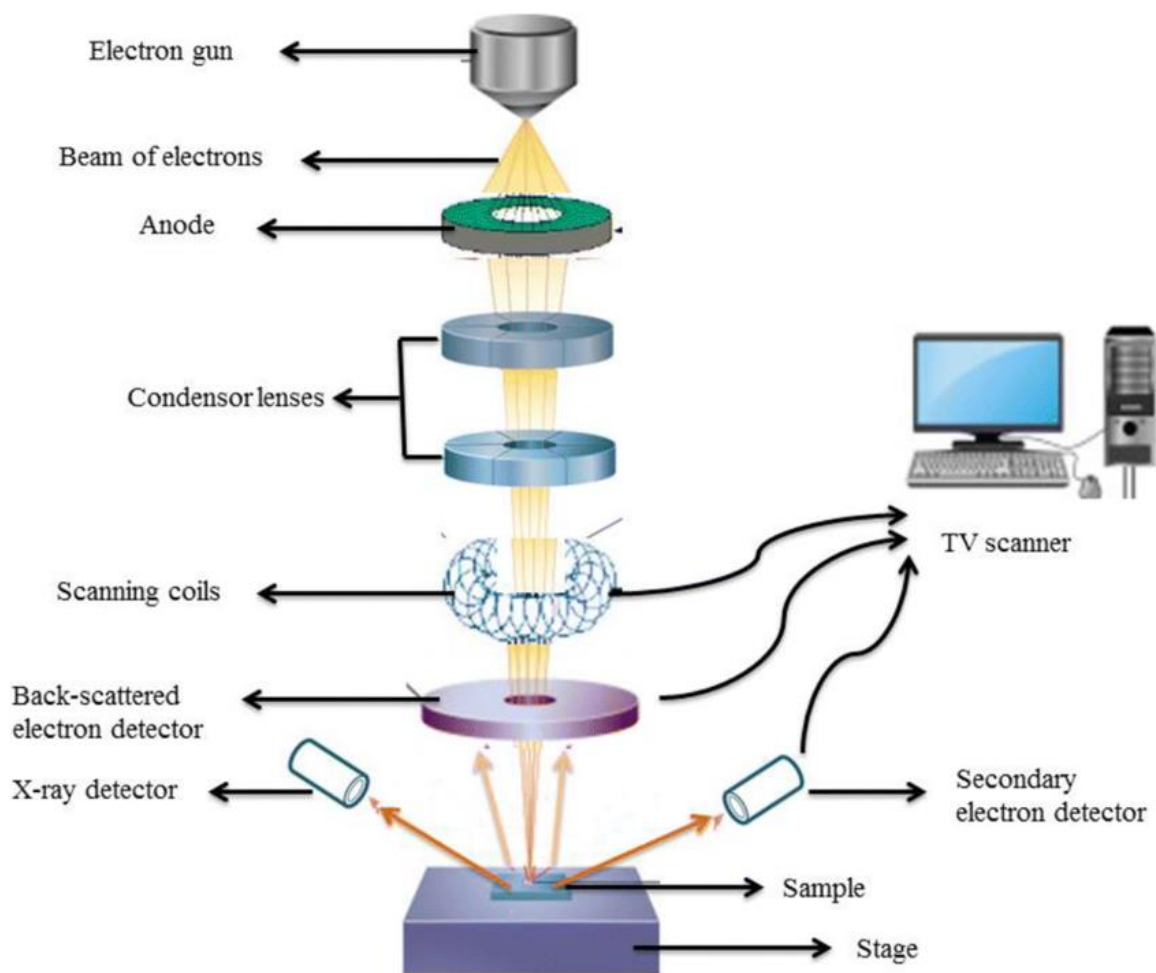


Figure 4.1: SEM working principle [143]

Secondary electrons play a crucial role in SEM imaging as they are responsible for revealing topography and morphology of the sample. Upon impact, the incident primary electrons

dislodge surface electrons of the sample. The dislodged electrons, known as secondary electrons, can be gathered by a secondary electron detector (SE detector) connected to a positively charged grid. These electrons are then converted into signals, which are subsequently amplified, interpreted, and converted into an image [144].

4.2.2 Sample preparation

Preparing a sample for SEM analysis is simple as it requires the sample to be conductive, which can be achieved by coating it with gold using a sputter coater.

4.3 XRD

XRD is a powerful non-destructive technique used for the characterization of materials using x-rays radiation. X-rays are a type of electromagnetic radiation that shares the same nature as light, but they have higher energy and a much shorter wavelength of approximately 1\AA . In 1912, German scientist Max von Laue and his colleagues discovered that crystalline substances could function as three-dimensional diffraction gratings at x-ray wavelengths that correspond to the spacing between planes in a crystal lattice.

XRD is employed to determine the specific crystalline phases present in a material and to analyze their structural properties. Additionally, it is employed for the assessment of microstructure analysis in polycrystalline and amorphous materials, measurement of film thickness, determination of unit cell dimensions, estimation of average particle size, and evaluation of sample purity.

4.3.1 Working principle

The specimen to be examined is exposed to a beam of X-rays as shown in Fig 4.2. Many materials consist of tiny crystals that have a regular arrangement of atoms. Every atom consists of a central nucleus that is surrounded by clouds of electrons. When x-rays interact with an atom, the electrons within the atom oscillate due to the influence of the incoming x-rays.

As a result, the electrons emit secondary x-rays with the same energy as the original x-rays. Constructive or destructive interference can occur when x-rays interact with each other, resulting in emission. Constructive interference occurs when the waves are in alignment, resulting in signal

amplification. Destructive interference, on the other hand, happens when the waves are not aligned, leading to signal destruction. The periodic arrangement of atoms in a crystal creates distinct planes that are clearly separated by specific distances.

When an x-ray beam is directed at the atomic planes, the evenly distributed atoms cause the x-rays to scatter. When the scattered waves align at precise angles and combine in a way that increases their strength, the emitted signals are greatly amplified. This phenomenon is commonly referred to as diffraction. The detector captures the diffracted x-rays and represents them as a graph [145]. The x-rays diffracted from a crystal are mathematically described by an equation called Bragg's law:

$$n\lambda = 2d\sin\theta$$

In this context, n represents the order of reflection, λ represents the wavelength, d represents the interplanar spacing of the crystal lattice planes that is responsible for a specific diffracted beam, and θ represents the angle between the incident beam and the lattice planes as shown in Fig 4.3.

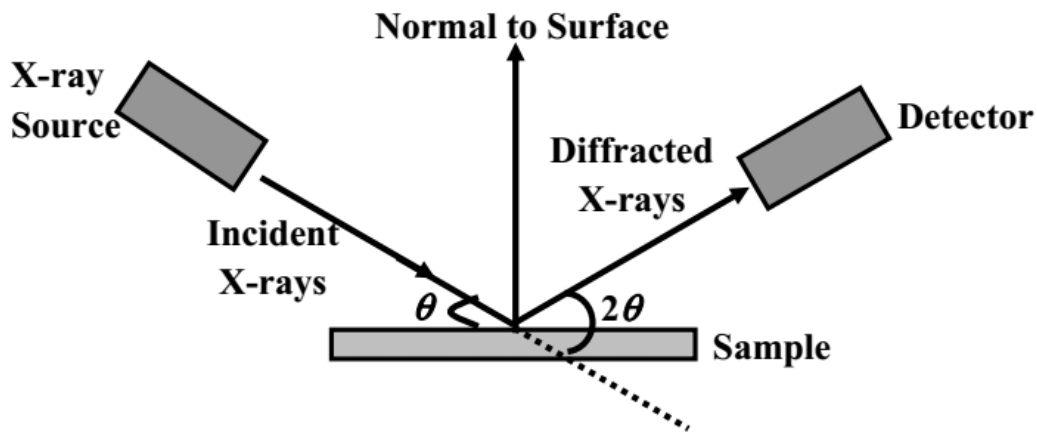


Figure 4.2: Schematic representation of X-ray diffraction [146]

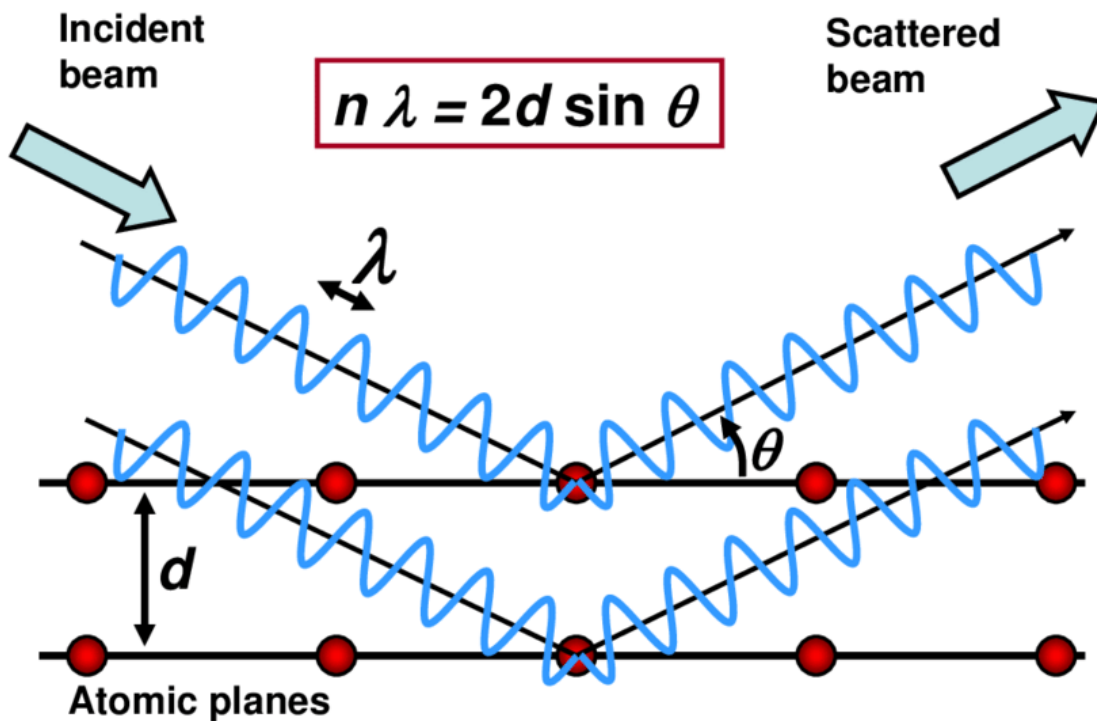


Figure 4.3: Schematic representation of Bragg's law [147]

4.4 FTIR Spectroscopy

FTIR spectroscopy examines the interaction between infrared radiation and material. Infrared radiation has a longer wavelength than visible light. FTIR is the predominant method for vibrational spectroscopy, commonly employed to determine the functional groups and chemical bond types. FTIR is a technique that enables the collection of an infrared spectrum over a broad range of wavenumbers. The dispersive method differs from this approach by collecting signals separately at each wavenumber to create a spectrum. Currently, FTIR has largely supplanted the dispersive method due to its significantly superior signal-to-noise ratio.

Infrared (IR) radiation is generated by a source of light and focused onto the sample. The sample selectively absorbs certain amounts of the passing light, while reflecting the rest. The residual light is transmitted, carrying the molecular data, and then captured by a detector to generate an electronic signal.

The Michelson interferometer plays a crucial role in the Fourier transforms infrared spectrometer. The infrared beam emitted by the source passes through the interferometer and is directed towards a beam splitter for measurement, as depicted in Fig 4.4.

The beam is subsequently divided and directed towards a fixed mirror and a mirror in motion, respectively. Subsequently, the beam is merged and aimed towards the sample material. All wavelengths' spectral information is simultaneously acquired. The mobile mirror alters the lengths of the optical paths to create interference of light between the two divided beams.

There will be no difference in the trajectories of the two split beams if the moving mirror is positioned at the same distance from the beam splitter as the fixed mirror. This is because their optical pathways will be identical. If the moving mirror is shifted away from the beam-splitter, an optical path difference (δ) will be produced.

The two divided beams will produce alternating destructive and constructive interference, with a consistent variation in the δ value.

Constructive interference occurs when:

$$\delta = n\lambda,$$

whereas when:

$$\delta = (1 / 2 + n) \lambda$$

then completely destructive interference occurs. Alteration in the position of a mobile mirror leads to a variation in the δ value.

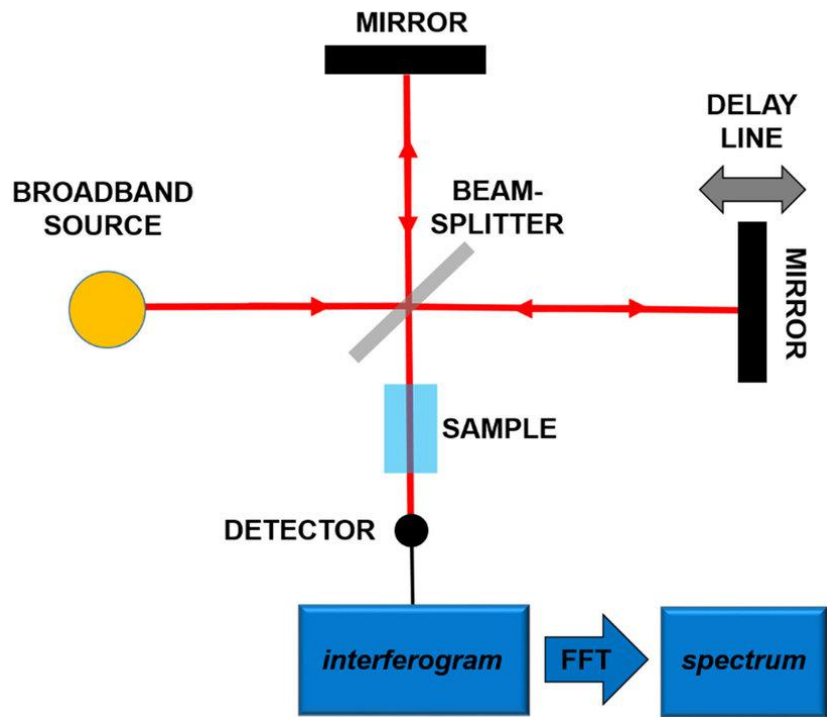


Figure 4.4: Schematic representation FTIR working [148]

An interferogram refers to a graphical representation of the intensity of light interference in relation to the difference in optical path. From an interferogram, the infrared spectrum depiction of light intensity as a function of wavenumber needs to be Fourier transformed. Interferogram signals are received by the FTIR detector and either transmitted to a sample or reflected from a sample. There is no infrared spectrum in the interferogram that was received from the detector. A computer utilizing FTIR technology produces the infrared spectrum through the implementation of the fast Fourier transform (FFT) algorithm.

The FTIR spectrum can be comparable to a chemical fingerprint. It has the capability to identify and authenticate known and unknown samples, as well as to analyze and describe novel materials. Especially valuable in the chemical and manufacturing sectors, as well as in research and development. FTIR spectroscopy can provide answers to a wide range of analytical questions across different industries, depending on the specific setup and procedure of the spectrometer [149].

4.5 CV

CV is a widely used electrochemical technique that involves sweeping the potential to gather information about the electrochemical process. The CV can be used to determine various processes, such as the redox process of electrode materials, the reactants involved, and the reaction kinetics of heterogeneous electron transfer reactions that occur in an electrochemical.

4.5.1 Working principle

In order to perform CV, an electrochemical cell is prepared by introducing an electrolyte solution and three electrodes. The potentiostat is employed to systematically vary the potential in a linear manner between the reference and working electrode until it reaches a pre-established threshold, at which point it is reversed and swept in the opposite direction.

The device measures the dynamic current between the counter and working probes in real-time by iteratively performing the scanning process. A cyclic voltammogram is the distinctive plot that is obtained as a result. Fig 4.7 provides an example.

The scan illustrated in Figure 4.7 begins at a voltage of -0.4V and progresses towards higher oxidative potentials. The initial voltage is insufficient for the oxidation of the analyte.

As the substance being analyzed undergoes oxidation at the surface of the working electrode, the current exhibits exponential growth (b) once the point of initial oxidation (Eonset) is reached. The current in the process is currently controlled through electrochemical methods, where the current increases in direct proportion to the voltage, while inside the diffuse double layer, the analyte's concentration gradient near the electrode surface stays constant. When the diffuse double layer increases in size and the analyte is used up, the current response no longer follows a straight line. At point c, the anodic peak current (i_{pa}) at the anodic peak potential (E_{pa}) reaches its maximum value. An increase in current is caused by higher positive potentials, while a decrease in analyte flux occurs at a The Nernst equation is not satisfied by the analyte's sluggish mass transfer from the bulk to the DDL interface, which limits the current. The current reduces as the potential is gradually scanned in a positive direction until it approaches a steady-state, at which point additional increases in potential have no impact. The reductive scan, which involves reversing the scan to negative potentials, proceeds to oxidize the analyte until the applied potential

reaches a specific value. This value enables the oxidized analyte that has accumulated on the electrode surface to be re-reduced.

With the scan direction changed, the reduction process is comparable to the oxidation process. Furthermore, at the cathodic peak potential (E_p^c) (f), a cathodic peak (i_p^c) is seen. The cathodic and anodic peak currents for a reversible process are expected to have similar magnitudes but opposing polarity [152].

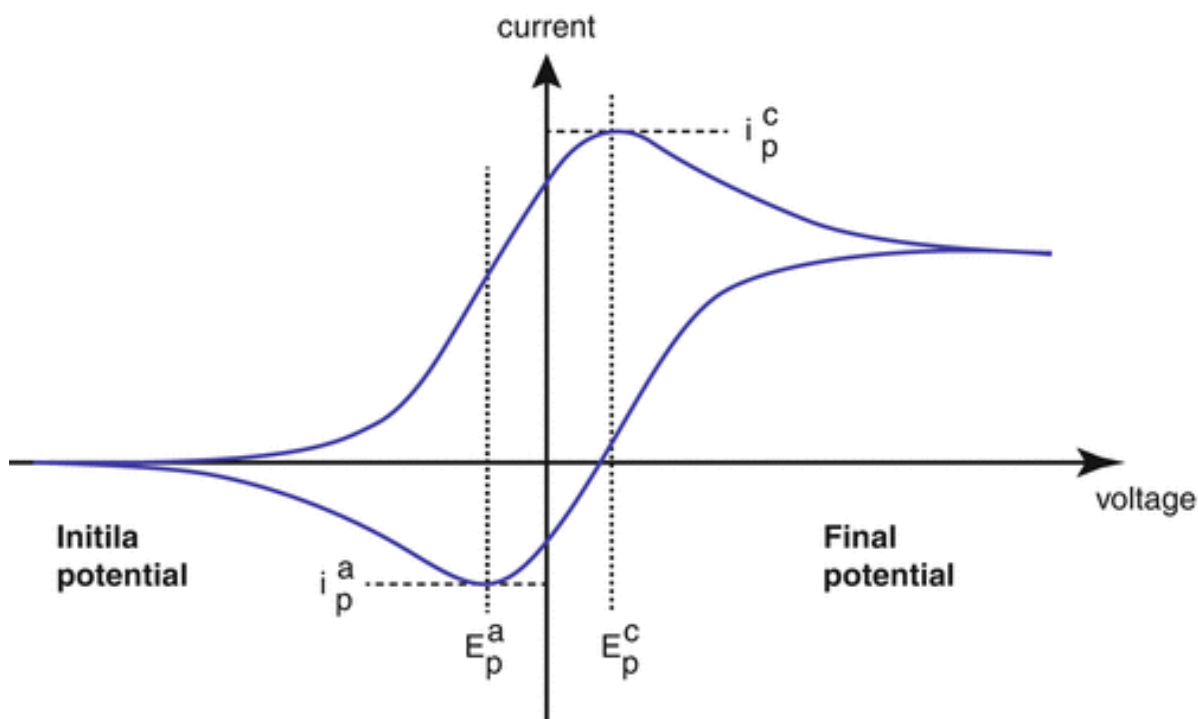


Figure 4.5: Cyclic voltammogram for an one-electron electrochemically reversible redox process [153]

4.6 Electrochemical Impedance Spectroscopy (EIS)

EIS is an electrochemical method that provides information on the processes and kinetics of different electrochemical systems. By providing a sinusoidal signal (alternating current or voltage) over a wide frequency range, electrochemical systems that are in a condition of balance or stability can be upset. This is known as electrochemical stimulation. The system's response with respect to voltage or current is then monitored. EIS is a technique that represents the relationship between the input signal (alternating voltage or alternating current) and the output signal

(alternating current or alternating voltage) across a wide range of frequencies, given that the electrochemical system under investigation is a linear time-invariant system, where the output signal is directly proportional to the input signal and the system's behavior remains constant over time [154].

It is extensively employed in the fields of corrosion studies, semiconductor science, energy conversion and storage technologies, chemical sensing and biosensing, as well as noninvasive diagnostics.

CHAPTER 5: RESULTS AND DISCUSSION

5.1 XRD

XRD analysis was performed to examine the structural formation of the fabricated samples. The intensities of the diffracted waves were measured within the angular range of 10° to 40° . The diffraction peaks of the Fe-MOF closely correspond to the simulated XRD pattern of MIL-FE-88B-NH₂, suggesting the successful synthesis of Fe-MOF. The XRD peaks (2θ) of the Fe-MOF at 9.2° (022), 10.3° (101), 13.0° (102), 16.7° (103), 18.5° (200), 19.0° (201), 20.7° (202), 26.4° (204), and 29.5° (302) match the characteristic peaks of the crystalline MIL-FE-88B-NH₂ as shown in Fig 5.1 [156]. Nevertheless, the γ -Fe₂O₃ crystalline phase is observed at $2\theta \approx 25.0^\circ$ and 29.5° due to the presence of a small quantity of Fe(III) ions [157]. The XRD plot of pure PANI reveals two distinct diffraction peaks at 24.9° and 19.3° which correspond to the crystallographic planes (322) and (113) respectively as shown in Fig 5.1 [158].

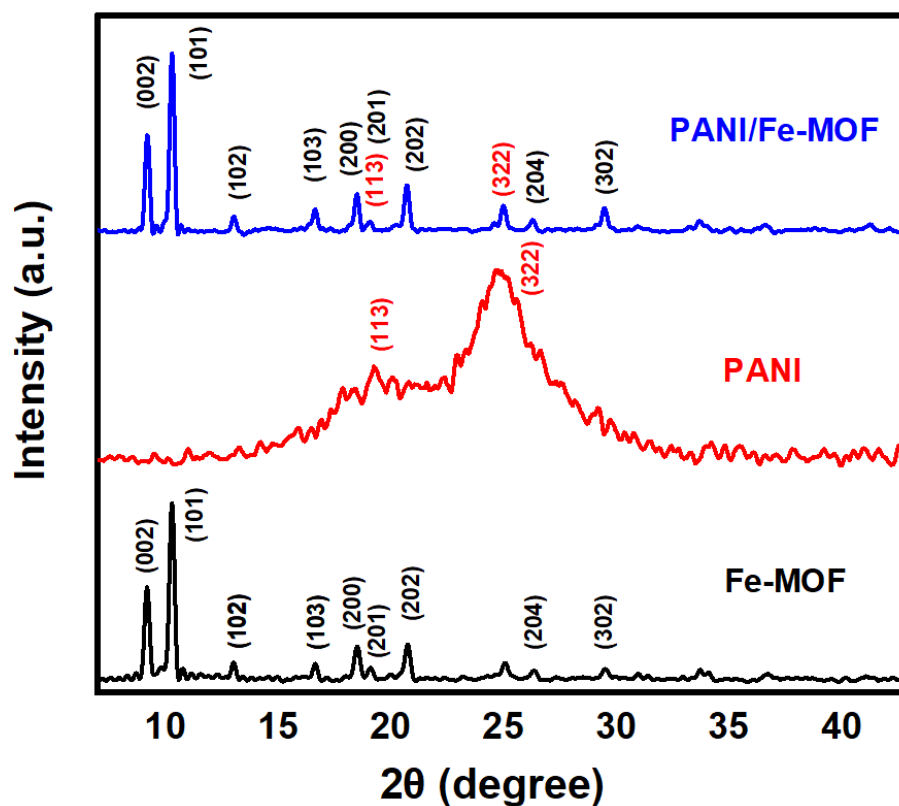


Figure 5.1: XRD Plots of Fe-MOF, PANI, PANI/Fe-MOF

The XRD pattern of the PANI/Fe-MOF composite, as shown in Fig 5.1 is very similar to that of MIL-FE-88B-NH₂, with only slight differences in peak intensities [156]. This suggests that the inclusion of PANI has little effect on the crystalline structure of the MOF. Given the small amount of PANI in the composite, the XRD pattern is primarily influenced by Fe-MOF. Furthermore, since the main peaks of polyaniline are close to the 2θ positions of Fe-MOF peaks, it is expected that they would overlap, which is evident in the XRD plot of the PANI/Fe-MOF composite. [136].

5.2 FTIR

The FTIR spectra of all synthesized samples were analyzed within the wavenumber range of 4000 cm⁻¹ to 500 cm⁻¹, (as illustrated in Fig. 5.2). The FTIR spectrum of Fe-MOF shows a band at 3424 cm⁻¹, indicating N–H bond stretching vibrations. The band at 1377 cm⁻¹ is associated with symmetric C–O stretching vibrations, while the band at 1584 cm⁻¹ corresponds to C=C vibrations. Another peak at 1629 cm⁻¹ suggests the presence of a carbonyl group (C=O), though it is partially masked by the strong C=C band. The bands at 1254 cm⁻¹ and 766 cm⁻¹ are assigned to the bending vibrations of C sp²–N and C sp²–H bonds, respectively. These features are observed in both the amino ligand and the synthesized materials. A characteristic band at 575 cm⁻¹ in the Fe-MOF spectrum indicates the FeO coordination bond between Fe³⁺ and the ligand. FTIR analysis thus confirms bond formation between Fe(III) and the ligand through the oxygen atom in the synthesized MOF. [157].

The FTIR spectrum of PANI shows the in-plane and out-of-plane bending vibrations of aromatic C–H at 1130 cm⁻¹ and 783 cm⁻¹, respectively. The bands at 1230 cm⁻¹ and 1294 cm⁻¹ correspond to the C–N stretching in the secondary aromatic ring. IR peaks at 1568 cm⁻¹ and 1455 cm⁻¹ are attributed to the stretching vibrations of the C=C bond in the Quinoid (N=Q=N) and Benzenoid (N–B–N) rings, respectively. A band at 2913 cm⁻¹ represents C–H stretching vibrations, while N–H stretching in the secondary amine appears at 3429 cm⁻¹. The FTIR spectrum of PANI is consistent with bands commonly reported in the literature. [158].

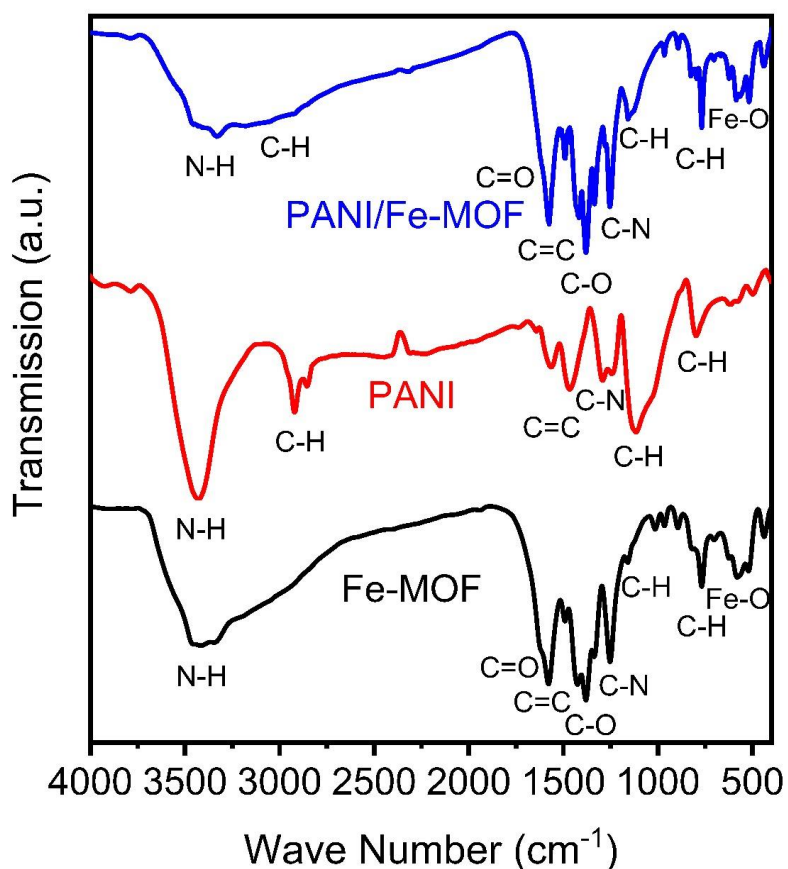


Figure 5.2: FTIR Spectra of Fe-MOF, PANI, Fe-MOF/PANI

The FTIR spectrum of the PANI/Fe-MOF composite shows characteristic bonds from both materials, with peaks at 1244 cm^{-1} and 1573 cm^{-1} , corresponding to the C–N stretching in the aromatic ring and C=C stretching in the benzenoid ring, respectively. Additionally, the bands at 1383 cm^{-1} and 581 cm^{-1} , attributed to C–O and FeO stretching, respectively, confirm the successful formation of the PANI/Fe-MOF composite.

5.3 Scanning Electron Microscope

The morphology of the synthesized samples was analyzed using a SEM. Figure 5.3 depicts the morphological characteristics of various materials, namely MIL-FE-88B-NH₂, PANI, Fe-MOF/PANI, Bare GF, Fe-MOF coated GF, and Fe-MOF/PANI coated GF and GF with attached Biofilm.

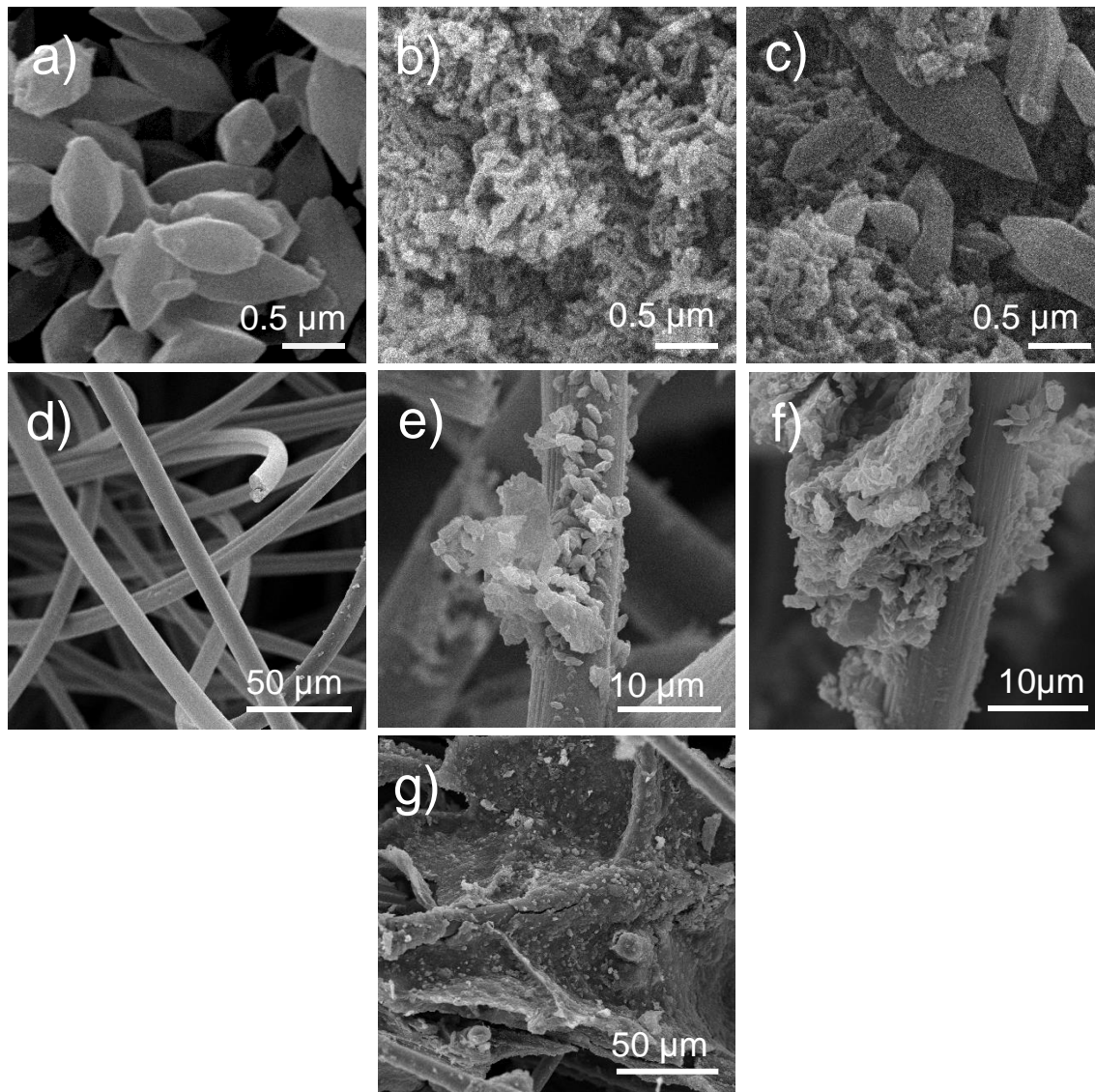


Figure 5.3: SEM images of (a) Fe-MOF (b) PANI (c) PANI/Fe-MOF (d) Bare GF (e) Fe-MOF Coated GF (f) PANI/Fe-MOF Coated GF (g) GF with attached Biofilm

SEM image revealed the successful preparation of spindle-shaped crystals with excellent dispersibility, having an average size of $10\ \mu\text{m}$ as shown in Fig 5.3 (a). Fig 5.3 (b) shows the SEM image of PANI which shows the formation of uniform nanotubes with an average size of $0.1\ \mu\text{m}$. Fig 5.3 (c) displays the SEM image of the Fe-MOF/PANI composite, revealing the presence of PANI nanotubes attached to the Fe-MOF crystals in a needle-like shape. Fig 5.3 (d) displays the SEM image of uncoated GF, revealing the presence of fine fibers with a diameter of $8\ \mu\text{m}$ and a smooth surface. Fig 5.3 (e) depicts the Fe-MOF@GF morphology. It is evident that the surface

of the fibers becomes rougher because of the attachment of MOF crystals, in contrast to the uncoated GF. This observation confirms the presence of the Fe-MOF coating. Fig 5.3 (f) depicts the attachment of PANI/Fe-MOF structure onto the fibers of GF. Fig 5.3 (g) displays SEM image of GF that have been modified with a biofilm. The image clearly reveals a substantial layer of biofilm covering the surface of the GF.

5.4 Contact angle

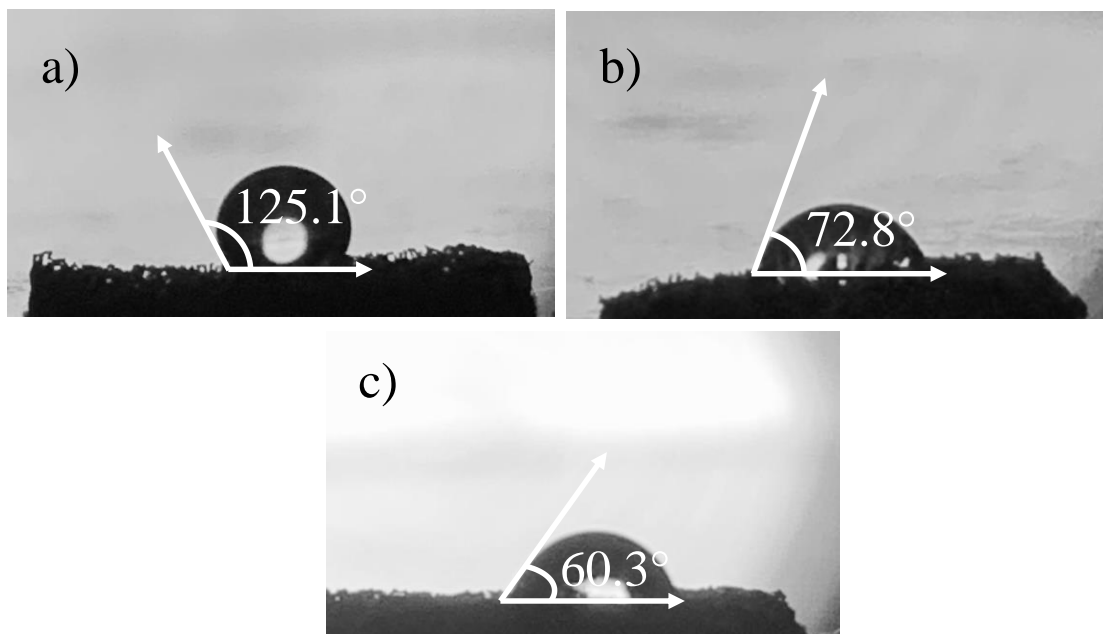


Figure 5.4: Contact angle of a) Bare GF, b) Fe-MOF@GF, c) PANI/Fe-MOF@GF

The contact angle was assessed on bare GF, Fe-MOF@GF, and PANI/Fe-MOF@GF to evaluate the wettability of the electrode materials (as seen in Fig 5.4). Untreated GF is hydrophobic; however, treatment with HCl and H₂O₂ renders it mildly hydrophilic.

Applying PANI/Fe-MOF and Fe-MOF to the GF substantially reduces the contact angle, hence improving its hydrophilicity. Fe-MOF displays a contact angle of 72.8°, significantly lower than that of bare GF at 125.1°, attributable to the presence of carboxylate groups. The incorporation of PANI into the MOF decreases the contact angle from 72.8° to 60.3°, resulting in a very hydrophilic material.

The enhanced hydrophilicity is due to the existence of positively charged sites along the polymer chain, which draw water molecules via ion-dipole interactions. This transition to hydrophilicity improves adhesion and biofilm proliferation on the anode surface.

5.5 Open and Close Circuit Voltage

Initially, we operate all three MFCs to allow sufficient time for the biofilm to develop on the electrode. Once the biofilm has developed and the cell has reached a peak value, we recorded open circuit voltage values throughout the cycle at a COD concentration of 1000.

Sodium acetate served as the primary carbon source. Each time the old medium is substituted with a new medium, the electrical voltage output progressively rises until it reaches a specific peak value. It remains at this level for a certain time period. However, once the carbon supply is exhausted, the voltage output of the batch fed with sodium acetate abruptly decreases.

Fig 5.5 (a) demonstrates that the MFC with a bare GF electrode reached a peak value of 430 mV, while the Fe-MOF@GF MFC achieved a higher peak value of 718 mV compared to the control MFC. The PANI/Fe-MOF@GF MFC recorded the highest value of 810 mV.

Figure 5.5 (b) illustrates the voltage values when a load of 1000 Ω is applied. The Control MFC reached a maximum voltage of 161 mV, whereas the Fe-MOF@GF MFC achieved a higher peak voltage of 202 mV compared to the Control MFC.

The PANI/Fe-MOF@GF MFC achieved the highest recorded value of 319 mV. Applying an additional layer of conductive and modified material to the GF anode improves its conductivity, leading to higher voltages and enhanced stability.

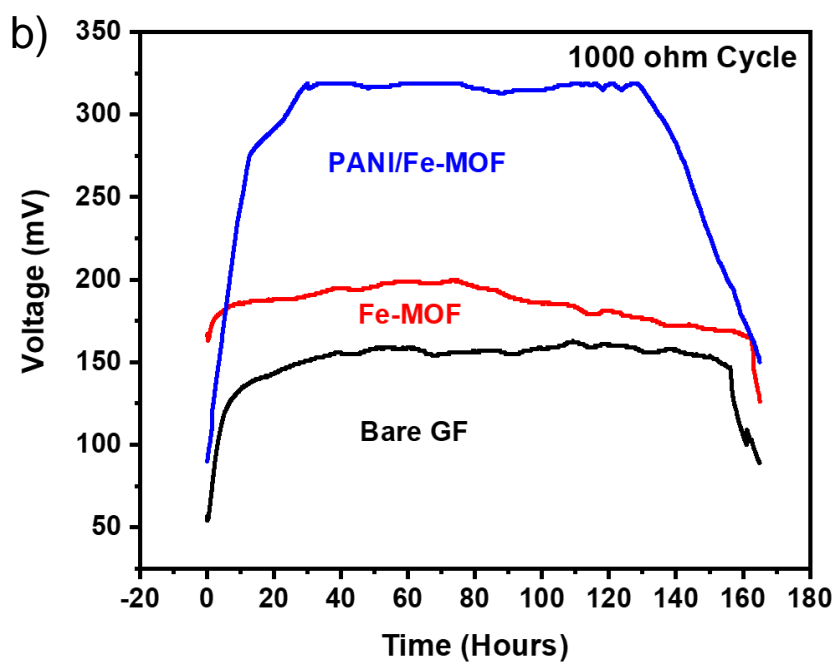
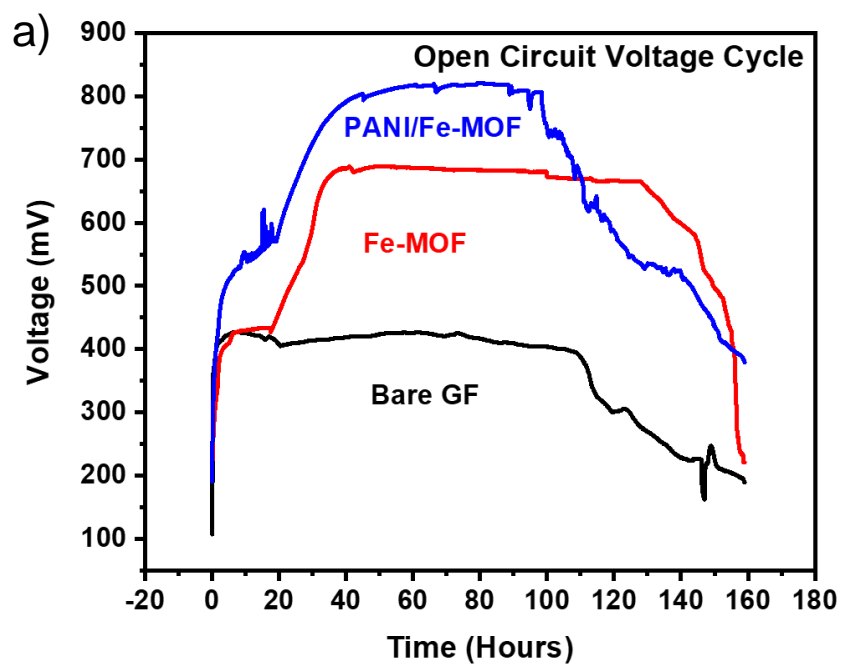


Figure 5.5: a) OCV Bare GF MFC, Fe-MOF@GF MFC, PANI/Fe-MOF@ GF MFC, b) 1000 Ω Voltage cycle for all three MFCs

5.6 Power Density

A polarization curve was plotted by systematically altering the external resistance within the range of 10 to 10000 Ω and logging the corresponding voltage measurements. Values were recorded at 2-minute intervals each time the external resistance was changed. The maximum power density of a MFC can be determined by identifying the highest point on the graph that plots between the current density (x-axis) and power density (y-axis).

The power densities for PANI/Fe-MOF@GF, Fe-MOF@GF, and bare GF MFCs were 277 mW/m^2 , 154 mW/m^2 , and 45 mW/m^2 , respectively, indicating enhancements of 6.16 and 3.43 times compared to bare GF. Heightened polarization diminishes the power output of the MFC. The gradient of a point on the polarization curve at a specific current density indicates the level of polarization at that location. The voltage for polarization curves decreased as the current density increased. The PANI/Fe-MOF@GF MFC demonstrated the least polarization among the other MFCs, indicating a minimal internal resistance of 250 Ω . The PANI/Fe-MOF@GF and Fe-MOF@GF MFCs had the lowest internal resistance at 250 Ω , compared to 1000 Ω for bare GF. Consequently, the MFC with Fe-MOF/PANI@GF anode exhibited superior performance.

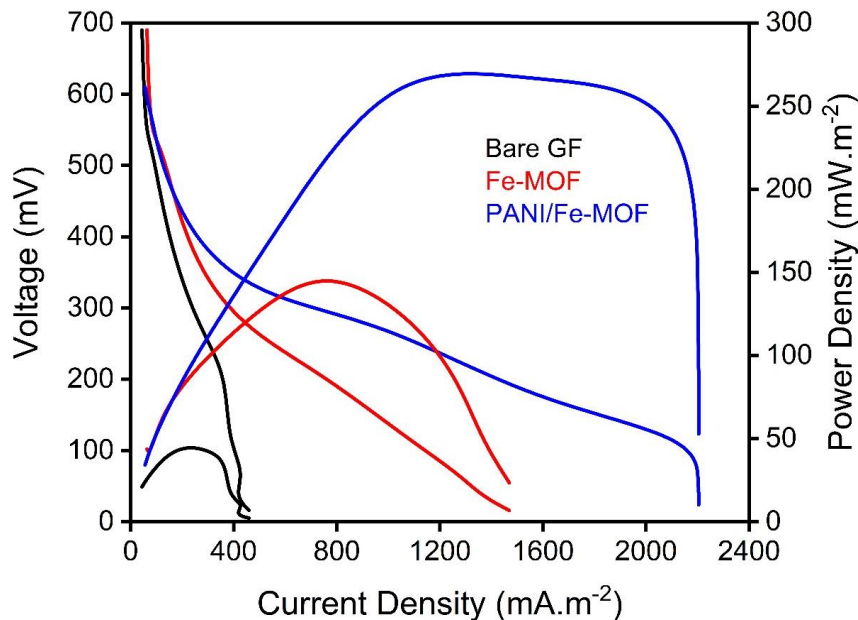


Figure 5.6: Power density and Current density Curves of all three MFCs

5.7 CV

The experimental setup consisted of three electrodes: an Ag/AgCl reference electrode, a working electrode GF/Material Coated GF, and a counter electrode made of platinum wire. The purpose of this setup was to conduct CV measurements in a 1 mM potassium ferricyanide ($K_3[Fe(CN)_6]$) within a 0.3 M potassium hydroxide (KOH) electrolyte solution.

A potential window ranging from -0.2 to 0.6 V was utilized and CV was performed at the scan rate of 10 mVs^{-1} . The anodes' performance was assessed by CV analysis (shown in Fig. 5.7 (a)). Modification of the GF electrode with Fe-MOF and Fe-PANI/Fe-MOF, resulted in an increase in the CV anodic current.

Fig 5(a) illustrates that the PANI/Fe-MOF@GF electrode produced the maximum current output (0.444 mA), succeeded by the Fe-MOF@GF electrode (0.198 mA), and the bare GF electrode (0.114 mA). The area enclosed by the CV curve can be employed to signify the number of electrons transferred at the electrode, indicating the electrode's capacitance. An increased capacitance offers a greater surface area for microbial attachment and additional redox-active sites to accept electrons from an external power source, thus enhancing the electron transfer process [34].

The PANI/Fe-MOF@GF electrode exhibits a capacitance of 16.5 mF/cm^2 , surpassing the Fe-MOF@GF at 8.46 mF/cm^2 and the bare GF electrode at 2.17 mF/cm^2 . This enhancement is attributed to the presence of PANI, which possesses superior redox properties due to nitrogen heteroatoms and the conjugation of π electrons along the polymeric chains, a characteristic lacking in the Fe-MOF and bare electrodes, resulting in lower capacitance values.

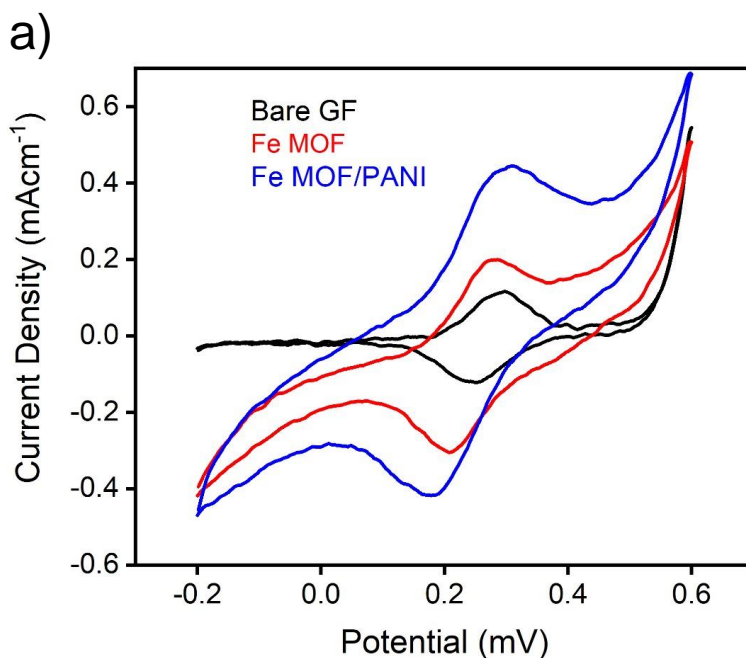
Additionally, to evaluate the bio-electrochemical performance and the role of exoelectrogens in the EET process, CV of bioanodes of PANI/Fe-MOF@GF, Fe-MOF@GF, and bare GF were performed under non-turnover conditions (as shown in Fig. 5.7 (b)).

The CV analysis reveals that the integration of PANI with Fe-MOF markedly enhances the anodic current and increases the number of electrons participating in the process, consequently illustrating better bioelectrocatalytic activity.

The redox peaks in the CV graph were not pronounced due to diminished Faradaic currents. The peaks were identified by analysing the CVs of PANI/Fe-MOF@GF, Fe-MOF@GF, and bare GF MFCs using the first derivative method (as illustrated in Fig 5.7(c)).

Numerous studies have demonstrated that a first derivative technique can uncover concealed redox peaks, which are beneficial for evaluating biofilm activity and tentatively identifying proteins involved in electron transfer processes. The derivative was determined by analysing anodic cyclic voltammograms from positive to negative voltage, revealing potential redox peaks.

More pronounced peaks were detected with PANI/Fe-MOF at potentials of -50 mV and +170 mV vs Ag/AgCl. The peak at approximately 170 mV can be attributed to C-type cytochromes, as confirmed in previous research. In contrast, Fe-MOF and bare GF exhibited diminished peaks, indicating reduced redox activity.



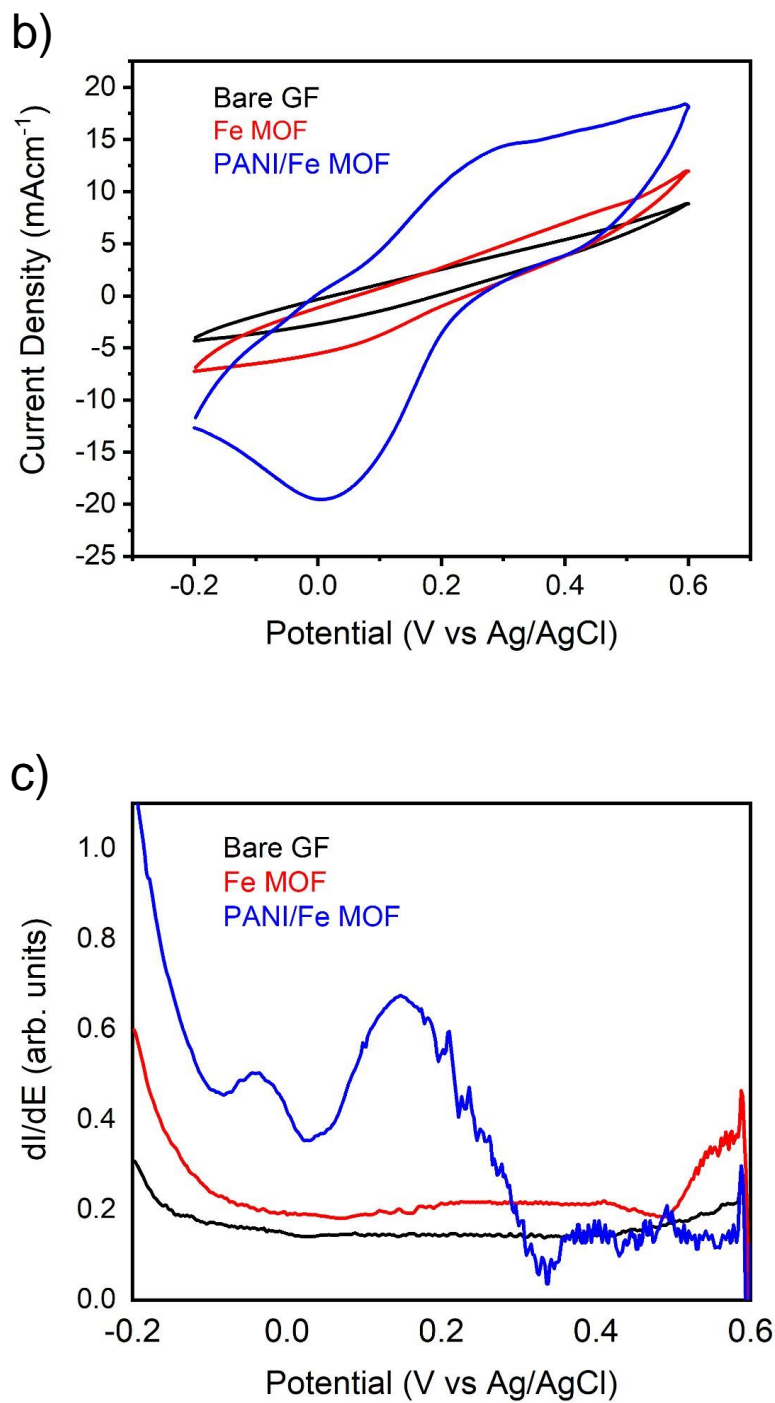


Figure 5.7: a) Cyclic Voltammogram of Bare GF, Fe-MOF@GF and PANI/Fe-MOF@GF, b) Cyclic Voltammogram of Bare GF MFC, Fe-MOF@GF MFC, PANI/Fe-MOF@GF MFC, c) First derivative of CV of Bare GF MFC, Fe-MOF@GF MFC, PANI/Fe-MOF@GF MFC

5.8 EIS

The electrocatalytic performance of PANI/Fe-MOF@GF, Fe-MOF@GF, and bare GF electrodes were evaluated using EIS in a conventional three-electrode configuration (shown in Fig. 5.8). The study indicates that bare GF possesses an Rct of 144 Ω , while Fe-MOF exhibits a Rct of 27.77 Ω . The PANI/Fe-MOF@GF composite exhibits the minimal Rct of 4.91 Ω , signifying optimal electron transfer efficiency in the composite anode. This discovery corresponds with the outcomes of the polarisation curve and voltage graphs.

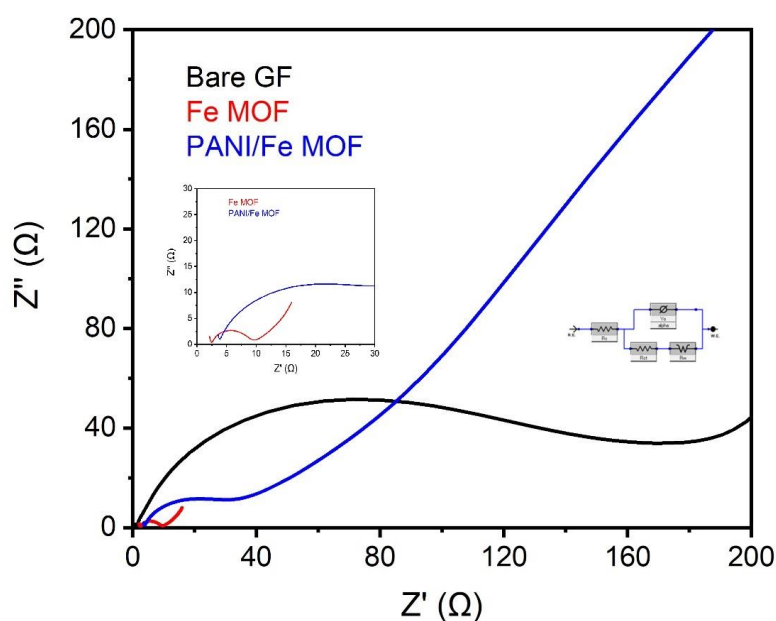


Figure 5.8: Nyquist plot of PANI/Fe-MOF@GF, Fe-MOF@GF, bare GF

CHAPTER 6: CONCLUSIONS AND FUTURE RECOMMENDATION

6.1 Conclusion

The objective of this study is to synthesize Fe-MOF and produce a composite material of PANI/Fe-MOF through an in-situ polymerization process. The materials were characterized using XRD, SEM, and FTIR analysis. Both samples were coated on GF using a straightforward dip and dry coating method. These electrodes were then employed in MFC and operated for several days, and their performance was evaluated.

The electrochemical experiments demonstrated that PANI/Fe-MOF exhibited superior performance compared to the other two electrodes in terms of R_{ct} and capacitance. The power density of PANI/Fe-MOF@GF was determined to be 277 mW/m^2 , while Fe-MOF@GF exhibited a power density of 154 mW/m^2 . In contrast, the uncoated/bare GF yielded a power density of 45 mW/m^2 . The study has verified that the PANI/Fe-MOF@GF anode exhibits higher voltage values at a load of 1000Ω and increased power density and lowered R_{ct} . The increased surface area and protonation of PANI confer positive charges, attracting negatively charged bacteria and facilitating the development of a dense microbial community on the anode, resulting in a reasonably thick biofilm on the PANI/Fe-MOF composite anode. The enhanced results demonstrate that the composite gains from a greater surface area attributed to the incorporation of PANI, efficient charge transfer pathways, and increased microbial adhesion and affinity due to better wettability. Our research provides significant insights into the application of Fe-MOF and its composites in MFCs. In conclusion, our study presents a simple and effective approach for synthesizing composite anode catalysts characterised by high surface area, electrical conductivity, hydrophilicity, and cost-efficiency, thereby markedly improving MFC performance.

6.2 Future Recommendations

There is a need to investigate the utilization of supplementary conductive polymers or nanomaterials in conjunction with Fe-MOF to reduce charge transfer resistance and enhance capacitance.

Examine the influence of different substrate materials and coating techniques on the effectiveness of composite electrodes.

Regarding the PANI/Fe-MOF composite, it is necessary to conduct more research on the interactions between different microbial communities and the composite. This will help us gain a better understanding of the mechanisms that contribute to enhanced biofilm formation and electron transfer. Conduct an experiment to modify the surface properties of the PANI/Fe-MOF composite to improve the attachment and proliferation of microorganisms. Performing a cost-benefit analysis to assess the economic feasibility of expanding the production of PANI/Fe-MOF composites for commercial purposes.

By implementing these suggestions, future research can build upon the positive findings of this study, enhancing the field of MFCs and the broader utilization of PANI/Fe-MOF materials in energy and environmental technology.

REFERENCES

- [1] B. E. Logan *et al.*, "Microbial Fuel Cells: Methodology and Technology," *Environmental Science & Technology*, vol. 40, no. 17, pp. 5181-5192, 2006/09/01 2006, doi: 10.1021/es0605016.
- [2] K. Rabaey *et al.*, "Microbial ecology meets electrochemistry: electricity-driven and driving communities," *The ISME Journal*, vol. 1, no. 1, pp. 9-18, 2007/05/01 2007, doi: 10.1038/ismej.2007.4.
- [3] Y. Zhang, B. Min, L. Huang, and I. Angelidaki, "Electricity generation and microbial community response to substrate changes in microbial fuel cell," *Bioresource Technology*, vol. 102, no. 2, pp. 1166-1173, 2011/01/01/ 2011, doi: <https://doi.org/10.1016/j.biortech.2010.09.044>.
- [4] G. Wareen *et al.*, "Comparison of pennywort and hyacinth in the development of membraned sediment plant microbial fuel cell for waste treatment," *Chemosphere*, vol. 313, p. 137422, 2023/02/01/ 2023, doi: <https://doi.org/10.1016/j.chemosphere.2022.137422>.
- [5] T. Niu, H. Zhu, B. Shutes, and C. He, "Gaseous carbon and nitrogen emissions from microbial fuel cell-constructed wetlands with different carbon sources: Microbiota-driven mechanisms," *Journal of Cleaner Production*, vol. 435, p. 140404, 2024/01/05/ 2024, doi: <https://doi.org/10.1016/j.jclepro.2023.140404>.
- [6] T. Cai *et al.*, "Application of advanced anodes in microbial fuel cells for power generation: A review," *Chemosphere*, vol. 248, p. 125985, 01/21 2020, doi: 10.1016/j.chemosphere.2020.125985.
- [7] S. Kitagawa, "Metal–organic frameworks (MOFs)," *Chemical Society Reviews*, vol. 43, no. 16, pp. 5415-5418, 2014.
- [8] H. Furukawa, K. E. Cordova, M. O’Keeffe, and O. M. Yaghi, "The chemistry and applications of metal-organic frameworks," *Science*, vol. 341, no. 6149, p. 1230444, 2013.

- [9] Q.-L. Zhu and Q. Xu, "Metal–organic framework composites," *Chemical Society Reviews*, vol. 43, no. 16, pp. 5468-5512, 2014.
- [10] H. Meng *et al.*, "Conductive metal–organic frameworks: design, synthesis, and applications," *Small Methods*, vol. 4, no. 10, p. 2000396, 2020.
- [11] C. P. Raptopoulou, "Metal-organic frameworks: Synthetic methods and potential applications," *Materials*, vol. 14, no. 2, p. 310, 2021.
- [12] S. A. E. Naser, K. O. Badmus, and L. Khotseng, "Synthesis, properties, and applications of metal organic frameworks supported on graphene oxide," *Coatings*, vol. 13, no. 8, p. 1456, 2023.
- [13] H. Roy *et al.*, "Microbial fuel cell construction features and application for sustainable wastewater treatment," *Membranes*, vol. 13, no. 5, p. 490, 2023.
- [14] A. A. Yaqoob, M. N. Mohamad Ibrahim, M. Rafatullah, Y. S. Chua, A. Ahmad, and K. Umar, "Recent advances in anodes for microbial fuel cells: An overview," *Materials*, vol. 13, no. 9, p. 2078, 2020.
- [15] S. Dharmalingam, V. Kugarajah, and M. Sugumar, "Membranes for microbial fuel cells," in *Microbial Electrochemical Technology*: Elsevier, 2019, pp. 143-194.
- [16] J. Khera and A. Chandra, "Microbial fuel cells: recent trends," *Proceedings of the National Academy of Sciences, India Section A: Physical Sciences*, vol. 82, pp. 31-41, 2012.
- [17] R. C. O. Tang *et al.*, "Review on design factors of microbial fuel cells using Buckingham's Pi Theorem," *Renewable and Sustainable Energy Reviews*, vol. 130, p. 109878, 2020.
- [18] N. Degrenne, B. Allard, F. Buret, F. Morel, S.-E. Adami, and D. Labrousse, "Comparison of 3 self-starting step-up DC: DC converter topologies for harvesting energy from low-voltage and low-power microbial fuel cells," in *Proceedings of the 2011 14th European Conference on Power Electronics and Applications*, 2011: IEEE, pp. 1-10.

- [19] R. Selvasembian *et al.*, "Recent progress in microbial fuel cells for industrial effluent treatment and energy generation: Fundamentals to scale-up application and challenges," *Bioresource technology*, vol. 346, p. 126462, 2022.
- [20] A. Nawaz *et al.*, "Microbial fuel cells: Insight into simultaneous wastewater treatment and bioelectricity generation," *Process Safety and Environmental Protection*, vol. 161, pp. 357-373, 2022.
- [21] J. D. López-Hincapié, A. R. Picos-Benítez, B. Cercado, F. Rodríguez, and A. Rodríguez-García, "Improving the conFIGuration and architecture of a small-scale air-cathode single chamber microbial fuel cell (MFC) for biosensing organic matter in wastewater samples," *Journal of Water Process Engineering*, vol. 38, p. 101671, 2020/12/01/ 2020, doi: <https://doi.org/10.1016/j.jwpe.2020.101671>.
- [22] K. Obileke, H. Onyeaka, E. L. Meyer, and N. Nwokolo, "Microbial fuel cells, a renewable energy technology for bio-electricity generation: A mini-review," *Electrochemistry Communications*, vol. 125, p. 107003, 2021.
- [23] A. T. Hoang *et al.*, "Microbial fuel cells for bioelectricity production from waste as sustainable prospect of future energy sector," *Chemosphere*, vol. 287, p. 132285, 2022.
- [24] I. M. Abu-Reesh, "Single- and Multi-Objective Optimization of a Dual-Chamber Microbial Fuel Cell Operating in Continuous-Flow Mode at Steady State," *Processes*, vol. 8, no. 7, doi: 10.3390/pr8070839.
- [25] Z. Du, H. Li, and T. Gu, "A state of the art review on microbial fuel cells: A promising technology for wastewater treatment and bioenergy," *Biotechnology advances*, vol. 25, pp. 464-82, 09/01 2007, doi: 10.1016/j.biotechadv.2007.05.004.
- [26] M. T. Matsena, B. Kholisa, and E. M. N. Chirwa, "Key operational parameters assessment for a chromium (VI)-reducing annular upflow microbial fuel cell," *Journal of Power Sources*, vol. 590, p. 233794, 2024/01/15/ 2024, doi: <https://doi.org/10.1016/j.jpowsour.2023.233794>.

- [27] L. Mekuto, A. Olowolafe, S. Pandit, N. Dyantyi, P. Nomngongo, and R. Huberts, "Microalgae as a biocathode and feedstock in anode chamber for a self-sustainable microbial fuel cell technology: A review," 01/01 2020, doi: 10.1016/j.sajce.2019.10.002.
- [28] I. A. Ieropoulos, J. Greenman, C. Melhuish, and J. Hart, "Comparative study of three types of microbial fuel cell," *Enzyme and microbial technology*, vol. 37, no. 2, pp. 238-245, 2005.
- [29] S. Prathiba, P. S. Kumar, and D.-V. N. Vo, "Recent advancements in microbial fuel cells: A review on its electron transfer mechanisms, microbial community, types of substrates and design for bio-electrochemical treatment," *Chemosphere*, vol. 286, p. 131856, 2022/01/01/ 2022, doi: <https://doi.org/10.1016/j.chemosphere.2021.131856>.
- [30] K. Watanabe, "Recent Developments in Microbial Fuel Cell Technologies for Sustainable Bioenergy," *Journal of Bioscience and Bioengineering*, vol. 106, no. 6, pp. 528-536, 2008/12/01/ 2008, doi: <https://doi.org/10.1263/jbb.106.528>.
- [31] K. Watanabe, "Recent developments in microbial fuel cell technologies for sustainable bioenergy," (in eng), no. 1347-4421 (Electronic).
- [32] P. Clauwaert *et al.*, "Minimizing losses in bio-electrochemical systems: the road to applications," *Applied microbiology and biotechnology*, vol. 79, pp. 901-913, 2008.
- [33] Y. Liu, F. Harnisch, K. Fricke, U. Schröder, V. Climent, and J. M. Feliu, "The study of electrochemically active microbial biofilms on different carbon-based anode materials in microbial fuel cells," *Biosensors and Bioelectronics*, vol. 25, no. 9, pp. 2167-2171, 2010/05/15/ 2010, doi: <https://doi.org/10.1016/j.bios.2010.01.016>.
- [34] S. A. Patil, F. Harnisch, B. Kapadnis, and U. Schröder, "Electroactive mixed culture biofilms in microbial bioelectrochemical systems: The role of temperature for biofilm formation and performance," *Biosensors and Bioelectronics*, vol. 26, no. 2, pp. 803-808, 2010/10/15/ 2010, doi: <https://doi.org/10.1016/j.bios.2010.06.019>.
- [35] F. Liang, Y. Xiao, and F. Zhao, "Effect of pH on sulfate removal from wastewater using a bioelectrochemical system," *Chemical Engineering Journal*, vol. 218, pp. 147-153, 2013.

- [36] J. Rousk *et al.*, "Soil bacterial and fungal communities across a pH gradient in an arable soil," *The ISME journal*, vol. 4, no. 10, pp. 1340-1351, 2010.
- [37] X. Zhang, X. Li, X. Zhao, and Y. Li, "Factors affecting the efficiency of a bioelectrochemical system: a review," *RSC advances*, vol. 9, no. 34, pp. 19748-19761, 2019.
- [38] M. A. Massoud, A. Tarhini, and J. A. Nasr, "Decentralized approaches to wastewater treatment and management: Applicability in developing countries," *Journal of Environmental Management*, vol. 90, no. 1, pp. 652-659, 2009/01/01/ 2009, doi: <https://doi.org/10.1016/j.jenvman.2008.07.001>.
- [39] S. P. Jung and S. Pandit, "Important factors influencing microbial fuel cell performance," in *Microbial electrochemical technology*: Elsevier, 2019, pp. 377-406.
- [40] S. Venkata Mohan, G. Velvizhi, J. Annie Modestra, and S. Srikanth, "Microbial fuel cell: Critical factors regulating bio-catalyzed electrochemical process and recent advancements," *Renewable and Sustainable Energy Reviews*, vol. 40, pp. 779-797, 2014/12/01/ 2014, doi: <https://doi.org/10.1016/j.rser.2014.07.109>.
- [41] J. Wei, P. Liang, and X. Huang, "Recent progress in electrodes for microbial fuel cells," *Bioresour. Technol.*, vol. 102, no. 20, pp. 9335-9344, 2011/10/01/ 2011, doi: <https://doi.org/10.1016/j.biortech.2011.07.019>.
- [42] P. Aelterman, M. Versichele, M. Marzorati, N. Boon, and W. Verstraete, "Loading rate and external resistance control the electricity generation of microbial fuel cells with different three-dimensional anodes," *Bioresour. Technol.*, vol. 99, no. 18, pp. 8895-8902, 2008/12/01/ 2008, doi: <https://doi.org/10.1016/j.biortech.2008.04.061>.
- [43] S. Oh, B. E. Min B Fau - Logan, and B. E. Logan, "Cathode performance as a factor in electricity generation in microbial fuel cells," (in eng), no. 0013-936X (Print).
- [44] J. K. Jang *et al.*, "Construction and operation of a novel mediator- and membrane-less microbial fuel cell," *Process Biochemistry*, vol. 39, no. 8, pp. 1007-1012, 2004/04/30/ 2004, doi: [https://doi.org/10.1016/S0032-9592\(03\)00203-6](https://doi.org/10.1016/S0032-9592(03)00203-6).

- [45] B. Min and B. E. Logan, "Continuous Electricity Generation from Domestic Wastewater and Organic Substrates in a Flat Plate Microbial Fuel Cell," *Environmental Science & Technology*, vol. 38, no. 21, pp. 5809-5814, 2004/11/01 2004, doi: 10.1021/es0491026.
- [46] D. Pant, G. Van Bogaert, L. Diels, and K. Vanbroekhoven, "A review of the substrates used in microbial fuel cells (MFCs) for sustainable energy production," *Bioresource Technology*, vol. 101, no. 6, pp. 1533-1543, 2010/03/01/ 2010, doi: <https://doi.org/10.1016/j.biortech.2009.10.017>.
- [47] D. Pant *et al.*, "Bioelectrochemical systems (BES) for sustainable energy production and product recovery from organic wastes and industrial wastewaters," *RSC Advances*, 10.1039/C1RA00839K vol. 2, no. 4, pp. 1248-1263, 2012, doi: 10.1039/C1RA00839K.
- [48] J. C. Biffinger, J. Pietron, R. Ray, B. Little, and B. R. Ringeisen, "A biofilm enhanced miniature microbial fuel cell using *Shewanella oneidensis* DSP10 and oxygen reduction cathodes," *Biosensors and Bioelectronics*, vol. 22, no. 8, pp. 1672-1679, 2007.
- [49] H. Lin, X. Wu, C. Miller, and J. Zhu, "Improved performance of microbial fuel cells enriched with natural microbial inocula and treated by electrical current," *Biomass and bioenergy*, vol. 54, pp. 170-180, 2013.
- [50] C. Abourached, M. J. English, and H. Liu, "Wastewater treatment by Microbial Fuel Cell (MFC) prior irrigation water reuse," *Journal of Cleaner Production*, vol. 137, pp. 144-149, 2016/11/20/ 2016, doi: <https://doi.org/10.1016/j.jclepro.2016.07.048>.
- [51] D. C. Holzman, "Microbe power!," ed: National Institute of Environmental Health Sciences, 2005.
- [52] R. Goswami and V. K. Mishra, "A review of design, operational conditions and applications of microbial fuel cells," *Biofuels*, vol. 9, no. 2, pp. 203-220, 2018.
- [53] M. Guo, W. Song, and J. Buhain, "Bioenergy and biofuels: History, status, and perspective," *Renewable and Sustainable Energy Reviews*, vol. 42, pp. 712-725, 2015, doi: 10.1016/j.rser.2014.10.013.

- [54] J. V. Boas, V. B. Oliveira, M. Simões, and A. M. F. R. Pinto, "Review on microbial fuel cells applications, developments and costs," *Journal of Environmental Management*, vol. 307, p. 114525, 2022/04/01/ 2022, doi: <https://doi.org/10.1016/j.jenvman.2022.114525>.
- [55] J. V. Boas, V. B. Oliveira, M. Simões, and A. M. Pinto, "Review on microbial fuel cells applications, developments and costs," *Journal of Environmental Management*, vol. 307, p. 114525, 2022.
- [56] H. M. Saeed *et al.*, "Microbial desalination cell technology: a review and a case study," *Desalination*, vol. 359, pp. 1-13, 2015.
- [57] K. Rabaey, S. D. Lissens G Fau - Siciliano, W. Siciliano Sd Fau - Verstraete, and W. Verstraete, "A microbial fuel cell capable of converting glucose to electricity at high rate and efficiency," (in eng), no. 0141-5492 (Print).
- [58] A. A. Yaqoob, M. N. M. Ibrahim, and C. Guerrero-Barajas, "Modern trend of anodes in microbial fuel cells (MFCs): An overview," *Environmental Technology & Innovation*, vol. 23, p. 101579, 2021/08/01/ 2021, doi: <https://doi.org/10.1016/j.eti.2021.101579>.
- [59] A. Singh, "Eco-Affectionate Face of Microbial Fuel Cells," *Critical Reviews in Environmental Science and Technology*, vol. 44, 01/01 2014, doi: [10.1080/10643389.2012.710445](https://doi.org/10.1080/10643389.2012.710445).
- [60] H. Zafar, N. Peleato, and D. Roberts, "A review of the role of pre-treatment on the treatment of food waste using microbial fuel cells," *Environmental Technology Reviews*, vol. 11, pp. 72-90, 12/31 2022, doi: [10.1080/21622515.2022.2058426](https://doi.org/10.1080/21622515.2022.2058426).
- [61] S. G. A. Flimban, I. M. I. Ismail, T. Kim, and S.-E. Oh, "Overview of Recent Advancements in the Microbial Fuel Cell from Fundamentals to Applications: Design, Major Elements, and Scalability," *Energies*, vol. 12, no. 17, doi: [10.3390/en12173390](https://doi.org/10.3390/en12173390).
- [62] V. R. Nimje *et al.*, "A single-chamber microbial fuel cell without an air cathode," (in eng), no. 1422-0067 (Electronic).

- [63] S. B. Velasquez-Orta, I. M. Head, T. P. Curtis, and K. Scott, "Factors affecting current production in microbial fuel cells using different industrial wastewaters," *Bioresource Technology*, vol. 102, no. 8, pp. 5105-5112, 2011/04/01/ 2011, doi: <https://doi.org/10.1016/j.biortech.2011.01.059>.
- [64] S. R. Babu Arulmani, H. L. Ganamuthu, V. Ashokkumar, G. Govindarajan, S. Kandasamy, and H. Zhang, "Biofilm formation and electrochemical metabolic activity of *Ochrobactrum* Sp JSRB-1 and *Cupriavidus* Sp JSRB-2 for energy production," *Environmental Technology & Innovation*, vol. 20, p. 101145, 2020/11/01/ 2020, doi: <https://doi.org/10.1016/j.eti.2020.101145>.
- [65] M. Rahimnejad, A. Adhami, S. Darvari, A. Zirepour, and S.-E. Oh, "Microbial fuel cell as new technology for bioelectricity generation: A review," *Alexandria Engineering Journal*, vol. 54, no. 3, pp. 745-756, 2015/09/01/ 2015, doi: <https://doi.org/10.1016/j.aej.2015.03.031>.
- [66] D. Das, *Microbial fuel cell : a bioelectrochemical system that converts waste to watts*, Cham, Switzerland: Springer Cham, Switzerland, 2018. [Online]. Available: <https://search.ebscohost.com/login.aspx?direct=true&scope=site&db=nlebk&db=nlabk&AN=1651387>.
- [67] H. Wang, L. Lu, D. Liu, F. Cui, and P. Wang, "Characteristic changes in algal organic matter derived from *Microcystis aeruginosa* in microbial fuel cells," *Bioresource Technology*, vol. 195, pp. 25-30, 2015/11/01/ 2015, doi: <https://doi.org/10.1016/j.biortech.2015.06.014>.
- [68] D. Bond and D. Lovley, "Bond DR, Lovley DR.. Evidence for involvement of an electron shuttle in electricity generation by *Geothrix fermentans*. *Appl Environ Microbiol* 71: 2186-2189," *Applied and environmental microbiology*, vol. 71, pp. 2186-9, 04/01 2005, doi: 10.1128/AEM.71.4.2186-2189.2005.
- [69] S. Roy, S. Marzorati, A. Schievano, and D. Pant, "Microbial Fuel Cells," 2016, pp. 1-15.

- [70] T. J. Park *et al.*, "Microbial community in microbial fuel cell (MFC) medium and effluent enriched with purple photosynthetic bacterium (*Rhodospseudomonas* sp.)," (in eng), no. 2191-0855 (Print).
- [71] M. Hatamoto, Y. Imachi H Fau - Yashiro, A. Yashiro Y Fau - Ohashi, H. Ohashi A Fau - Harada, and H. Harada, "Detection of active butyrate-degrading microorganisms in methanogenic sludges by RNA-based stable isotope probing," (in eng), no. 1098-5336 (Electronic).
- [72] A. Popova *et al.*, "Enrichment strategy for enhanced bioelectrochemical hydrogen production and the prevention of methanogenesis," *International Journal of Hydrogen Energy*, vol. 41, 02/01 2016, doi: 10.1016/j.ijhydene.2016.01.014.
- [73] A. A. Mier *et al.*, "A review of recent advances in electrode materials for emerging bioelectrochemical systems: From biofilm-bearing anodes to specialized cathodes," (in eng), no. 1879-1298 (Electronic).
- [74] X. Xie *et al.*, "Three-Dimensional Carbon Nanotube–Textile Anode for High-Performance Microbial Fuel Cells," *Nano Letters*, vol. 11, no. 1, pp. 291-296, 2011/01/12 2011, doi: 10.1021/nl103905t.
- [75] J. M. Sonawane, A. Yadav, P. C. Ghosh, and S. B. Adeloju, "Recent advances in the development and utilization of modern anode materials for high performance microbial fuel cells," (in eng), no. 1873-4235 (Electronic).
- [76] X. Wang, Y. Cheng S Fau - Feng, M. D. Feng Y Fau - Merrill, T. Merrill Md Fau - Saito, B. E. Saito T Fau - Logan, and B. E. Logan, "Use of carbon mesh anodes and the effect of different pretreatment methods on power production in microbial fuel cells," (in eng), no. 0013-936X (Print).
- [77] H. Cai, J. Wang, Y. Bu, and Q. Zhong, "Treatment of carbon cloth anodes for improving power generation in a dual-chamber microbial fuel cell," *Journal of Chemical Technology and Biotechnology*, vol. 88, 04/01 2013, doi: 10.1002/jctb.3875.

- [78] W. Zhu *et al.*, "Enhanced extracellular electron transfer between *Shewanella putrefaciens* and carbon felt electrode modified by bio-reduced graphene oxide," *Science of The Total Environment*, vol. 691, pp. 1089-1097, 2019/11/15/ 2019, doi: <https://doi.org/10.1016/j.scitotenv.2019.07.104>.
- [79] X. Li, S. Mettu, G. J. O. Martin, M. Ashokkumar, and C. S. K. Lin, "Ultrasonic pretreatment of food waste to accelerate enzymatic hydrolysis for glucose production," *Ultrasonics Sonochemistry*, vol. 53, pp. 77-82, 2019/05/01/ 2019, doi: <https://doi.org/10.1016/j.ultsonch.2018.12.035>.
- [80] C. Chen, A. Chaudhary, and A. Mathys, "Nutritional and environmental losses embedded in global food waste," *Resources, Conservation and Recycling*, vol. 160, p. 104912, 2020/09/01/ 2020, doi: <https://doi.org/10.1016/j.resconrec.2020.104912>.
- [81] Y. Shen, Y. Zhou, S. Chen, F. Yang, S. Zheng, and H. Hou, "Carbon Nanofibers Modified Graphite Felt for High Performance Anode in High Substrate Concentration Microbial Fuel Cells," *The Scientific World Journal*, vol. 2014, p. 130185, 2014/04/22 2014, doi: [10.1155/2014/130185](https://doi.org/10.1155/2014/130185).
- [82] H.-F. Cui, L. Du, P.-B. Guo, B. Zhu, and J. H. T. Luong, "Controlled modification of carbon nanotubes and polyaniline on macroporous graphite felt for high-performance microbial fuel cell anode," *Journal of Power Sources*, vol. 283, no. C, pp. 46-53, 2015, doi: [10.1016/j.jpowsour.2015.02.088](https://doi.org/10.1016/j.jpowsour.2015.02.088).
- [83] H. Chen *et al.*, "Impact of liquid velocity and stacking modes on the performance of anaerobic fluidized bed microbial fuel cell," *Powder Technology*, vol. 433, p. 119264, 2024/01/15/ 2024, doi: <https://doi.org/10.1016/j.powtec.2023.119264>.
- [84] J. X. Leong, W. R. W. Daud, M. Ghasemi, K. B. Liew, and M. Ismail, "Ion exchange membranes as separators in microbial fuel cells for bioenergy conversion: A comprehensive review," *Renewable and Sustainable Energy Reviews*, vol. 28, pp. 575-587, 2013/12/01/ 2013, doi: <https://doi.org/10.1016/j.rser.2013.08.052>.

- [85] H. Liu, S. Cheng, and B. E. Logan, "Power Generation in Fed-Batch Microbial Fuel Cells as a Function of Ionic Strength, Temperature, and Reactor ConFIGuration," *Environmental Science & Technology*, vol. 39, no. 14, pp. 5488-5493, 2005/07/01 2005, doi: 10.1021/es050316c.
- [86] T. Liu, Y.-y. Yu, D. Li, H. Song, X. Yan, and W. N. Chen, "The effect of external resistance on biofilm formation and internal resistance in *Shewanella* inoculated microbial fuel cells," *RSC Advances*, 10.1039/C5RA26125B vol. 6, no. 24, pp. 20317-20323, 2016, doi: 10.1039/C5RA26125B.
- [87] Z. Wang *et al.*, "Effects of soluble flavin on heterogeneous electron transfer between surface-exposed bacterial cytochromes and iron oxides," *Geochimica et Cosmochimica Acta*, vol. 163, pp. 299-310, 2015/08/15/ 2015, doi: <https://doi.org/10.1016/j.gca.2015.03.039>.
- [88] B. Min, B. E. Cheng S Fau - Logan, and B. E. Logan, "Electricity generation using membrane and salt bridge microbial fuel cells," (in eng), no. 0043-1354 (Print).
- [89] B. E. Logan, "Exoelectrogenic bacteria that power microbial fuel cells," *Nature Reviews Microbiology*, vol. 7, no. 5, pp. 375-381, 2009/05/01 2009, doi: 10.1038/nrmicro2113.
- [90] J. I. Chang, J. J. Tsai, and K. H. Wu, "Thermophilic composting of food waste," *Bioresource Technology*, vol. 97, no. 1, pp. 116-122, 2006/01/01/ 2006, doi: <https://doi.org/10.1016/j.biortech.2005.02.013>.
- [91] A. Nandy and P. Kundu, "ConFIGurations of Microbial Fuel Cells," 2018.
- [92] X. Jin, N. Yang, Y. Liu, F. Guo, and H. Liu, "Bifunctional cathode using a biofilm and Pt/C catalyst for simultaneous electricity generation and nitrification in microbial fuel cells," (in eng), no. 1873-2976 (Electronic).
- [93] F. Wang *et al.*, "Synchronously electricity generation and degradation of biogas slurry using microbial fuel cell," *Renewable Energy*, vol. 142, 04/01 2019, doi: 10.1016/j.renene.2019.04.063.

- [94] C. Santoro *et al.*, "Cathode materials for ceramic based microbial fuel cells (MFCs)," *International Journal of Hydrogen Energy*, vol. 40, no. 42, pp. 14706-14715, 2015/11/09/2015, doi: <https://doi.org/10.1016/j.ijhydene.2015.07.054>.
- [95] K.-Y. Kim, W. Yang, and B. E. Logan, "Impact of electrode configurations on retention time and domestic wastewater treatment efficiency using microbial fuel cells," *Water Research*, vol. 80, pp. 41-46, 2015/09/01/2015, doi: <https://doi.org/10.1016/j.watres.2015.05.021>.
- [96] L. Zhang, L. Jun, X. Zhu, D. Ye, Q. Fu, and Q. Liao, "Startup Performance and Anodic Biofilm Distribution in Continuous-Flow Microbial Fuel Cells with Serpentine Flow Fields: Effects of External Resistance," *Industrial & Engineering Chemistry Research*, vol. 56, 03/22 2017, doi: [10.1021/acs.iecr.6b04619](https://doi.org/10.1021/acs.iecr.6b04619).
- [97] M. Zhang, Z. Ma, N. Zhao, K. Zhang, and H. Song, "Increased power generation from cylindrical microbial fuel cell inoculated with *P. aeruginosa*," (in eng), no. 1873-4235 (Electronic).
- [98] M. Zhou, M. Chi, J. Luo, H. He, and T. Jin, "An overview of electrode materials in microbial fuel cells," *Journal of Power Sources*, vol. 196, no. 10, pp. 4427-4435, 2011/05/15/2011, doi: <https://doi.org/10.1016/j.jpowsour.2011.01.012>.
- [99] E. Ji *et al.*, "Interface resistances of anion exchange membranes in microbial fuel cells with low ionic strength," (in English), *Biosensors and Bioelectronics*, vol. 26, no. 7, pp. 3266-3271, 2011, doi: [10.1016/j.bios.2010.12.039](https://doi.org/10.1016/j.bios.2010.12.039).
- [100] S. E. Oh, J. H. Kim Jr Fau - Joo, B. E. Joo Jh Fau - Logan, and B. E. Logan, "Effects of applied voltages and dissolved oxygen on sustained power generation by microbial fuel cells," (in eng), no. 0273-1223 (Print).
- [101] S. V. Raghavulu, S. V. Mohan, R. K. Goud, and P. N. Sarma, "Effect of anodic pH microenvironment on microbial fuel cell (MFC) performance in concurrence with aerated and ferricyanide catholytes," *Electrochemistry Communications*, vol. 11, no. 2, pp. 371-375, 2009, doi: [10.1016/j.elecom.2008.11.038](https://doi.org/10.1016/j.elecom.2008.11.038).

- [102] A. Kaushik and A. Chetal, "Power generation in microbial fuel cell fed with post methanation distillery effluent as a function of pH microenvironment," *Bioresource Technology*, vol. 147, pp. 77-83, 2013/11/01/ 2013, doi: <https://doi.org/10.1016/j.biortech.2013.08.004>.
- [103] M. Wang, Z. Wang, X. Gong, and Z. Guo, "The intensification technologies to water electrolysis for hydrogen production – A review," *Renewable and Sustainable Energy Reviews*, vol. 29, pp. 573-588, 2014, doi: 10.1016/j.rser.2013.08.090.
- [104] S. Puig, M. Serra M Fau - Coma, M. Coma M Fau - Cabré, M. D. Cabré M Fau - Balaguer, J. Balaguer Md Fau - Colprim, and J. Colprim, "Effect of pH on nutrient dynamics and electricity production using microbial fuel cells," (in eng), no. 1873-2976 (Electronic).
- [105] A. P. Borole, C. O'Neill H Fau - Tsouris, S. Tsouris C Fau - Cesar, and S. Cesar, "A microbial fuel cell operating at low pH using the acidophile *Acidiphilium cryptum*," (in eng), no. 0141-5492 (Print).
- [106] M. Dopson, G. Ni, and T. H. J. A. Sleutels, "Possibilities for extremophilic microorganisms in microbial electrochemical systems," *FEMS Microbiology Reviews*, vol. 40, no. 2, pp. 164-181, 2016, doi: 10.1093/femsre/fuv044.
- [107] V. B. Oliveira, M. Simões, L. F. Melo, and A. M. F. R. Pinto, "Overview on the developments of microbial fuel cells," *Biochemical Engineering Journal*, vol. 73, pp. 53-64, 2013/04/15/ 2013, doi: <https://doi.org/10.1016/j.bej.2013.01.012>.
- [108] P. Nouri and G. Najafpour Darzi, "Impacts of process parameters optimization on the performance of the annular single chamber microbial fuel cell in wastewater treatment," (in eng), no. 1618-0240 (Print).
- [109] S. Venkata Mohan, S. Veer Raghavulu, and P. N. Sarma, "Biochemical evaluation of bioelectricity production process from anaerobic wastewater treatment in a single chambered microbial fuel cell (MFC) employing glass wool membrane," *Biosensors and Bioelectronics*, vol. 23, no. 9, pp. 1326-1332, 2008/04/15/ 2008, doi: <https://doi.org/10.1016/j.bios.2007.11.016>.

- [110] A. Larrosa-Guerrero, K. Scott, I. M. Head, F. Mateo, A. Ginesta, and C. Godinez, "Effect of temperature on the performance of microbial fuel cells," *Fuel*, vol. 89, no. 12, pp. 3985-3994, 2010/12/01/ 2010, doi: <https://doi.org/10.1016/j.fuel.2010.06.025>.
- [111] I. S. Michie, J. R. Kim, R. M. Dinsdale, A. J. Guwy, and G. C. Premier, "The influence of psychrophilic and mesophilic start-up temperature on microbial fuel cell system performance," *Energy & Environmental Science*, 10.1039/C0EE00483A vol. 4, no. 3, pp. 1011-1019, 2011, doi: 10.1039/C0EE00483A.
- [112] K. A. Dwivedi, S. J. Huang, C. T. Wang, and S. Kumar, "Fundamental understanding of microbial fuel cell technology: Recent development and challenges," (in eng), no. 1879-1298 (Electronic).
- [113] K. P. Katuri, K. Scott, I. M. Head, C. Picioreanu, and T. P. Curtis, "Microbial fuel cells meet with external resistance," *Bioresour. Technol.*, vol. 102, no. 3, pp. 2758-2766, 2011/02/01/ 2011, doi: <https://doi.org/10.1016/j.biortech.2010.10.147>.
- [114] Y. Ahn and B. E. Logan, "A multi-electrode continuous flow microbial fuel cell with separator electrode assembly design," (in eng), no. 1432-0614 (Electronic).
- [115] Y. Fan, E. Sharbrough, and H. Liu, "Quantification of the Internal Resistance Distribution of Microbial Fuel Cells," *Environmental Science & Technology*, vol. 42, no. 21, pp. 8101-8107, 2008/11/01 2008, doi: 10.1021/es801229j.
- [116] A. Elmekawy, X. Hegab Hm Fau - Dominguez-Benetton, D. Dominguez-Benetton X Fau - Pant, and D. Pant, "Internal resistance of microfluidic microbial fuel cell: challenges and potential opportunities," (in eng), no. 1873-2976 (Electronic).
- [117] A. Doug, C. Tsouris, Y. Hamilton, and A. Borole, "Assessment of the Effects of Flow Rate and Ionic Strength on the Performance of an Air-Cathode Microbial Fuel Cell Using Electrochemical Impedance Spectroscopy," *Energies*, vol. 3, 04/01 2010, doi: 10.3390/en3040592.

- [118] O. Lefebvre, S. Tan Z Fau - Kharkwal, H. Y. Kharkwal S Fau - Ng, and H. Y. Ng, "Effect of increasing anodic NaCl concentration on microbial fuel cell performance," (in eng), no. 1873-2976 (Electronic).
- [119] G. Velvizhi and S. Venkata Mohan, "Electrogenic activity and electron losses under increasing organic load of recalcitrant pharmaceutical wastewater," *International Journal of Hydrogen Energy*, vol. 37, no. 7, pp. 5969-5978, 2012/04/01/ 2012, doi: <https://doi.org/10.1016/j.ijhydene.2011.12.112>.
- [120] S. Rikame, A. Mungray, and A. K. Mungray, "Electricity generation from acidogenic food waste leachate using dual chamber mediator less microbial fuel cell," *International Biodeterioration & Biodegradation*, vol. 75, pp. 131–137, 11/01 2012, doi: 10.1016/j.ibiod.2012.09.006.
- [121] C. Nagendranatha Reddy and B. Min, "Biological Conversion of Food Waste to Value Addition in Microbial Fuel Cell," 2019, pp. 211-238.
- [122] S. Venkata Mohan, P. N. Mohanakrishna G Fau - Sarma, and P. N. Sarma, "Composite vegetable waste as renewable resource for bioelectricity generation through non-catalyzed open-air cathode microbial fuel cell," (in eng), no. 1873-2976 (Electronic).
- [123] J. Babauta, R. Renslow, Z. Lewandowski, and H. Beyenal, "Electrochemically active biofilms: facts and fiction. A review," *Biofouling*, vol. 28, no. 8, pp. 789-812, 2012/09/01 2012, doi: 10.1080/08927014.2012.710324.
- [124] S. Jung and J. M. Regan, "Influence of external resistance on electrogenesis, methanogenesis, and anode prokaryotic communities in microbial fuel cells," (in eng), no. 1098-5336 (Electronic).
- [125] A. J. Stams, C. M. de Bok Fa Fau - Plugge, M. H. A. Plugge Cm Fau - van Eekert, J. van Eekert Mh Fau - Dolfing, G. Dolfing J Fau - Schraa, and G. Schraa, "Exocellular electron transfer in anaerobic microbial communities," (in eng), no. 1462-2912 (Print).

- [126] V. Sharma and P. P. Kundu, "Biocatalysts in microbial fuel cells," *Enzyme and Microbial Technology*, vol. 47, no. 5, pp. 179-188, 2010/10/06/ 2010, doi: <https://doi.org/10.1016/j.enzmictec.2010.07.001>.
- [127] S. Prathiba, P. S. Kumar, and D. N. Vo, "Recent advancements in microbial fuel cells: A review on its electron transfer mechanisms, microbial community, types of substrates and design for bio-electrochemical treatment," (in eng), no. 1879-1298 (Electronic).
- [128] R. Kumar, L. Singh, and A. W. Zularisam, "Exoelectrogens: Recent advances in molecular drivers involved in extracellular electron transfer and strategies used to improve it for microbial fuel cell applications," *Renewable and Sustainable Energy Reviews*, vol. 56, pp. 1322-1336, 2016/04/01/ 2016, doi: <https://doi.org/10.1016/j.rser.2015.12.029>.
- [129] D. Lovley, "Microbial fuel cells: novel microbial physiologies and engineering approaches," *Current opinion in biotechnology*, vol. 17, pp. 327-32, 07/01 2006, doi: [10.1016/j.copbio.2006.04.006](https://doi.org/10.1016/j.copbio.2006.04.006).
- [130] D. R. Lovley, "Bug juice: harvesting electricity with microorganisms," *Nature Reviews Microbiology*, vol. 4, no. 7, pp. 497-508, 2006/07/01 2006, doi: [10.1038/nrmicro1442](https://doi.org/10.1038/nrmicro1442).
- [131] D. R. Lovley and K. P. Nevin, "Electrobiocommodities: powering microbial production of fuels and commodity chemicals from carbon dioxide with electricity," *Current Opinion in Biotechnology*, vol. 24, no. 3, pp. 385-390, 2013/06/01/ 2013, doi: <https://doi.org/10.1016/j.copbio.2013.02.012>.
- [132] U. Schröder, "Anodic electron transfer mechanisms in microbial fuel cells and their energy efficiency," *Physical chemistry chemical physics : PCCP*, vol. 9, pp. 2619-29, 07/01 2007, doi: [10.1039/b703627m](https://doi.org/10.1039/b703627m).
- [133] Y. Qiao, C. M. Li, S.-J. Bao, and Q.-L. Bao, "Carbon nanotube/polyaniline composite as anode material for microbial fuel cells," *Journal of Power Sources*, vol. 170, no. 1, pp. 79-84, 2007/06/30/ 2007, doi: <https://doi.org/10.1016/j.jpowsour.2007.03.048>.

- [134] J. Benito *et al.*, "Fabrication of ultrathin films containing the metal organic framework Fe-MIL-88B-NH₂ by the Langmuir–Blodgett technique," *Colloids and Surfaces A: Physicochemical and Engineering Aspects*, vol. 470, pp. 161-170, 2015.
- [135] P. Sivakumar, S. Priyatharshni, K. Nagashanmugam, A. Thanigaivelan, and K. Kumar, "Chitosan capped nanoscale Fe-MIL-88B-NH₂ metal-organic framework as drug carrier material for the pH responsive delivery of doxorubicin," *Materials Research Express*, vol. 4, no. 8, p. 085023, 2017.
- [136] W. Wang, C. Wen, D. Zheng, C. Li, J. Bian, and X. Wang, "Simultaneous degradation of RhB and reduction of Cr (VI) by MIL-53 (Fe)/Polyaniline (PANI) with the mediation of organic acid," *Chinese Journal of Chemical Engineering*, vol. 42, pp. 55-63, 2022.
- [137] T. David, J. K. Mathad, T. Padmavathi, and A. Vanaja, "Part-A: Synthesis of polyaniline and carboxylic acid functionalized SWCNT composites for electromagnetic interference shielding coatings," *Polymer*, vol. 55, no. 22, pp. 5665-5672, 2014.
- [138] M. Salami, Z. Talebpour, and R. Alizadeh, "Fabrication of a new SPME fiber based on Polyacrylic acid/MIL-88 (Fe)-NH₂ composite as a self-healing coating for the analysis of breast cancer biomarkers in the urine sample," *Journal of Pharmaceutical and Biomedical Analysis*, vol. 219, p. 114902, 2022.
- [139] C. Bi, Q. Wen, Y. Chen, and H. Xu, "Boosting power output in microbial fuel cell with sulfur-doped MXene/polypyrrole hydrogel anode for enhanced extracellular electron transfer process," *Journal of Applied Electrochemistry*, pp. 1-15, 2024.
- [140] A. Sumisha and K. Haribabu, "Modification of graphite felt using nano polypyrrole and polythiophene for microbial fuel cell applications-a comparative study," *International Journal of Hydrogen Energy*, vol. 43, no. 6, pp. 3308-3316, 2018.
- [141] K. Tahir *et al.*, "Nickel ferrite/MXene-coated carbon felt anodes for enhanced microbial fuel cell performance," *Chemosphere*, vol. 268, p. 128784, 2021.
- [142] K. Tahir *et al.*, "MnCo₂O₄ coated carbon felt anode for enhanced microbial fuel cell performance," *Chemosphere*, vol. 265, p. 129098, 2021.

- [143] N. Munir, M. Hanif, D. A. Dias, and Z. Abideen, "The role of halophytic nanoparticles towards the remediation of degraded and saline agricultural lands," *Environmental Science and Pollution Research*, vol. 28, no. 43, pp. 60383-60405, 2021.
- [144] B. J. Inkson, "Scanning electron microscopy (SEM) and transmission electron microscopy (TEM) for materials characterization," in *Materials characterization using nondestructive evaluation (NDE) methods*: Elsevier, 2016, pp. 17-43.
- [145] J. Epp, "X-ray diffraction (XRD) techniques for materials characterization," in *Materials Characterization Using Nondestructive Evaluation (NDE) Methods*, 2016, pp. 81-124.
- [146] W. W. Andualem, "Green Synthesis of CuO Nanoparticles for the Application of Dye Sensitized Solar Cell," ed, 2020.
- [147] S. N. Salisu Nasir, M. Z. H. Mohd Zobir Hussein, Z. Z. Zulkarnain Zainal, N. A. Y. Nor Azah Yusof, M. Syazwan Afif, and I. M. A. Ibrahim Mustapha Alibe, "Potential valorization of by-product materials from oil palm: a review of alternative and sustainable carbon sources for carbon-based nanomaterials synthesis," 2019.
- [148] B. Patrizi, M. Siciliani de Cumis, S. Viciani, and F. D'Amato, "Dioxin and related compound detection: Perspectives for optical monitoring," *International Journal of Molecular Sciences*, vol. 20, no. 11, p. 2671, 2019.
- [149] V. Țucureanu, A. Matei, and A. M. Avram, "FTIR spectroscopy for carbon family study," *Critical reviews in analytical chemistry*, vol. 46, no. 6, pp. 502-520, 2016.
- [150] A. Marcelli, A. Cricenti, W. M. Kwiatek, and C. Petibois, "Biological applications of synchrotron radiation infrared spectromicroscopy," *Biotechnology advances*, vol. 30, no. 6, pp. 1390-1404, 2012.
- [151] A. Marcelli, A. Cricenti, W. Kwiatek, and C. Petibois, "Biological applications of synchrotron radiation infrared spectromicroscopy," *Synchrotron Radiation in Natural Science*, vol. 9, no. 1-2, p. 43, 2010.

- [152] N. K. Bakirhan, B. Uslu, and S. A. Ozkan, "Chapter 3 - Sensitive and Selective Assay of Antimicrobials on Nanostructured Materials by Electrochemical Techniques," in *Nanostructures for Antimicrobial Therapy*, A. Fikai and A. M. Grumezescu Eds.: Elsevier, 2017, pp. 55-83.
- [153] S. Bilal, "Cyclic Voltammetry," in *Encyclopedia of Applied Electrochemistry*, G. Kreysa, K.-i. Ota, and R. F. Savinell Eds. New York, NY: Springer New York, 2014, pp. 285-289.
- [154] A. C. Lazanas and M. I. Prodromidis, "Electrochemical impedance spectroscopy— a tutorial," *ACS Measurement Science Au*, vol. 3, no. 3, pp. 162-193, 2023.
- [155] J. Li, G. Luo, L. He, J. Xu, and J. Lyu, "Analytical approaches for determining chemical oxygen demand in water bodies: a review," *Critical reviews in analytical chemistry*, vol. 48, no. 1, pp. 47-65, 2018.
- [156] Y. Li *et al.*, "TiO₂ nanoparticles anchored onto the metal–organic framework NH₂-MIL-88B (Fe) as an adsorptive photocatalyst with enhanced fenton-like degradation of organic pollutants under visible light irradiation," *ACS sustainable chemistry & engineering*, vol. 6, no. 12, pp. 16186-16197, 2018.
- [157] L. T. Tran, H. T. Dang, H. V. Tran, G. T. Hoang, and C. D. Huynh, "MIL-88B (Fe)-NH₂: An amine-functionalized metal–organic framework for application in a sensitive electrochemical sensor for Cd²⁺, Pb²⁺, and Cu²⁺ ion detection," *RSC advances*, vol. 13, no. 32, pp. 21861-21872, 2023.
- [158] A. Nisar, M. A. Khan, and Z. Hussain, "Synthesis and characterization of PANI/MOF-199/Ag nanocomposite and its potential application as non-enzymatic electrochemical sensing of dopamine," *Journal of the Korean Ceramic Society*, vol. 59, no. 3, pp. 359-369, 2022.

